



HAL
open science

PET imaging for the characterization of tauopathies : Alzheimer's disease and chronic traumatic encephalopathy

Maëva Dhaynaut

► **To cite this version:**

Maëva Dhaynaut. PET imaging for the characterization of tauopathies : Alzheimer's disease and chronic traumatic encephalopathy. Medical Imaging. Sorbonne Université, 2019. English. NNT : 2019SORUS197 . tel-02968207

HAL Id: tel-02968207

<https://theses.hal.science/tel-02968207v1>

Submitted on 15 Oct 2020

HAL is a multi-disciplinary open access archive for the deposit and dissemination of scientific research documents, whether they are published or not. The documents may come from teaching and research institutions in France or abroad, or from public or private research centers.

L'archive ouverte pluridisciplinaire **HAL**, est destinée au dépôt et à la diffusion de documents scientifiques de niveau recherche, publiés ou non, émanant des établissements d'enseignement et de recherche français ou étrangers, des laboratoires publics ou privés.

THÈSE

École doctorale ED 30 : Informatique, télécommunications et
électronique de Paris

Pour obtenir le grade de docteur délivré par :

L'Université Pierre et Marie Curie

Spécialité doctorale : Neurosciences et imagerie biomédicale

PET imaging for the characterization of tauopathies: Alzheimer's Disease and Chronic Traumatic Encephalopathy

présentée et soutenue publiquement par

Maeva DHAYNAUT

le 18 décembre 2019

Jury

Mme. Aurélie Kas, professor, LIB Paris, Sorbonne Université UPMC

M. Georges El Fakhri, professor, Gordon Center for Medical Imaging
Boston, Harvard medical School, Massachusetts General Hospital

Mme. Marie-Odile Habert, MCP, LIB Paris, Sorbonne Université
UPMC

M. Alain Prigent, professor, Faculté Médecine Paris Sud

M. Vincent Lebon, professor, Paris Sud University

M. Damien Galanaud, professeur, Hospital Pitié Salpêtrière, UPMC

Directeur de thèse : **Georges El Fakhri, Aurélie Kas**

Approved by:

Date Approved:

PET imaging for the characterization of tauopathies: Alzheimer's Disease and Chronic Traumatic Encephalopathy

Abstract

Tauopathies are neurodegenerative diseases characterized by intracerebral aggregation of abnormal Tau proteins. These incurable diseases are really heterogeneous with the aggregation of different isoforms of Tau protein. Many fields of research are working on therapeutical targets. During this university thesis, we studied by Positron Emission Tomography (PET) imaging the Tau burden in Alzheimer's Disease (AD) and Chronic Traumatic Encephalopathy (CTE), two different tauopathies with similar Tau isoforms. In this context, our first objective was to determine the ability of Tau PET imaging to improve the diagnosis of AD and to determine the viability of a new potential treatment. We have established that Tau PET imaging was able to detect the beneficial effect of a non-invasive brain stimulation, called transcranial alternating current stimulation (tACS) in people with AD. Our second objective was to determine the usefulness of Tau PET imaging *in vivo* in a population of American football players to help the early detection of CTE. We have demonstrated that in our population, Tau PET imaging was able to highlight the Tau pathology in early stages of CTE. In parallel, we have studied by autoradiography post-mortem from patients with neuro-pathological diagnosis of AD and CTE the binding pattern of three radiotracers widely used in research for Tau imaging. We directly compared the binding properties of [¹⁸F]-AV-1451 with [¹⁸F]-MK-6240 and [¹⁸F]-PI-2620 in the same specimens. These three tracers showed similar strong binding pattern to Tau protein in AD and a lack of binding in CTE brain slices. The off-target binding profiles were also similar between the three radiotracers, with uptake observed in neuromelanin-containing neurons and hemorrhage, validating our *in vivo* assessments. In total, these experiments allow to confirm the potential utility of Tau PET tracers for the reliable detection, quantification of Tau aggregates and disease-progression tracking in AD, while it remains questionable for CTE.

Imagerie TEP pour la caractérisation des tauopathies: maladie d'Alzheimer et encéphalopathie traumatique chronique

Résumé

Les tauopathies sont des maladies neurodégénératives caractérisées par une agrégation intracérébrale de protéines Tau anormales. Cependant, ces maladies incurables sont hétérogènes avec l'agrégation de différentes isoformes de la protéine Tau. De nombreux domaines de recherche travaillent sur des cibles thérapeutiques. Au cours de ce travail doctoral, nous avons étudié par tomographie par émission de positons (TEP) l'imagerie des agrégats Tau dans la maladie d'Alzheimer (MA) et l'encéphalopathie traumatique chronique (ETC). Dans ce contexte, notre premier objectif était de déterminer la capacité de l'imagerie Tau-TEP à améliorer le diagnostic de la MA et de déterminer la viabilité d'un nouveau traitement potentiel. Nous avons établi que l'imagerie Tau-TEP était capable de détecter l'effet bénéfique d'une stimulation cérébrale non invasive, appelée stimulation transcrânienne à courant alternatif (tACS) chez les personnes atteintes de MA. Notre deuxième objectif était de déterminer l'utilité de l'imagerie Tau *in vivo* dans une population de joueurs de football américains pour aider à la détection précoce de l'ETC. Nous avons démontré que, dans notre population, l'imagerie Tau était en mesure de mettre en évidence les premières étapes de la maladie. En outre, nous avons étudié par autoradiographie post-mortem chez des patients diagnostiqués MA et ETC, le schéma de liaison de trois radiotraceurs largement utilisés en recherche. Nous avons directement comparé les propriétés de liaison de [¹⁸F]-AV-1451 avec [¹⁸F]-MK-6240 et [¹⁸F]-PI-2620 dans les mêmes échantillons. Ces trois traceurs ont montré un modèle similaire de forte liaison à la protéine Tau dans la MA et un manque de liaison dans le cas de l'ETC. Les profils de liaison hors cible étaient également similaires, avec une rétention observée dans les neurones contenant de la neuromélanine et une hémorragie, en accord avec nos évaluations *in vivo*. Au total, ces expériences ont permis de confirmer l'utilité potentielle de l'imagerie Tau-TEP pour la détection, quantification des agrégats de Tau avec le suivi de la progression de la maladie dans la MA, tout en restant incertain pour l'ETC.

Summary

- Publications.....10
- List of tables.....13
- List of figures.....14
- List of symbols and abbreviations.....16

- INTRODUCTION.....18

- PART 1 : Background.....19
- TAUOPATHIES.....20
- 1. Tau protein.....20
 - 1.1. Structure.....20
 - 1.2. Functions.....22
 - a. Regulation of microtubule stability.....22
 - b. Axonal transport.....23
 - c. Other functions of Tau.....24
- 2. Different types of tauopathies.....24
- 3. Alzheimer’s Disease.....25
 - 3.1. Clinical signs.....25
 - 3.2. Risks factors.....26
 - 3.3. Physiopathology.....26
- 4. Chronic Traumatic Encephalopathy in traumatic brain injuries.....29
 - 4.1. Clinical signs.....30
 - 4.2. Risks factors.....30

4.3. Physiopathology.....	31
POSITRON EMISSION TOMOGRAPHY.....	32
1. Principles of PET imaging.....	32
1.1 Radiotracers.....	33
1.2. Physical interactions.....	33
2. Clinical applications in neurology.....	36
3. Tau protein in PET imaging.....	37
GOALS.....	39
PART 2 : Autoradiographic characterization of p-Tau PET tracers [F-18]-AV-1451, [F-18]-MK-6240, [F-18]-PI-2620 in AD and CTE.....	40
PROBLEM STATEMENT.....	41
MATERIALS AND METHODS.....	42
1. Autoradiography principles.....	42
2. Tissue samples.....	42
3. Radiotracers.....	43
4. Phosphor screen autoradiography.....	43
RESULTS.....	45
1. Autoradiography of AD cases.....	45
2. Autoradiography of CTE cases.....	48
3. Autoradiography of off-target binding.....	51
DISCUSSION.....	53

PART 3 : Tau PET imaging in AD : Effect of modulation gamma oscillations by transcranial alternating current stimulation on brain structures in humans.....	58
PROBLEM STATEMENT.....	59
MATERIALS AND METHODS.....	61
1. Subject selection.....	61
2. Data acquisition.....	61
3. Image reconstruction and processing.....	62
4. Biostatistical analysis.....	63
RESULTS.....	64
1. Amyloid-beta imaging.....	64
2. Hyperphosphorylated Tau imaging.....	66
DISCUSSION.....	70
PART 4 : Tau PET Imaging in CTE in athletes: a sequela of TBI.....	72
PROBLEM STATEMENT.....	73
MATERIALS AND METHODS.....	74
1. Subject selection.....	74
2. Data acquisition.....	75
3. Image reconstruction and processing.....	75
4. Biostatistical analysis.....	76
RESULTS.....	77
1. Amyloid-beta imaging.....	78
2. Hyperphosphorylated Tau imaging.....	79
DISCUSSION.....	83

CONCLUSIONS AND PERSPECTIVES.....86

Acknowledgments.....88

References.....89

Annexes.....111

Publications

(1) Autoradiography validation of novel tau PET tracer [F-18]-MK-6240 on human postmortem brain tissue. *Acta Neuropathol Commun.* 2019 Mar 11;7(1):37. doi: 10.1186/s40478-019-0686-6.

CinthyA Agüero, MD, PhD, **Maeva Dhaynaut**, MS, Marc D. Normandin, PhD, Ana C. Amaral, PhD, Nicolas Guehl, MS, PhD, Kimberly Nguyen, BA, Victoria Fleming, BA, Keith A. Johnson, MD Matthew P. Frosch, MD, PhD and Teresa Gómez-Isla, MD, PhD

(2) [¹⁸F]-AV-1451 binding profile in Chronic Traumatic Encephalopathy: a postmortem case series. *Acta Neuropathol Commun.* 2019 Oct 28;7(1):164. doi: 10.1186/s40478-019-0808-1.

Marta Marquié, MD, PhD*; CinthyA Agüero, MD, PhD*; Ana C. Amaral, PhD; Alberto Villarejo-Galende, MD, PhD; Prianca Ramanan, BA; Michael Siao Tick Chong, BA; Nil Sáez-Calveras; Rachel E. Bennett, PhD; Eline Verwer, PhD; Sally Ji Who Kim, PhD; **Maeva Dhaynaut** MS; Victor E. Alvarez, MD; Keith A. Johnson, MD; Ann C. McKee, MD; Marc Normandin, PhD; Matthew P. Frosch, MD, PhD; and Teresa Gómez-Isla, MD, PhD

(3) Evaluation of pharmacokinetic modeling strategies for in-vivo quantification of tau with the radiotracer [18-F]-MK6240 in human subjects. *Eur J Nucl Med Mol Imaging.* 2019 Sep;46(10):2099-2111. doi: 10.1007/s00259-019-04419-z. Epub 2019 Jul 22.

Nicolas J. Guehl & Dustin W. Wooten & Daniel L. Yokell & Sung-Hyun Moon
Maeva Dhaynaut & Samantha Katz & Kirsten A. Moody & Codi Gharagouzloo
& Aurélie Kas & Keith A. Johnson & Georges El Fakhri & Marc D. Normandin

Publications in preparation related to PhD work

(4) Autoradiographic characterization of novel tau PET tracer [18F]-PI-2620 in human postmortem brain tissue. (*Abstract presented at SfN 2019*)

Maeva Dhaynaut MS*, Cinthya Agüero MD, PhD*, Ramesh Neelamegam PhD, S-H Moon PhD, Marc D. Normandin PhD, Georges El Fakhri PhD DABR, Matthew P. Frosch MD, PhD and Teresa Gómez-Isla MD, PhD

(5) Pathologic correlations of *in vivo* [18F]-AV-1451 imaging in autopsy-confirmed Alzheimer's disease, Frontotemporal lobar degeneration with TDP-43 inclusions and control cases.

Cinthya Agüero, MD, PhD, **Maeva Dhaynaut**, MS, Ana C. Amaral, PhD, Nicolas Guehl, MS, PhD, Kimberly Nguyen, BA, Victoria Fleming, BA, Marc D. Normandin, PhD, Derek H. Oakley, MD, PhD, Stephen N. Gomperts, MD, PhD Keith A. Johnson, MD Matthew P. Frosch, MD, PhD and Teresa Gómez-Isla, MD, PhD

Other projects

(6) Pharmacokinetic evaluation of the 5-HT₆ radiotracer [18-F]2FNQ1P in rhesus macaque. (*Abstract presented at SNMMI 2019*)

M Dhaynaut, TM Shoup, NJ Guehl, S-H Moon, G El Fakhri, MD Normandin

(7) Evaluation of [18-F]3F4AP in non-human primates: a PET tracer for demyelinating diseases. (*paper in preparation*)

Guehl NJ, Ramos-Torres K, **Dhaynaut M**, Moon SH, Neelamegam R, Correia J, Basuli F, Zhang X, Popko B, El Fakhri G, Reich DS, Herscovitch P, Normandin MD, Brugarolas P.

(8) Functional neuroimaging using dynamic 3D UTE MRI. (*paper in preparation*)

Codi A. Gharagouzloo, Chao Ma, Eline E. Verwer, Chuan Huang, **Dhaynaut M**, Joseph B. Mandeville, Srinivas Sridhar, Georges El Fakhri, Dustin W. Wooten, Marc D. Normandin.

(9) Fluorinated Cromolyn Derivatives for Potential Alzheimer's Disease Treatment. *(Paper in preparation)*

TM Shoup, MD Normandin, K Takahashi, A Griciuc, L Quinti, **M Dhaynaut**, S-H Moon, NJ Guehl, P Brugarolas, RE Tanzi, G El Fakhri, DR Elmaleh

(10) GE-179 PET imaging of NMDA receptor availability in amyotrophic lateral sclerosis. *(Poster)*

Liu J, Guehl NJ, Wooten DW, Weise S, Babu S, Alshikho MJ, **Dhaynaut M**, Moon SH, Carter R, Yokell D, El Fakhri G, Normandin MD, Atassi N.

(11) Novel ¹¹C-labeled tracer for K⁺ channels in the brain: synthesis and imaging in non-human primates. *(Paper in preparation)*

Ramesh Neelamegam, PhD, Nicolas J. Guehl, Jorge E. Sanchez-Rodriguez, PhD, Kazue Takahashi, Karla M. Ramos-Torres, PhD, **Maeva DHAYNAUT**, Alyssa Bravin, Sung-Hyun Moon, PhD, Georges N. El Fakhri, PhD, Moses Q. Wilks, PhD, Marc D. Normandin, PhD, Pedro Brugarolas, PhD.

(12) Radiosynthesis and in vitro evaluation of [¹⁸F]N-decyl-6-fluoronicotinamide-TEMPO as a PET/MR probe of oxidative stress in cell membranes.

Sung-Hyun Moon, PhD, Moses Q. Wilks, PhD, Kazue Takahashi, Ph.D, Paul Han, Ph.D, Chao Ma, PhD, Hushan Yuan, Ph.D, **Dhaynaut M**, Guehl NJ, Georges N. El Fakhri, PhD, Timothy M. Shoup, PhD, Marc D. Normandin, PhD.

List of tables

Table 1: Aβ scores for each subject.....64
Table 2: Aβ scores for each subject.....78

List of figures

Figure 1: Isoforms of Tau protein.....	21
Figure 2: Phosphorylation of Tau and regulation of axonal transport...23	23
Figure 3: Tau pathology in Alzheimer’s disease.....27	27
Figure 4: Spatio-temporal evolution of the Tau lesions according to Braak.....28	28
Figure 5: Nuclear reaction of β + type disintegration.....34	34
Figure 6: Principles of PET imaging.....35	35
Figure 7 : Chemical structure of the Tau PET radioligands [¹⁸F]-AV-1451, [¹⁸F]-MK-6240 and [¹⁸F]-PI-2620.....43	43
Figure 8: [¹⁸F]-AV-1451 phosphor screen images of brain slices from AD and control cases.....46	46
Figure 9: [¹⁸F]-MK-6240 phosphor screen images of brain slices from AD and control cases.....47	47
Figure 10: [¹⁸F]-PI-2620 phosphor screen images of brain slices from AD and control cases.....48	48
Figure 11: [¹⁸F]-AV-1451 phosphor screen images of brain slices from CTE cases.....49	49
Figure 12: [¹⁸F]-PI-2620 and [¹⁸F]-MK-6240 phosphor screen images of brain slices from CTE cases.....50	50
Figure 13: Representative images of phosphor screen autoradiography experiments with and without ethanol washing steps.....51	51
Figure 14: [¹⁸F]-PI-2620 and [¹⁸F]-MK-6240 phosphor screen images off-target binding.....52	52
Figure 15: SUVR parametric images of [¹¹C]-PiB for all subjects using the cerebellum no vermis as reference region.....65	65

Figure 16: Change in [¹¹C]-PiB binding across the 5 subjects in the temporal lobe.....	66
Figure 17: SUVR parametric images of [¹⁸F]-AV-1451 for all subjects using the white matter as reference region.....	67
Figure 18: Change in [¹⁸F]-AV-1451 binding across the 5 subjects in the temporal Lobe.....	68
Figure 19: Change in [¹⁸F]-AV-1451 binding across the 5 subjects in regions of interest.....	69
Figure 20: SUVR parametric images of [¹¹C]-PiB and [¹⁸F]-AV-1451 for all subjects.....	77
Figure 21: Mean SUVR values for [¹¹C]-PiB across 10 subjects in the regions of interest.....	79
Figure 22: [¹⁸F]AV-1451 binding in temporal lobe and pallidum of TBI and control subjects.....	81
Figure 23: Mean SUVR values for [¹⁸F]-AV-1451 across the 10 subjects in the regions of interest.....	82

List of symbols and abbreviations

Tubulin associated unit (Tau)
microtubule-associated protein tau (MAPT)
microtubules (MT)
neurofibrillary tangles (NFTs)
paired helical filaments (PHFs)
microtubule-associated proteins (MAP)
Alzheimer's Disease (AD)
Chronic traumatic encephalopathy (CTE)
frontotemporal dementia linked to chromosome 17 (FTDP-17)
corticobasal degeneration (CBD)
progressive supranuclear palsy (PSP)
argyrophylic grain dementia (AGD)
Lewis Body Dementia (DLB)
amyloid beta ($A\beta$)
Amyloid Precursor Protein (APP)
mild cognitive impairment (MCI)
Fludeoxyglucose-Positron Emission Tomography (FDG-PET)
Traumatic brain injuries (TBIs)
Positron emission tomography (PET)
Single Photon Emission Computed Tomography (SPECT)
High Performance Liquid Chromatography (HPLC)
Line of Response (LOR)
Computed Tomography (CT)
magnetic resonance imaging (MRI)
coronary artery disease (CAD)
Methionine (MET)
fluoroethyl-l-tyrosine (FET)
Phospho-Tau (p-Tau)
Boston University (BU)
Alzheimer's Disease Research Center (ADRC)

standardized uptake values (SUVR)
region of interests (ROIs)
Monoamine Oxydase B (MAO-B)
transcranial alternating current stimulation (tACS)
Allen Center for Non-Invasive Brain Stimulation (CNBS)
Beth Israel Deaconess Medical Center (BIDMC)
Mini-Mental State Examination (MMSE)
Clinical Dementia Rating (CDR)
Massachusetts General Hospital (MGH)
full width at half maximum (FWHM)
Montreal Neurological Institute (MNI)
mesial temporal cortex (MTC)
Telephone Montreal Cognitive Assessment (T-MoCA)
Alzheimer's Disease Cooperative Study (ADCS-ADL)
Neuropsychiatric Inventory–Questionnaire (NPI-Q)
magnetization-prepared rapid gradient-echo (MPRAGE)

Introduction

Tauopathies are incurable diseases characterised by an abnormal intracellular amount of Tau protein hyperphosphorylated. These pathologies lead to neurodegeneration and dementia. Dementia is one of the biggest health problems facing our society. In the United States, the cost of caring for these patients is more than \$200 billion per year. In **PART 1**, we will give a brief presentation of tauopathies and the implication of Tau protein in the disease. We will focus mainly on two tauopathies with similar Tau isoforms, Alzheimer's Disease (AD) and Chronic Traumatic Encephalopathy (CTE).

Positron Emission Tomography (PET) is a functional imaging modality that has become a useful method in clinic. As we will see in **PART 1**, PET enables the imaging of a radiotracer injected in patient's body allowing the visualisation of physiological or pathological processes. In this work, we will look closer at the distribution of hyperphosphorylated Tau protein in the brain by PET imaging.

The aim of this thesis is to demonstrate the role of PET imaging in accurately estimate the changes in hyperphosphorylated Tau protein deposition in the brain of subjects with tauopathies as AD and CTE.

In order to have a correct interpretation of the PET images it is essential to validate the biological targets and to identify potential off-target binding of these imaging agents. That's why in **PART 2** we will investigate, by autoradiography on post-mortem slices of brain from patients with diagnosed AD and CTE, the binding pattern of three radiotracers for Tau imaging.

Then, we will study the ability of Tau PET imaging to improve the diagnosis of AD and to determine the viability of a new potential treatment in **PART 3**. In **PART 4**, we will scrutinize in a population of American football players the aptitude of Tau PET imaging in the early detection of CTE.

PART 1 : Background

TAUOPATHIES

Tauopathies are a group of neurodegenerative diseases characterized by the presence in neurons and glial cells of intracellular aggregates of Tubulin associated unit (Tau) proteins hyperphosphorylated. The accumulation causes neurodegeneration in specific brain regions, leading to cognitive impairments and ultimately dementia.

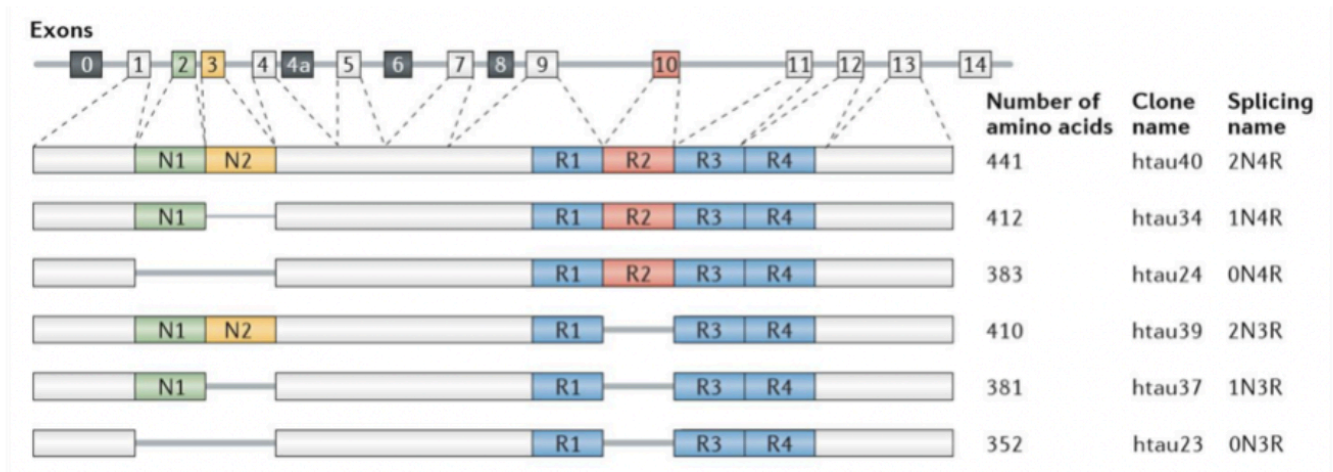
1. Tau protein

Human Tau protein is encoded by a single microtubule-associated protein tau (MAPT) gene localized on chromosome 17q21 (Neve et al., 1986). Six main isoforms of the protein are present in the adult brain, arising from the alternative splicing of exons 2, 3 and 10 (Goedert et al., 1988) (Figure 1).

1.1. Structure

The Tau protein is a highly polarized protein, hydrophilic and heat-resistant (Lee et al., 1989; Weingarten et al., 1975). It is formed by four protein domains: the N-terminal region, the proline-rich region, the microtubule binding region and the C-terminal region. The proline-rich region is very basic and would allow spacing microtubules (MT) between themselves constituting the "projection domain" (Chen et al., 1992). The N-terminal part of the protein presents a predominantly acidic composition while the C-terminal part is neutral (Himmler et al., 1989). The different isoforms depend on the number of inserts localized in the N-terminal part of the protein (Goedert et al., 1989; Lee et al., 1989), encoded by exons 2 and 3, creating isoforms with either zero, one or two inserts (0N, 1N and 2N). In addition, alternative splicing of exon 10 leads to the production of isoforms 3R and 4R with 3 or 4 repeats in the C-terminal domain (Goedert et al., 1988, 1989). In the peripheral nervous

system, Tau is found in the larger isoform corresponding to the 2N4R form with the addition of exon 4a (Mandelkow and Mandelkow, 2011).



Taken from Wang (2016)

Figure 1: Isoforms of Tau protein. The alternative splicing of MAPT gene leads to the formation of isoforms 4R and 3R with respectively 4 and 3 repeats in the C-terminal part of the protein and of isoforms with zero (0N), one (1N) or two (2N) N-terminal repeats (Wang et al., 2016).

Tau proteins are natively unfolded and disordered with no stable secondary or tertiary structure (Mylonas et al., 2008, Mukrasch et al., 2009). Few transient secondary structures (α -helix, β -strand, poly-proline II helix) are observed along the protein, conferring a very flexible conformation sensitive to variations of the environment (Dunker et al., 2008).

Tau protein is the major constituent of neurofibrillary tangles (NFTs) corresponding to intracellular aggregation of abnormally hyperphosphorylated insoluble Tau proteins (Brion et al., 1985). These assemblies are classified as straight, twisted or paired helical filaments (PHFs) and are found in neurons, astrocytes, and oligodendrocytes (Arima et al., 2006). These pathological filaments PHF are excellent

ultrastructural markers of neurodegenerative processes present in tauopathies (Delacourte et al., 1994).

1.2. Functions

Tau proteins belong to the family of microtubule-associated proteins (MAP). A role of Tau *in vitro* is to induce microtubules polymerization from free tubulin (Cleveland et al., 1977; Weingarten et al., 1975). In the brain, Tau is abundantly expressed in neurons (Binder et al., 1985; Goedert et al., 1989; Kosik et al., 1989), in dendrites (Ittner et al., 2010), in the nucleus (Sultan et al., 2011) and highly at the axonal level (Binder et al., 1985; Dotti et al., 1987). Tau proteins are also observed in a minor amount in glial cells as oligodendrocytes and astrocytes (LoPresti et al., 1995). The pattern of isoforms expression may differ between neuronal populations. Indeed, 3R and 4R isoforms are present in pyramidal cells of the cortex, while the granular cells of the dentate gyrus express only 3R Tau isoforms (Goedert et al., 1989). This implies that all the isoforms have functional differences.

a. Regulation of microtubule stability

Microtubules of the cytoskeleton are particularly abundant in neurons where they are involved in cytoplasmic transport, an essential function for neuronal activity. A major function of Tau proteins is to bind microtubules and regulate their polymerization (Weingarten et al., 1975, Drubin et al., 1986).

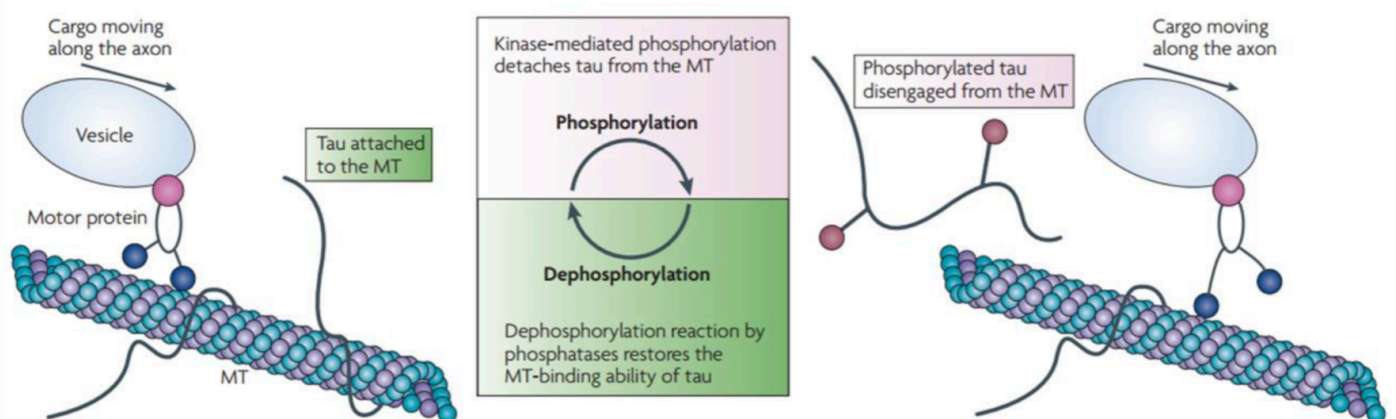
The binding of Tau proteins to microtubules is possible by their phosphorylation and the presence of repeated microtubule binding domains (Himmler et al., 1989, Ennulat et al., 1989). These repeat domains can be 3 or 4 and the 4th binding domain increases the affinity of Tau 4R isoforms to microtubules, the polymerization and the stabilization (Butner et al., 1991, Goedert et al., 1990).

Tau is normally phosphorylated but in tauopathies Tau is hyperphosphorylated on serine-threonine (Noble et al., 2013) and no longer able to bind to microtubules, increasing its intracellular cytosolic levels (Maas et al., 2000).

b. Axonal transport

Axonal transport is a two-way communication from the cell body of the neuron to the synaptic axonal endings by going through the cytoplasm of its axon. Axonal transport is essential for neuronal functions because it allows the movement and the recycling of synaptic vesicles, proteins, mitochondria, nutrients or other organelles. Microtubules are the main component of the cytoskeleton involved in this intracellular transport (Mandelkow et al., 2007). By regulating the stability of microtubules and participating in morphogenesis, Tau proteins intervene indirectly in axonal transport.

Tau proteins also have the ability to act directly on axonal transport (Figure 2; Ballatore et al., 2007). Indeed, Kinesin motors, which are the proteins responsible for the transport of vesicles from the soma to the synapse, are inhibited by encountering microtubule bound Tau proteins (Dixit et al., 2008). Tau and Kinesin are in competition with each other for binding microtubules. Tau can also affect the association between Kinesin and cargoes (Wang et al., 2016). It has been shown *in vitro* and *in vivo* in transgenic mice, that overexpressing Tau proteins disturb the axonal transport (Ebner et al., 1998; Stamer et al., 2002; Ishihara et al., 1999; Ittner et al., 2008).



Taken from Ballatore (2007)

Figure 2: Phosphorylation of Tau and regulation of axonal transport. (Ballatore et al., 2007). Tau phosphorylation allows the motor protein to go to the synapse and deliver the cargo.

c. Other functions of Tau

The brain accumulation of Tau protein has been seen correlated with synaptic loss (Ingelsson et al., 2004), but the mechanisms are still not well understood. The lack of mitochondrial transport at synapses could be involved in that process (Shahpasand et al., 2012). Small quantities of Tau protein are also observed in dendrites where they play an important role in the protein composition of the postsynaptic region (Ittner et al., 2010) which is implicated in long term potentiation and synaptic plasticity (Mondragón Rodríguez et al., 2012).

Some Tau isoforms were found to be enriched in the nucleus (Liu et al., 2013) where they bind to DNA at adenosine-thymine dimers (Sultan et al., 2011; Sjöberg et al., 2006) and RNA (Violet et al., 2014). This binding would play a protective role against stress-induced degradation (Sultan et al., 2011; Violet et al., 2014).

2. Different types of tauopathies

The isoform composition of aggregated Tau proteins makes it possible to classify tauopathies in four classes (Sergeant et al., 2008).

In class I, all six isoforms of Tau are present into the aggregates. This classical profile is characteristic of Alzheimer's Disease (AD) (Sergeant et al., 1997), Chronic traumatic encephalopathy (CTE) (Hof et al., 1992; Schmidt et al., 2001), Down's syndrome-related dementia (Hof et al., 1995), Niemann-Pick disease type C (Love et al., 1995), and some frontotemporal dementia linked to chromosome 17 (FTDP-17) (Sergeant et al., 2005).

In class II, it is mainly the 4R isoforms that are aggregated. This is the case for corticobasal degeneration (CBD), progressive supranuclear palsy (PSP), argyrophilic grain dementia (AGD) and most cases of FTDP-17 associated with mutations in the MAPT gene (Sergeant et al., 1999; Tolnay et al., 2002).

Class III is characterized by the aggregation of 3R forms and corresponds to Pick's disease and some familial cases of FTDP-17 (Buée et al., 1996; Delacourte et al., 1996).

Finally, a tauopathy called myotonic dystrophy can be observed in the brain of patients with type I and II. This disease is characterized by an aggregation of small size isoforms of insoluble Tau proteins (the foetal Tau isoform ON_3R) and a strong downregulation of isoforms containing N-terminal repeats (Vermersch et al., 1996). This constitutes class IV.

In this PhD research work we focused mainly our interest on two tauopathies, AD and CTE. In following, we are going to talk in more details about these two pathologies.

3. Alzheimer's Disease

AD is an irreversible neurodegenerative disease and the most common cause of dementia, especially after 65 years old where it accounts for about 60-70% of dementia (Fratiglioni et al., 2000). Affecting over 5 million people in the United States alone, and over 30 million worldwide (Hebert et al., 2013), the prevalence of AD is expected to increase significantly in the future as the population ages. The therapeutic options are very limited, no treatments can avoid the progression of the disease.

3.1. Clinical signs

The clinical symptoms are related to the topographic distribution of the lesions and suggest the involvement of specific brain structures. Commonly AD is characterized by lesions at the entorhinal cortex and the hippocampus, leading to memory disorders particularly for the episodic memory. The disease can reach other brain regions including the associative isocortex and cortical areas. Other cognitive functions are then affected as a progressive loss of speech, impairments in executive functions and orientation (time and space), praxies and gnosies. Some noncognitive symptoms can also be developed including anxiety, depression, psychotic symptoms, sleep disorders, incontinence and cerebrovascular symptoms. In the final stage of the disease, the patient can have his motor functions altered (Cacabelos et al., 1996).

3.2. Risks factors

Age is the most important risk factor for developing this tauopathy. There are many others factors of risk as genetic and environmental factors.

Most genetic risk factors associated with the development of tauopathies seem to affect the regulation of Tau expression, leading to an increase in the production of the protein, inducing an increase in the 4R/3R isoforms ratio for AD (Myers et al. 2005; 2007). Other variations rising the expression of Tau have been associated with AD as DNA hypomethylations (Barrachina and Ferrer, 2009; Iwata et al., 2014), a non-causative mutation (Coppola et al., 2012) and duplications of MAPT gene (Hooli et al., 2014).

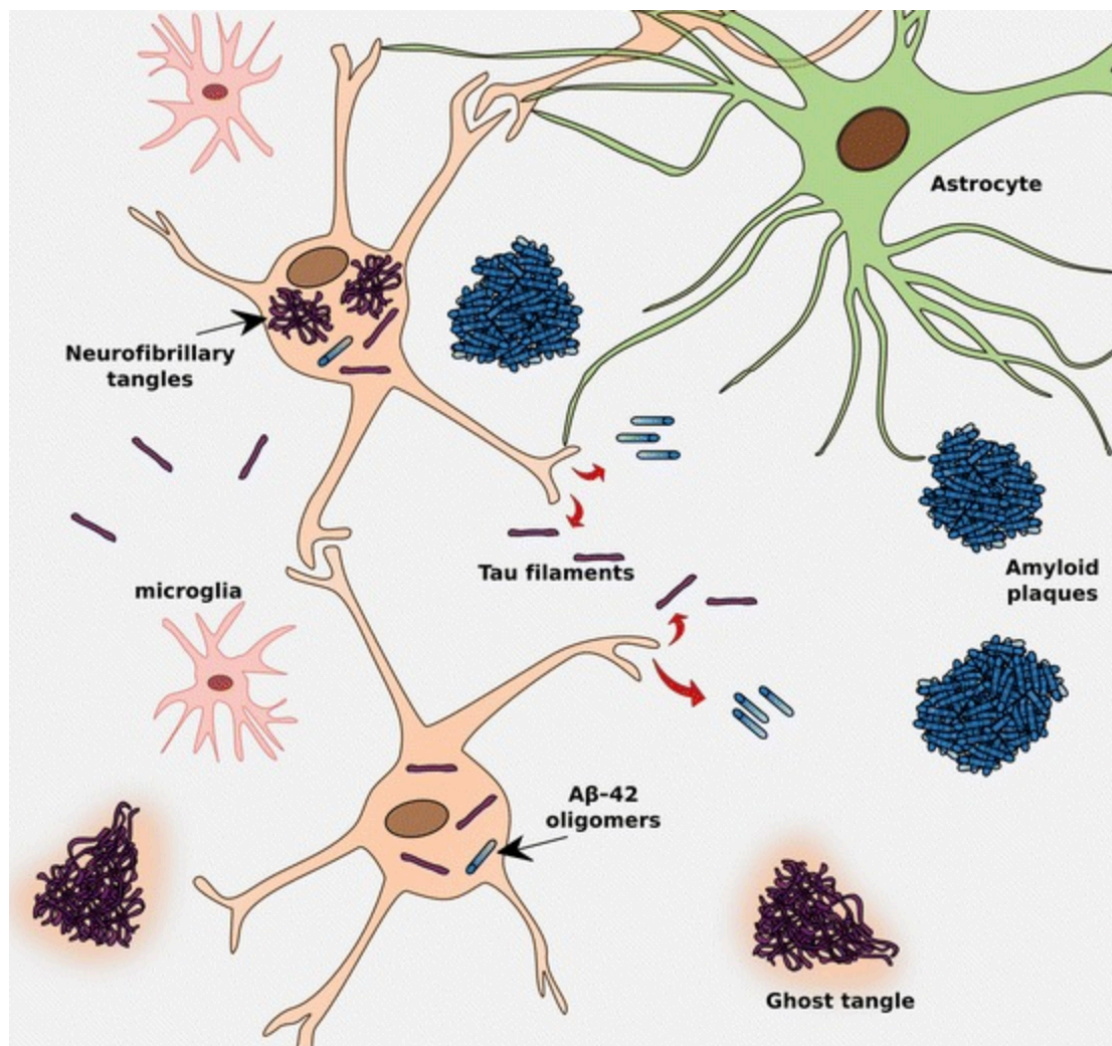
Some rare autosomal dominant family forms of AD are related to amyloid beta (A β) as mutation in Amyloid Precursor Protein (APP), PSEN1 (Sherrington et al., 1995) or PSEN2 (Levy-Lahad et al., 1995) genes. The two genes PSEN encode the presenilin protein, a subunit of the gamma secretase complex, involve in the generation of A β from APP (Schellenberg et al., 1992). These familial forms of AD have a similar clinical and histological pattern and they begin earlier in life, around 50 years old (Ryman et al., 2014). In addition, many AD susceptibility genes with different levels of risk have been identified including the APOE e4 allele (Corder et al., 1993, Strittmatter et al., 1993). The polymorphism of the APOE e4 allele is common in the population and the risk of having AD is greater in people with one and two copies of the APOE e4 allele than in people without this allele (Farrer et al., 1997).

Some environmental risks have also been identified as air quality, aluminium, pesticides and vitamin D deficiency (Killin et al., 2016).

3.3. Physiopathology

AD is characterized by the presence of two major pathological characteristics : extra-neuronal plaques constituted of A β peptides, and NFTs composed of the aggregation of all Tau protein isoforms (Villain et al. 2012; Villemagne et al. 2013; Saint-Aubert et al., 2017) (Figure 3). A large number of Tau phosphorylation sites were found to reduce Tau-MT interaction (Cho and Johnson, 2003, 2004; Fischer et

al., 2009) promoting Tau aggregation and reducing the stabilisation of MT (Liu et al., 2007).



Taken from Saint-Aubert (2017)

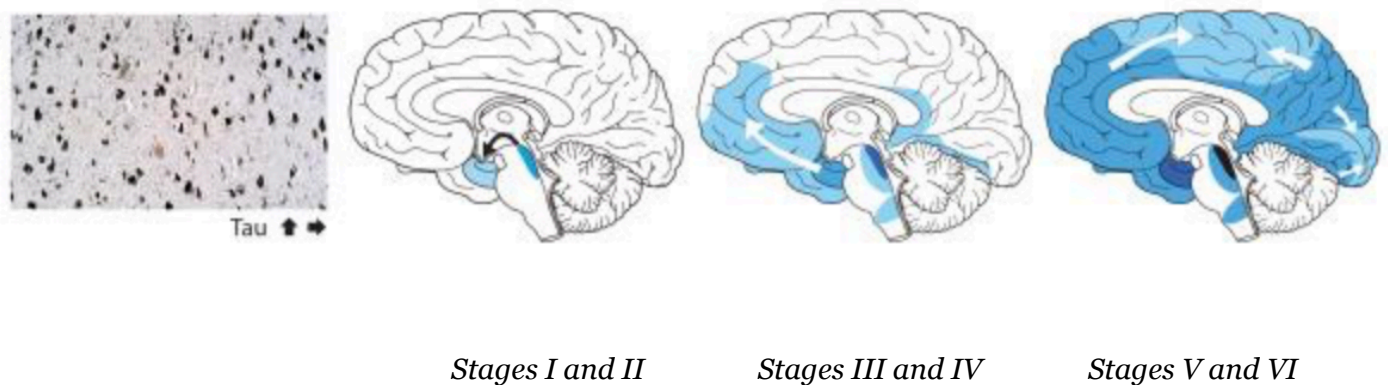
Figure 3: Tau pathology in Alzheimer's disease. Unlike A β , Tau aggregates primarily in intracellular. Some tangles, called ghost tangles, can be seen outside of cells where the host neuron died.

The evolution and the spreading of these A β and the NFTs are characterized and classified into different stages. The stages of Amyloid plaques deposition in AD are described by Thal (Thal et al., 2002). NFTs follow a well-defined sequential path of propagation classified into 10 stages according to the Delacourte classification (Delacourte et al., 1999) and 6 stages according to the Braak classification (Braak &

Braak, 1991; Braak et al., 2006 (Figure 4). It is this classification of Braak which is the most used in current practice.

The most vulnerable brain structures and the first affected by NFTs are the locus coeruleus and the transentorhinal cortex (Braak stage I). Then the disease can reach the enthorinal cortex (Braak stage II). These two stages correspond to a long preclinical period asymptomatic and the presence of Tau in the entorhinal cortex after 75 years old is similar to normal brain aging. Braak stage III corresponds to early lesions of the hippocampus. In stage IV, NFTs are extended on the hippocampus and reach to the temporal cortex and limbic regions and then to all associative cortical regions. Stages III and IV correspond to the beginning of AD and are called mild cognitive impairment (MCI). Finally, stages V and VI correspond to a major impairment of the isocortex affecting the entire cortex. The primary, visual and motor cortical regions are among the last brain regions affected by the disease (Jucker et al., 2011).

The spreading of Tau may occur *via* trans-synaptic propagation through anatomically connected synapses, glial cells as oligodendrocytes and microglia (Wang et al., 2017; Ferrer et al., 2019; Perez et al., 2019).



Adapted from Jucker (2011)

Figure 4: Spatio-temporal evolution of the Tau lesions according to Braak. Neurofibrillary tangles follow a progression in six stages characterized after anatomopathological examination of AD brains patients post-mortem.

In clinic, a lot of progress have been made to improve the pathological diagnosis. For example, biological markers of AD in the cerebrospinal fluid (CSF) are now used in practice routine but this technique stays really invasive (Ortega et al., 2019). Also, the spatial distribution of cerebral glucose metabolism illustrated by FDG-PET (Fludeoxyglucose-Positron Emission Tomography) can help in differentiating AD from other causes of dementia (Gilman et al., 2005; Minoshima et al., 2001; Foster et al., 2008) and to predict the conversion of MCI to dementia (Davison et al., 2014; Ishii et al., 2014; Mosconi et al., 2006; Hoffman et al., 2000). The mean cerebral glucose metabolism has been found to gradually decrease with age (Kuhl et al., 1982), and the specific glucose metabolism pattern in AD allows a better diagnostic. In clinic, it is important to differentiate patients with Lewis Body Dementia (DLB) or FTD from patients with AD because they can have adverse effects to symptomatic treatments given to AD patients as neuroleptic treatment or anticholinesterase inhibitors. However this technique presents some variability in diagnostic performance representing the main limitation in the use of FDG-PET in clinical practice (Smailagic et al., 2015). According to this statement, it is important to develop new biomarkers.

4. Chronic traumatic encephalopathy in traumatic brain injuries

Traumatic brain injuries (TBIs) are a major public health problem with an incidence of 10 million people worldwide (Hyder et al, 2007) and over 1.7 million in the United States (Namjoshi et al., 2013).

Repetitive traumatic brain injuries can cause a neurodegenerative disorder called Chronic traumatic encephalopathy (CTE) characterized by the deposition of hyperphosphorylated Tau aggregates in the brain (Critchley, 1957). This condition has been among others described in players of contact sport (Gavett et al., 2011) as with professional American football athletes.

4.1. Clinical signs

A multitude of neurological and psychiatric symptoms are related to this pathology, including irritability, aggression, depression, memory loss (McKee et al. 2009), altered neuromuscular function, delayed reaction time, diminished postural control, altered gait and impulse control (Covassin et al., 2013; Howell et al., 2013; Reynolds et al., 2016; 2017). This disease can eventually progress to dementia (Gavett et al., 2010).

4.2. Risks factors

TBIs are clinically grouped by severity: mild, moderate and severe. Mild TBIs, also called concussion, is the most common form of TBI (~80-90% of cases (McCrorry et al., 2013)). Recent studies have revealed that extensive brain injury does not necessarily involve a single severe event but can be sustained through repeated sub-concussive injuries (sport contact such as American football) and causing CTE. Indeed, a recent study on rodents has demonstrated that repetitive mild TBIs led to more severe behavioral injuries than a single severe TBI and the effects of accumulation may be associated with increased inflammation in the brain (Gao et al, 2017).

Studies involving American football players revealed that the absorbed head impacts rises in an exponential fashion with age: around 80 hits (ages 7-8); >240 hits (ages 9-12); >1000 hits (high school); and 420-492 (college) (McKee et al, 2009; Center for disease control and prevention, 1997; Sports legacy institute, 2012). The National Football League (NFL) reported an average concussion incidence of 131.2 ± 26.8 concussions per year, a rate of 0.41 concussions per game (Pellman et al, 2004). This suggests that an individual sport player suffers multiple damaging head blows and/or concussions that may produce accumulative damage over the years.

4.3. Physiopathology

The pathophysiology of the TBI is complex and remains poorly understood. While the pathology typically begins with a mechanical focal trauma to the brain, it is rapidly followed by the activation of multiple molecular and neurochemical pathways that can lead to diffuse axonal injury (Sharp et al., 2014; Smith et al., 2013). Enhanced Tau protein phosphorylation occurs following severe neuronal injuries (Yang et al., 2017) and this hyperphosphorylation leads to the destabilization of microtubules, interrupting axonal transport and provoking synaptic dysfunction. The axonal injury may provide the initial perturbation of Tau, by promoting its dissociation from microtubules, facilitating its phosphorylation and aggregation. Altered Tau dynamics may then be exacerbated by the chronic persistent inflammatory response that has been shown to persist for decades following the initial impact (Collins-Praino et al., 2017).

Repetitive concussive events, like with the athletes engaged in high impact sports, increase the risk of CTE. CTE is characterized by accumulation in neurons, astrocytes and cell around blood vessels of varying amounts of A β and neurofibrillary tangles composed of the six isoforms of Tau hyperphosphorylated including both forms with 3 and 4 repeats of the microtubule binding domain (Smith et al., 2013; Mckee et al., 2013; 2016; Schmidt et al., 2001). Four progressive stages of CTE have been described following the abundance and distribution of Tau lesions (Mckee et al., 2013).

Tau Pathology in CTE follows a prion-like propagation. It appears along anatomical connections suggesting cell-to-cell transfer of toxic Tau through neuronal cell contacts (Goedert et al., 2017; Dujardin et al., 2014; Zanier et al., 2018).

Consequently, Tau plays a critical role in AD and CTE pathogenesis. Many advances are still needed for the therapeutic management of patients with these diseases. A first step is to detect these pathologies earlier and for this we need to have good *in vivo* tools for the detection of biomarkers, less invasive and sufficiently sensitive and specific, as in Positron Emission Tomography.

POSITRON EMISSION TOMOGRAPHY

Positron emission tomography (PET) is a functional imaging technique that tracks physiological processes at the molecular level by injecting a molecule labeled with a positron-emitting radioactive isotope or radionuclide. PET provides access to quantitative and dynamic measurements of biochemical parameters *in vivo* and enables a fast and easy assessment of various conditions. It has been reported as the most specific and sensitive technique for *in vivo* imaging of molecular interactions (Jones et al., 1996) as its performance exceeds the Single Photon Emission Computed Tomography (SPECT) (Bailey et al., 1994). Oncology is the main field of application of PET imaging, but it is also a technique of great interest for neuroimaging. PET is a non-invasive technique that has the advantage of being a translational technique that can be used from rodent to human and that allows to follow physiopathological processes or the effect of chronic treatment during longitudinal studies (Lancelot and Zimmer, 2010; Zimmer and Luxen, 2012). Coregistration of MRI and PET data enables the interpretation of functional data with localizing high-resolution structural information, leading to the prevalence of PET imaging in clinical applications (Anand et al., 2009).

1. Principles of PET imaging

A PET study begins by the injection of a radioactive tracer. After injection, the subject is placed within the field of view of the scanner where detectors can register incident gamma rays. The radionuclide decays and emits positrons, which then annihilate with an electron to produce two photons travelling in opposite directions. The gamma rays emitted can be detected by the scanner's detectors. The emitted positrons rapidly lose their energy in tissue, so the annihilation event is usually very close to the site of positron emission. Detection of the two coincident gamma rays defines a line, which intersects the position of the annihilation event. These "coincidence events" can be stored in arrays corresponding to projections through the patient, generating a map of the distribution of the radiotracer, creating a PET image.

The raw data collected by the PET scanner is then mathematically reconstructed to produce tomographic images of *in vivo* concentration of radiotracer (Bailey et al., 2006; Cherry et al., 2012).

1.1. Radiotracers

The synthesis of the radiotracer requires a precursor and a radionuclide. A precursor is a molecule with a structure close to the tracer with a group that can be substituted by the radioactive element. This design has to allow the radiotracer to behave the same way as the original molecule and not interfere with the physiologic process that is being imaged. The radionuclide of interest is produced by a particle accelerator, a cyclotron, which operates by the combined action of an electric field and a magnetic field.

From the radionuclide and the precursor, the radiosynthesis allows to obtain the radiotracer. At the end of the radiosynthesis, the product is purified and a quality control is assured essentially by High Performance Liquid Chromatography (HPLC). The specific activity (radioactive activity per quantity of molecules) must be high enough to avoid the dilution with non-radiolabeled molecules (Passchier et al., 2002).

The most commonly used labelling radionuclide in PET imaging is fluorine 18 (^{18}F). Its half-life of 109 minutes is long enough to perform an imaging study and short enough to limit the radiation exposure.

The radiotracer undergoes radioactive decay inside the body leading to a cascade of physical interactions.

1.2. Physical interactions

The radionuclide has a nucleus rich in protons. With this excess of positive charges it is unstable and decays spontaneously to a stable state by the transformation of a proton into a neutron. This results in the emission of a positron (e^+) and a neutrino and is called β^+ disintegration (Figure 5). The main radionuclides β^+ used in PET are carbon 11 (^{11}C), fluorine 18 (^{18}F), nitrogen 13 (^{13}N) and oxygen 15 (^{15}O).

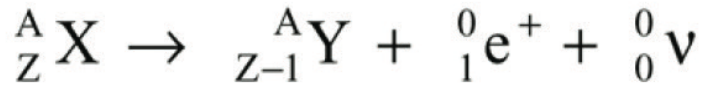
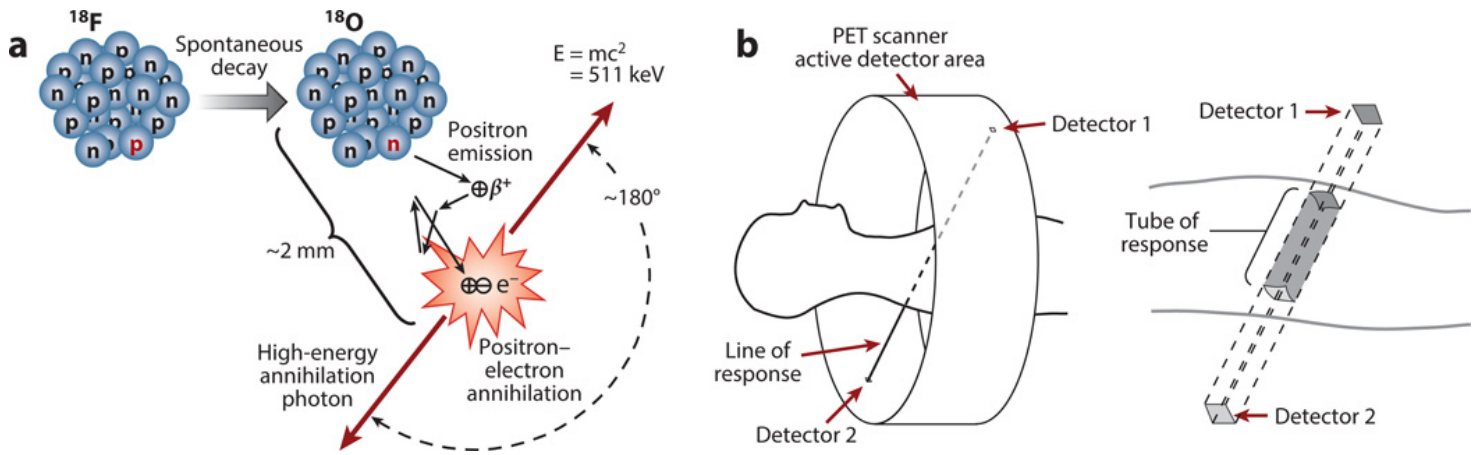


Figure 5: Nuclear reaction of β^+ type disintegration.

When incorporated into an organic material, the positron emitted by radioactive decay travels a distance of about one-two millimeters and annihilates itself by interacting with an electron to emit two gamma photons of 511 KeV at 180°. These photons are detected simultaneously by two opposite detectors of the PET camera (Figure 6). A PET scanner contains blocs of photons detectors arranged in concentric rings around the object to be imaged. They absorb the incident photon and convert it into visible light photons. A photomultiplier tube detects these photons and produces a proportional electric signal that contains information about the time when the incident photon was detected, its energy, and its position. Only a pair of colinear photons each at 511 keV arriving to the detectors at the same time constitute a counted event. The recording of these pairs of photons from the same annihilation on a line connecting two detectors constitutes the raw signal of the PET, stored in list-order mode of arrival. The two detectors, and the 3D tube between them, are commonly called the Line of Response (LOR). The constitution of the 3D quantitative image of the distribution of the radioactivity in the organism is carried out by tomographic reconstruction. The PET data collected by the scanner is a matrix indexing every possible LOR and saves its assigned count reflecting the distribution of the radiotracer along that LOR. Image reconstruction algorithms transform this matrix into a 3D image and some correction techniques can be applied to yield a quantitative image.



Taken from Vaquero (2015)

Figure 6: Principles of PET imaging. (a) The radionuclide fluorine-18 (^{18}F) spontaneously decays to the stable radionuclide oxygen-18 (^{18}O) by converting a proton to a neutron, leading to the emission of a positron. *Via* random scattering on a short distance the positron encounters its antiparticle, the electron. The resulting annihilation of both particles generates two anticollinear 511 keV annihilation photons. (b) The patient is surrounded by a ring of detectors. When two annihilation photons are detected the two points of interaction define a line of response schematically representing the ensemble of coincidences that fall inside the tube of response (Vaquero et al., 2015).

PET imaging provides information at the molecular level but is not accurate for the anatomical identification of areas highly concentrated in radioactivity. For this reason, PET cameras can be coupled with imaging techniques that provide anatomical information, such as X-ray CT (Computed Tomography) and MRI (magnetic resonance imaging).

The multitude of radiotracers and their different abilities explains how PET imaging is prevalent in clinical applications due to its ability of quantifying the imaged function. For example, in oncology PET imaging is valuable for diagnostics and for patient follow-up post-treatment (Jones et al., 2017) by localizing tumors (Dechow et al., 2010) and exploring the presence of cancer metastasis (Rajendran et al., 2003).

PET imaging is also useful in cardiology where it enables the measurements of myocardial perfusion (Driessen et al., 2017, Grüner et al., 2011) monitoring patients' response to therapy, lifestyle changes or the comprehensive evaluation of coronary artery disease (CAD) allowing subjects to access to preventive therapy (Schindler et al., 2010). PET imaging has also a high diagnostic value in assessing the myocardial viability of subjects with known CAD (Slart et al., 2006).

Since the early 1980s, the development of hundreds of brain radiotracers has greatly contributed to the understanding of the brain and psychiatric or neurological pathologies. As it is the topic of this dissertation, we are going to look into these clinical applications in neurology in more details.

2. Clinical applications in neurology

In standard medical care, [^{18}F]-FDG, an analogue of glucose, is employed to explore the regional glucose uptake testifying increased glucose entry and its intracellular accumulation. In the most common neurological studies, PET imaging has been used to indirectly evaluate neuronal activity by measuring glucose consumption through the fluorinated analogue [^{18}F]-FDG during neurodegenerative pathologies (Zimmer et al., 2012). [^{18}F]-FDG PET is a biomarker for neuronal degeneration in dementia (McKhann et al., 2011), its spatial distribution enables clinicians to make early diagnosis and to distinguish between different subtypes of dementia (Shivamurthy, et al. 2015).

Among the use of PET for neurodegenerative diseases, [^{18}F]-DOPA is very useful in the diagnostic of Parkinson Disease which is clinically challenging (Ibrahim et al., 2016).

In AD, *in vivo* imaging of amyloid deposits with [^{18}F]-labeled radiopharmaceuticals (18F-florbetapir, 18F-florbetaben and 18F-flutemetamol) has been shown accurate for discriminating AD from healthy controls and some other forms of dementia. However, the correct place of the PET amyloid imaging in the diagnostic workflow of dementia is still a debated issue (Filippi et al., 2018).

In epilepsy, [¹⁸F]-FDG PET permits the localization of the seizure foci (Hwang et al., 2001) needed in case of surgical therapy (Chassoux et al., 2010; Lee et al., 2009). Also, [¹¹C]-flumazenil PET is able to detect epileptic foci due to reduced binding of the GABA receptor inhibitory ligand (Hammers et al., 2002).

PET imaging can also be used in the diagnostic and management of brain cancers in addition with other imaging techniques as MRI. An increased [¹⁸F]-FDG uptake is indicative of cancer in the brain, and in the case of gliomas, it allows to assess the tumor grade and the survival rates (Padma et al., 2003). Nowadays, non-FDG radiotracers are widely tested and among them [¹¹C]-MET (methionine) and [¹⁸F]-FET (fluoroethyl-l-tyrosine) appear to be the most useful dedicated glioma radiotracers (Herholz et al., 2017; Gulyas et al., 2012).

During cerebral hypoxia-ischemia, dynamic changes in glucose metabolism occurring during and after injury, may be detectable in PET (Ouyang, et al., 2015, Heiss et al., 2000). PET is not systematically included in the diagnostic assessment of neurovascular disease such as Stroke (vasculo-cerebral accident), however it can help to determine the potentially recoverable tissues and identify affected regions in ischemic stroke (Heiss et al., 2000).

PET imaging of the brain covers many other areas as most of the brain radiotracers are specific ligands of proteins including enzymes, transporters and neurotransmitter receptors (Zimmer et al., 2012). Much effort has recently been put into the development of PET radiotracers for *in vivo* quantification of Tau protein, not FDA (Food and Drug Administration)-approved yet.

3. Tau protein in PET imaging

PET has proved to be an important tool for the detection of A β aggregates in the brain allowing a better diagnosis and clinical management of AD (Ariza et al., 2015; Rabinovici et al., 2019). However, neurological deficits and clinical signs of AD do not correlate well with amyloid pathology in contrast to Tau pathology. In AD, the

cognitive decline level is correlated to the spreading of Tau neurofibrillary tangles across the brain (Pontecorvo et al., 2017). Phospho-Tau (p-Tau) may be a relevant target of therapies for AD. This aggregation of Tau protein is common in tauopathies (Buée et al., 2000) supporting the need for the development of Tau-targeting treatments.

Several PET tracers targeting Tau deposits with a high binding affinity and selectivity have been developed (Okamura et al, 2016) and tested in humans. They are still not used in clinic but they are widely used in research. They contributed to improve diagnostic accuracy and understanding of the pathophysiology of AD (Villemagne et al, 2015; 2016). [¹⁸F]-AV-1451 (previously known as flortaucipir and T807) was recently developed for PET imaging of paired helical filaments of hyperphosphorylated Tau. Patients clinically diagnosed with dementia of AD type and MCI exhibit brain areas with a higher [¹⁸F]-AV-1451 signal than cognitively normal individuals. These regions are known to contain an elevated burden of Tau lesions in AD (Brier et al., 2016; Cho et al., 2016; Johnson et al., 2016; , Pontecorvo et al., 2017, Scholl et al., 2016; Wang et al., 2016).

For individuals at high risk of CTE, as with American football players occurring mild repetitive TBIs, Tau PET has the potential to advance our understanding of disease mechanisms and provide early stage diagnostic and prognostic biomarkers.

GOALS

Until very recently, it was only possible to see Tau aggregates in post-mortem by immunohistochemistry, because Tau deposits are mainly intracellular and it may be more difficult to access *in vivo*. Many neurological diseases are related to abnormal Tau. It becomes critical to be able to visualise this protein *in vivo*.

In that context it is necessary to develop new biomarkers to detect tauopathies earlier. Once this is done, interventions that decrease the intracerebral Tau burden could potentially be an important clinical advance. This could allow to treat these pathologies more quickly in order to limit the importance of neurological deficits.

The work carried out during this thesis aims to promote the use of non-invasive imaging techniques to explore the distribution of the Tau protein *in vivo* in the context of two taupopathies, AD and CTE.

The first experimental part is to study in phosphor screen autoradiography post-mortem the pattern binding of the most common used Tau radioligand in PET research, [¹⁸F]-AV-1451 in slices from AD and CTE brains. We compared the behaviour of this radiotracer with two novel second generation tracers, [¹⁸F]-MK-6240 and [¹⁸F]-PI-2620.

The second experimental part is the evaluation of the usefulness *in vivo* of [¹⁸F]-AV-1451 in the diagnostic and follow-up of patients with AD ensuing a potential treatment decreasing the intracerebral Tau burden.

The third experimental part is the use of the Tau PET imaging *in vivo* in a population of American football players to help the early detection of CTE and to have a better understanding of this pathology.

**PART 2: Autoradiographic characterization of
p-Tau PET tracers [¹⁸F]-AV-1451, [¹⁸F]-
MK-6240, [¹⁸F]-PI-2620 in AD and CTE**

PROBLEM STATEMENT

Tau aggregates are a pathological hallmark in such tauopathies as AD and CTE. Recently, several radiotracers were reported to show potential for imaging p-Tau by PET imaging *in vivo*. This gave the opportunity of utilizing them to improve diagnostic in tauopathies and to quantify Tau pathology burden in the human brain *in vivo*, allowing a following up of patients after potential treatments.

[¹⁸F]-AV-1451 has been described as the first promising ligand for detection of 3R/4R Tau isoform accumulation in the brain (Xia et al., 2013). Indeed, in AD patients compared to controls, an increased uptake of [¹⁸F]-AV-1451 has been observed in cortical regions containing NFTs (Brier et al., 2016; Cho et al., 2016; Johnson et al., 2016; Pontecorvo et al., 2017; Scholl et al., 2016; Wang et al., 2016). The same distinction has been discerned in regions where Tau lesions are expected between controls group and patients with tauopathies non-AD (Brier et al., 2016; Cho et al., 2016).

As a Tau PET radiotracer of first generation, [¹⁸F]-AV-1451 showed high affinity to the 3R/4R Tau isoform (Villemagne et al. 2015; 2018; Lois et al. 2019) with however some limitations as off-target binding as well as ante-mortem *versus* post-mortem inconsistencies (Villemagne et al. 2015; 2018; Harada et al., 2018; Lois et al., 2019). Second generation selective Tau PET radiotracers, such as [¹⁸F]-PI-2620 and [¹⁸F]-MK-6240 have been preclinically evaluated and demonstrated high affinity, selectivity and specificity so far (Lois et al. 2019).

The aim of our study was to investigate [¹⁸F]-AV-1451 binding patterns in pathologically confirmed AD and CTE post-mortem tissue using phosphor screen autoradiography. Also, we compared the binding patterns of [¹⁸F]-AV-1451 with [¹⁸F]-MK-6240 and [¹⁸F]-PI-2620, to verify if this new generation of Tau PET tracer could be more useful as biomarkers in AD and CTE than first generation tracers.

MATERIALS AND METHODS

1. Autoradiography principles

In vitro Autoradiography is a semi-quantitative histochemical technique aims to detect the anatomical distribution of a molecule of interest coupled to a radioactive isotope on tissue sections. The method is based on the specific binding of a radioligand to its target. The frozen tissue sections are incubated with the radioligand solution and brought into contact with a phosphor screen, which allows the visualization of the binding sites of the molecule of interest. Phosphor screens are ideal for imaging short-lived radionuclides, where expose time are limited, such as [¹¹C] and [¹⁸F] used to label radioligands for PET.

2. Tissue samples

In these studies are included postmortem brain, retina tissue samples from the Massachusetts and the Boston University (BU) Alzheimer's Disease Research Center (ADRC) Brain Bank.

Blocks of frozen tissue from AD, CTE and age-matched controls free of neurodegenerative disease subjects were embedded in optimal cutting temperature compound and cut into 10µm thick slices in a cryostat (Thermo-Shandon SME Cryostat). Then they were mounted on Histobond adhesion glass slides (StatLab, TX) and stored at -80°C.

3. Radiotracers

[¹⁸F]-AV-1451, [¹⁸F]-MK-6240 and [¹⁸F]-PI-2620 (Figure 7) have been used for phosphor screen autoradiography. It has been demonstrated that they all target the 3R/4R Tau isoform (Tiepol et al., 2019).

[¹⁸F]-AV-1451 and [¹⁸F]-MK-6240 were synthesized as previously described by our Center (Shoup et al., 2013; Collier et al., 2017) and experiments were performed using aliquots from material prepared for *in vivo* imaging on the same day. [¹⁸F]-PI-2620 was produced onsite in our Center specifically for this experiment the same day.

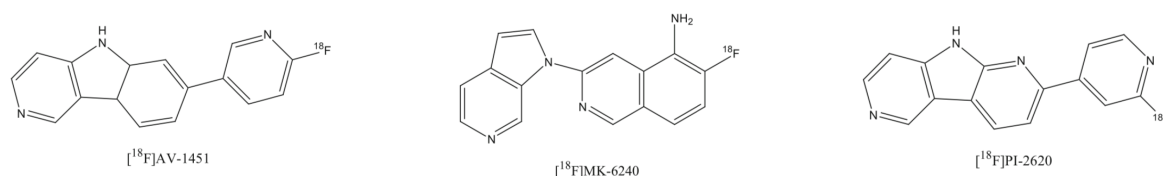


Figure 7: Chemical structure of the Tau PET radioligands [¹⁸F]-AV-1451, [¹⁸F]-MK-6240 and [¹⁸F]-PI-2620 (Tiepol et al., 2019).

4. Phosphor screen autoradiography

Frozen brain sections were fixed in 100% methanol at room temperature for 20 min and then transferred to a bath containing high specific activity of the radiotracer in 10mM PBS with a radioactivity concentration of approximately 20 μ Ci/ml (0,74 MBq/ml) for [¹⁸F]-AV-1451 and 10 μ Ci/ml (0,37 MBq/ml) for [¹⁸F]-MK-6240 and [¹⁸F]-PI-2620.

Adjacent brain slices were set in a blocking condition bath with the tracer unlabeled. An appropriate cold dose of each tracer was added to saturate all available specific binding sites of Tau, 500 nM of MK-6240 and 1 μ M of AV-1451 or PI-2620 (Xia et al., 2013).

After incubation for 60 minutes, sections were washed to remove unbound radiotracer as following : 10 mM PBS for 1 min, 70% ethanol/30% PBS for 2 min, 30% ethanol/70% PBS for 1min, and 100% 10 mM PBS for 1 min.

Sections were then air dried before transferring to a storage phosphor screen (MultiSensitive Phosphor Screen, PerkinElmer Life and Analytic Sciences, Shelton, CT) that had been photobleached by being exposed to a white light for at least 15 minutes. The slides and phosphor screen were enclosed in an aluminum film cassette and set in a dark area overnight.

Under red lighting conditions, the slides were removed from the exposed screen, which was mounted to the carousel of the digital imaging system (Cyclone Plus Storage Phosphor Scanner, PerkinElmer Life and Analytic Sciences). Scanning of screens was controlled by the manufacturer's OptiQuant software package using the highest available resolution of 600 dpi (approximately 50 μm sampling interval). Images from adjacent brain slices incubated in the unblocked and blocking conditions were compared to determine total and non-specific binding of the radiotracer in the tissue. All experiments were ran in triplicates.

To eliminate the possibility that the ethanol washing steps may have removed some weaker tracer binding, parallel experiments with a radioactivity concentration of approximately 1 $\mu\text{Ci/ml}$ (0,037 MBq/ml), an incubation of 90 minutes and only 100% 10 mM PBS in the washing conditions were also performed.

RESULTS

1. Autoradiography of AD cases

In AD cases, phosphor screens autoradiography experiments confirmed strong binding of AV-1451 to brain slices containing neurofibrillary tangles (Figure 8). This binding was blocked after incubating the slides with 1 μ M unlabeled AV-1451, demonstrating the selectivity of the signal. No AV-1451 signal has been noticed in slices from control cases with the exception of binding to layer II entorhinal cortex showing age-related tangles, the substantia nigra and the choroid plexus demonstrating off-target binding. AV-1451 binding was absent in the cerebellum, a region free of tangles in AD.

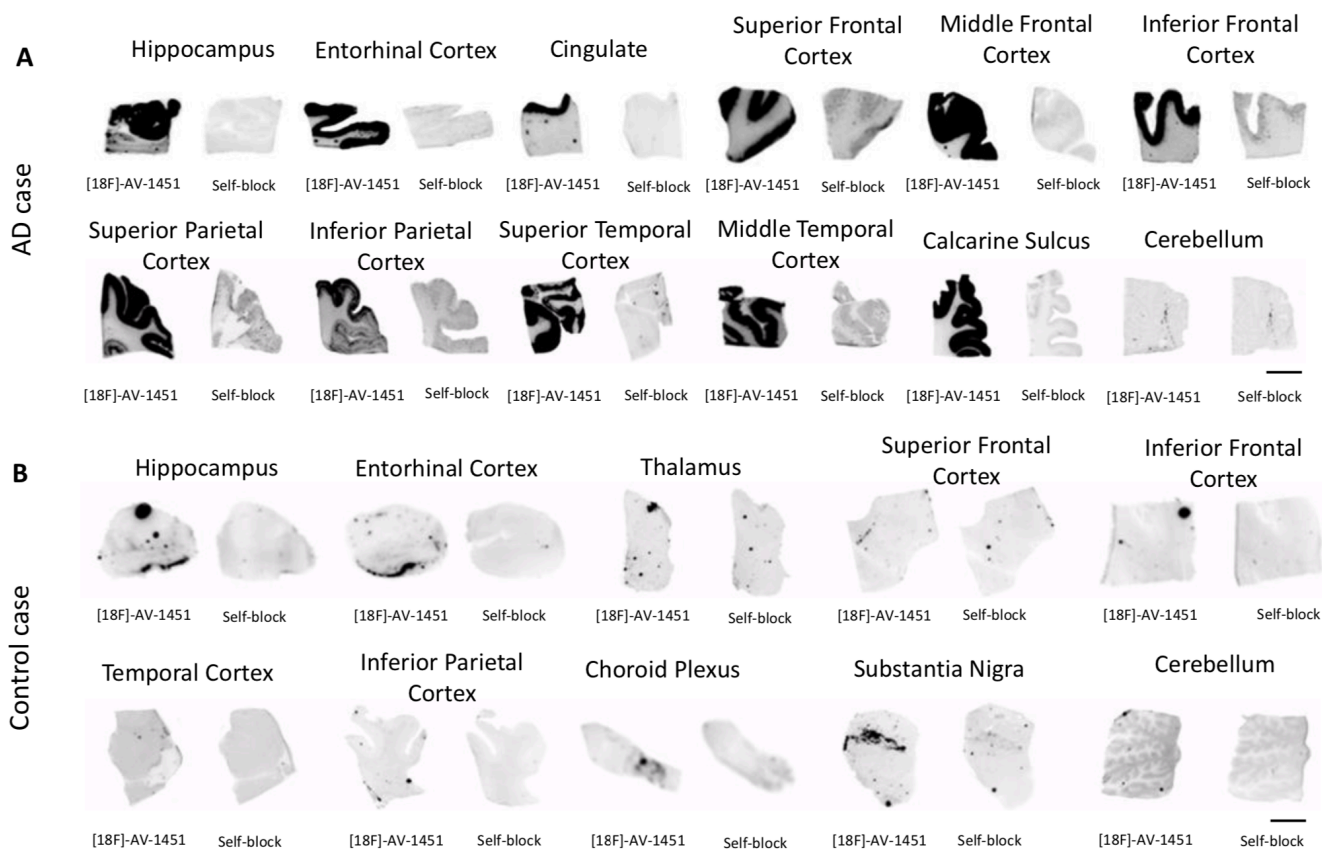


Figure 8: [18F]-AV-1451 phosphor screen images of brain slices from AD and control cases. Strong [18F]-AV-1451 binding was observed in cortical regions containing NFTs from AD brains. The signal was blocked by adding 1 μ M unlabeled AV-1451. No [18F]-AV-1451 signal was detected in the cerebellum (A). Slices from a control case free of pathology did not show detectable [18F]-AV-1451 binding. [18F]-AV-1451 binding was confined to incidental age-related PHF-tangle pathology in superficial layers of entorhinal cortex, substantia nigra and choroid plexus in control serving as internal positive control for the experiments (B). Scale bar=1 cm.

According to phosphor screen autoradiography experiments, the binding patterns of [18F]-MK-6240 (Figure 9) and [18F]-PI-2620 (Figure 10) were similar to those reported for [18F]-AV-1451 with a strong binding to neurofibrillary tangles in AD.

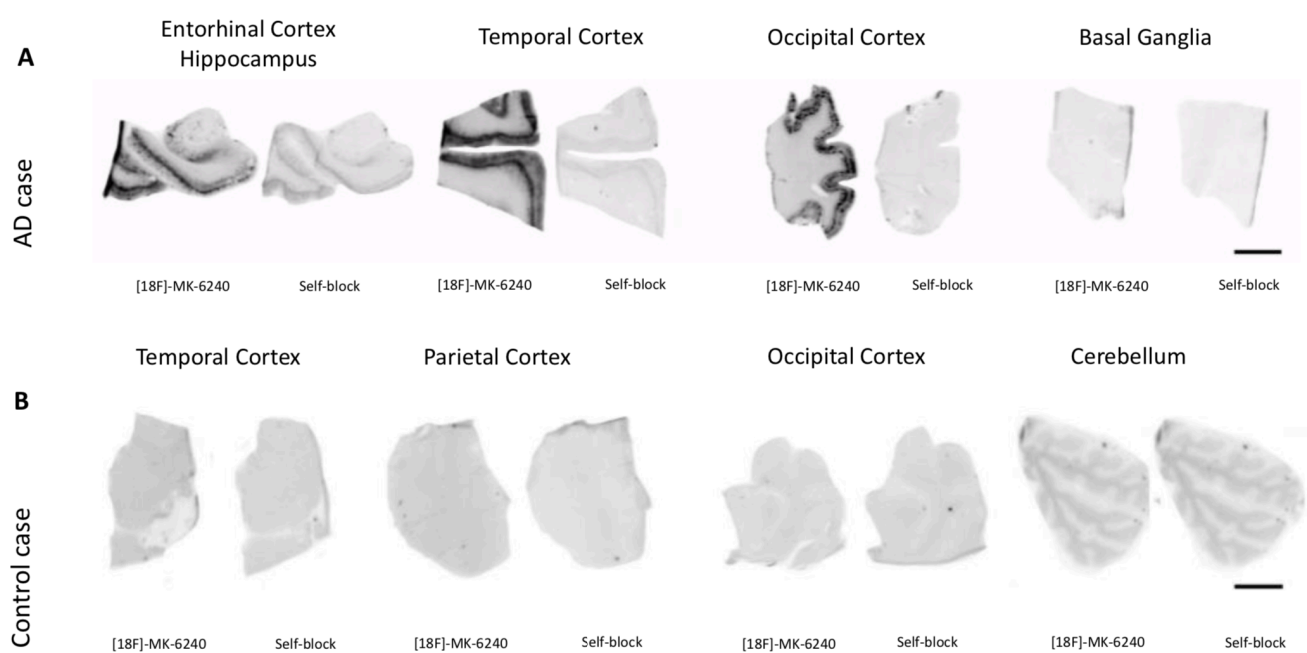


Figure 9: [18F]-MK-6240 phosphor screen images of brain slices from AD and control cases. From AD brains, strong [18F]-MK-6240 signal was detected in cortical regions containing tangles. No signal was observed in basal ganglia, a region free of tangles. Unlabeled MK-6240 permitted to block the signal (A). Slices from a control case free of pathology did not show detectable binding (B).

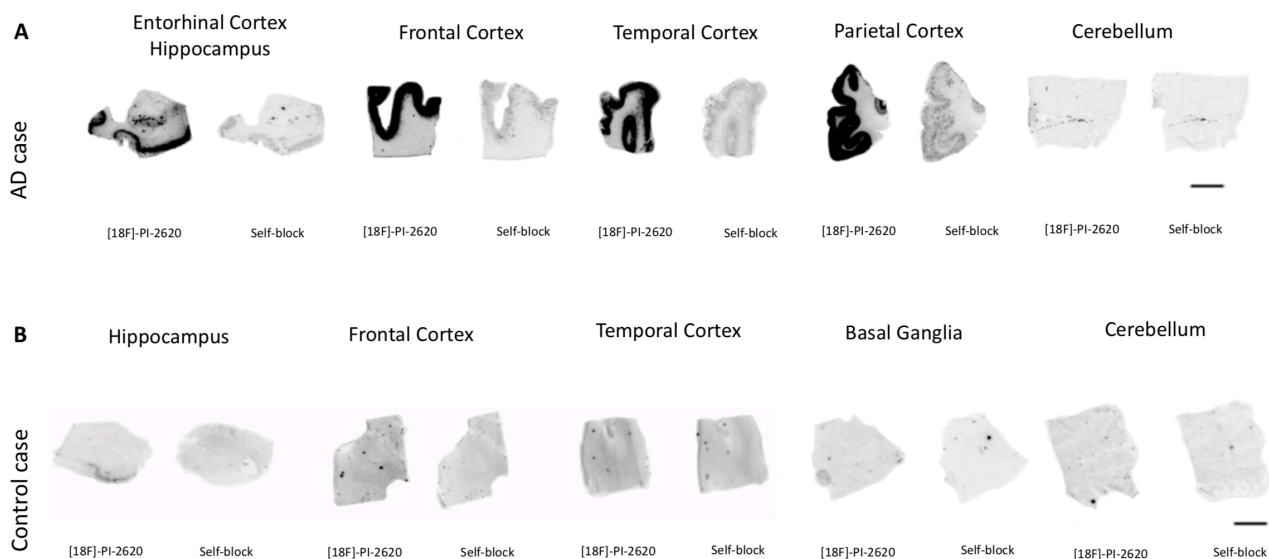


Figure 10: [18F]-PI-2620 phosphor screen images of brain slices from AD and control cases. Strong [18F]-PI-2620 binding was detected in cortical regions containing NFTs from AD brains. The signal was blocked by adding 1 μ M unlabeled PI-2620. No [18F]-PI-2620 signal was perceived in the cerebellum, area free from tangles (A). Slices from a control case free of pathology did not show detectable [18F]-PI-2620 binding. [18F]-PI-2620 binding was remarked in the hippocampus (age-related PHF-tangle pathology) serving as internal positive control for the experiments (B). Scale bar=1 cm.

2. Autoradiography of CTE cases

In the CTE cases, no autoradiographic signal could be detected with AV-1451 across multiple cortical regions known to contain Tau aggregates (Figure 11).

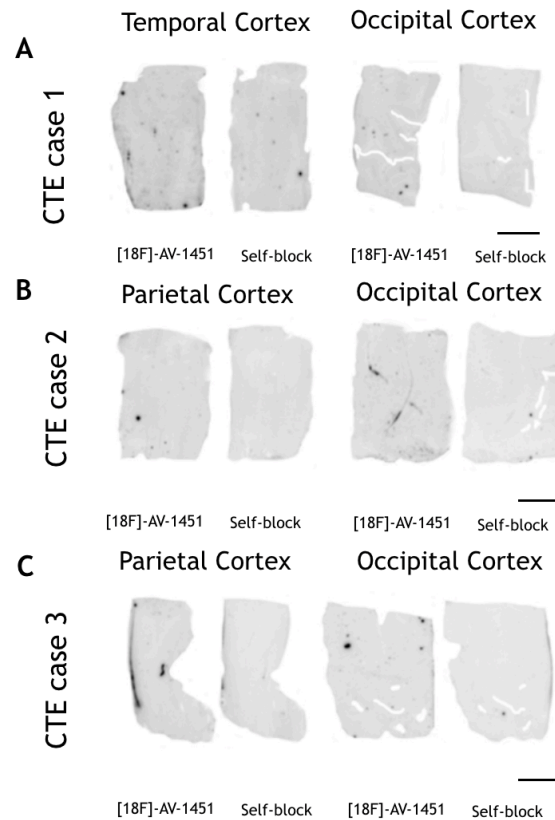


Figure 11: [18F]-AV-1451 phosphor screen images of brain slices from CTE cases. No [18F]-AV-1451 binding was detected in CTE slices. Scale bar = 1cm.

Like AV-1451, PI-2620 (Figure 12, A) and MK-6240 (Figure 12, B) seem to have a relatively low affinity for Tau aggregates in non-AD tauopathies as CTE. Indeed, no detectable binding with these two tracers have been identified in brain slices containing non-PHF Tau aggregates from CTE cases.

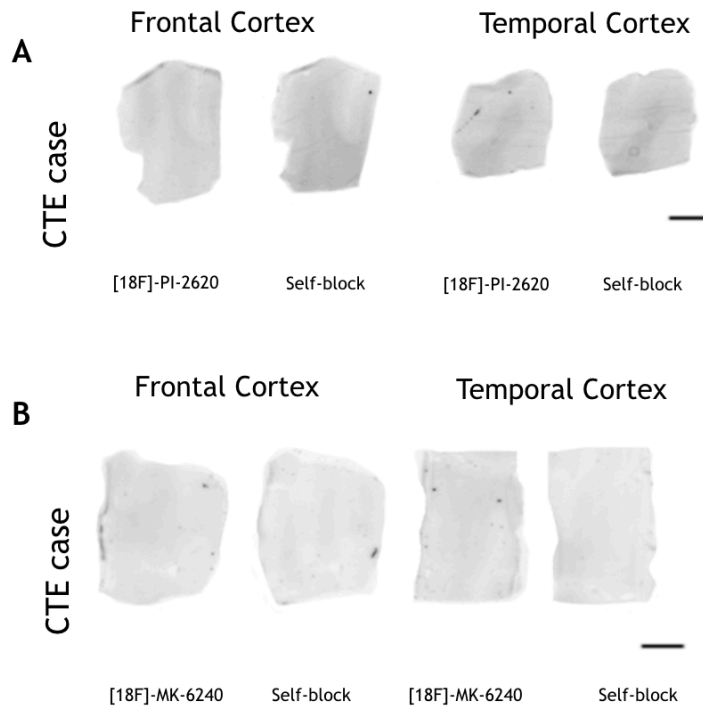


Figure 12: $[^{18}\text{F}]\text{-PI-2620}$ and $[^{18}\text{F}]\text{-MK-6240}$ phosphor screen images of brain slices from CTE cases. No $[^{18}\text{F}]\text{-PI-2620}$ (A) and $[^{18}\text{F}]\text{-MK-6240}$ (B) binding were detected in CTE slices. Scale bar = 1cm.

Parallel autoradiographic experiments performed with adjacent tissue slices and eliminating ethanol from the washing conditions yielded identical results, avoiding the possibility that the ethanol washing steps may have removed some weaker tracer binding (Figure 13).

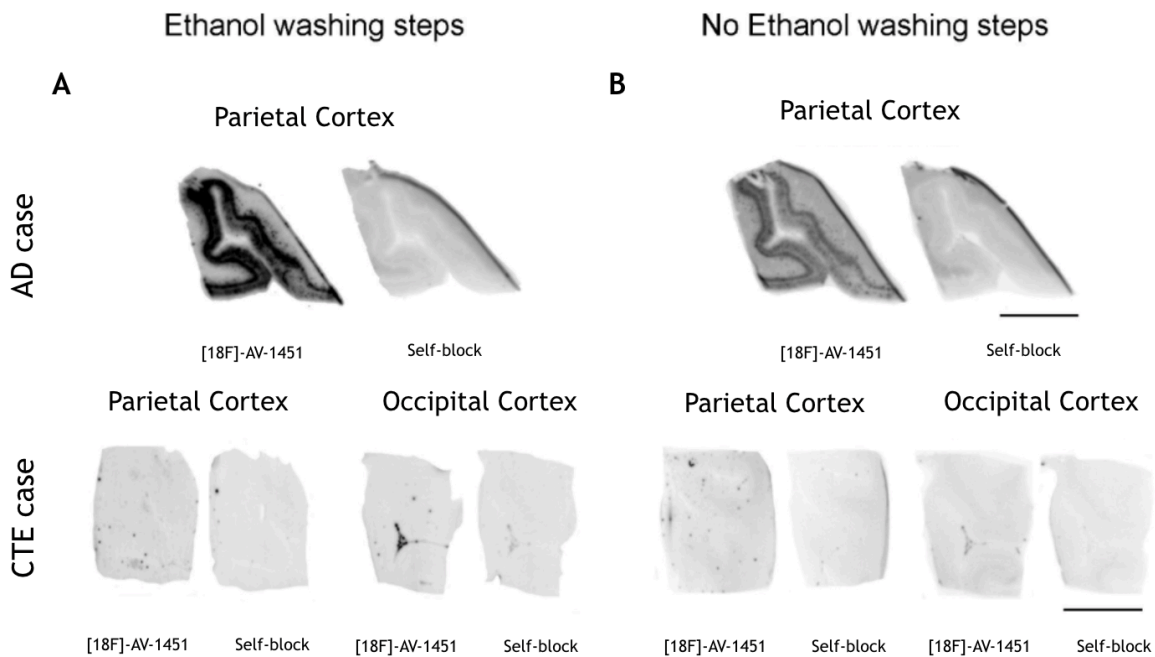


Figure 13: Representative images of phosphor screen autoradiography experiments with and without ethanol washing steps. The results of the protocol using ethanol in the washing steps are displayed on A, the ones from the protocol avoiding the use of ethanol in the washing steps are shown on B. Identical results were observed in comparison of both protocols using adjacent brain tissue slices. A strong $[^{18}\text{F}]\text{-AV-1451}$ binding signal was observed in cortical regions containing tangles in AD but no $[^{18}\text{F}]\text{-AV-1451}$ binding was detected in CTE slices with the exception of the off-target to leptomeningeal melanocytes. Scale bar = 1cm.

3. Autoradiography of off-target binding

MK-6240 and PI-2620 exhibit similar off-target binding patterns than described by $[^{18}\text{F}]\text{-AV-1451}$ (Marquié et al., 2015). Indeed, a strong off-target binding was present in midbrain slices containing substantia nigra, retinal pigment epithelium, brain metastatic melanoma, brain slices containing parenchymal hemorrhages and extracutaneous meningeal melanocytes (Figure 14).

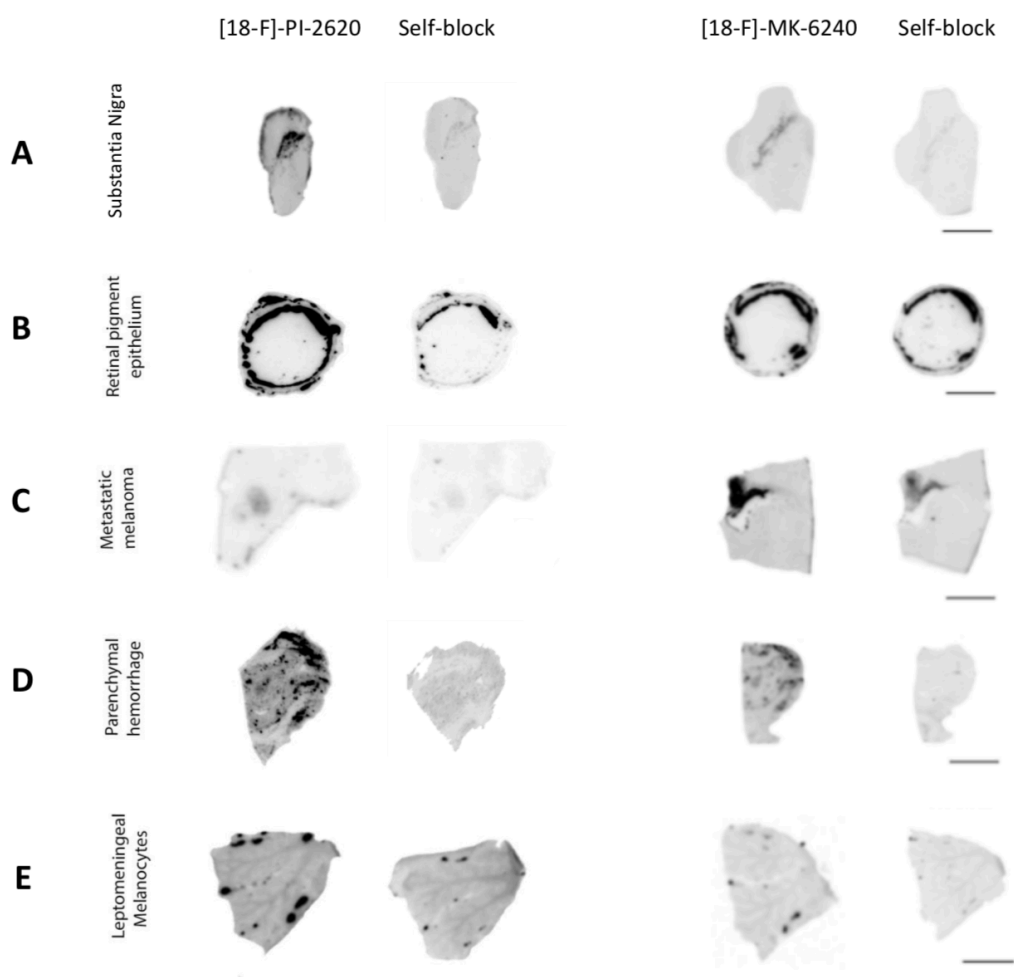


Figure 14: [¹⁸F]-PI-2620 and [¹⁸F]-MK-6240 phosphor screen images off-target binding. Strong [¹⁸F]-PI-2620 and [¹⁸F]-MK-6240 signal were discerned in neuromelanin-containing neurons of substantia nigra (A), melanin containing granules in the retinal pigment epithelium (B), malignant melanocytes in metastatic melanoma (C), parenchyme hemorrhage (D) and extracutaneous leptomenigeal melanocytes (E). [¹⁸F]-PI-2620 phosphor screen autoradiography images are displayed in (A-E) left panels. [¹⁸F]-MK-6240 phosphor screen autoradiography images are displayed in (A-E) right panels. Scale bar=1 cm.

DISCUSSION

Recently multiple novel PET tracers have been reported allowing the detection of Tau pathology *in vivo* for human. However, for the correct interpretation of the PET images it is essential to validate the biological targets and to identify potential off-target binding of these imaging agents.

Tau tracers in AD

Using autoradiography approaches in postmortem brain tissue samples we have seen that [¹⁸F]-AV-1451 has a high binding affinity for Tau aggregates in the form of NFTs in AD.

We have also carefully characterized the autoradiographic binding patterns of novel Tau tracers [¹⁸F]-MK-6240 and [¹⁸F]-PI-2620. Some early studies point to a higher *in vivo* retention of these radioligands in neocortical and medial temporal brain regions of AD patients compared to elderly cognitively normal individuals (Lohith et al., 2018; Kroth et al., 2019). Because these ligands are already being incorporated into clinical trial research, validation studies are crucial to evaluate the potential usefulness of these ligands as a reliable marker of human brain Tau lesions. In an attempt to advance towards that goal, we applied [¹⁸F]-MK-6240 and [¹⁸F]-PI-2620 phosphor screen to the study of a series of autopsy samples from individuals with a definitive diagnosis of AD and control brains free of neurodegenerative pathology. Overall, [¹⁸F]-MK-6240 and [¹⁸F]-PI-2620 autoradiographic binding patterns in AD were really similar to those of [¹⁸F]-AV-1451.

In our research groups some additional studies have been carried out, as autoradiography using a fine grain nuclear emulsion and immunohistochemistry. Regional and laminar autoradiographic patterns of distribution of [¹⁸F]-MK-6240 (Aguero et al., 2019) (Annexe 1) and [¹⁸F]-PI-2620 closely matched those of classic PHF-tangles in AD brains (Arnold et al., 1991; Lewis et al., 1987), confirming that [¹⁸F]-MK-6240 and [¹⁸F]-PI-2620 labeled lesions were NFTs. Also, PHF-tau load was

determined by immunohistochemistry, showing concomitant signal with the autoradiographic pattern (Aguero et al., 2019) (Annexe 1). This suggests that these lesions are the main pathological substrate of [¹⁸F]-MK-6240 and [¹⁸F]-PI-2620 binding.

To accurately interpret Tau neuroimaging of these radioligands, the correlation between *in vivo* retention and postmortem *in vitro* binding is the gold standard. We are running in our group this comparison of *in vivo* measures of [¹⁸F]-AV-1451 relative standardized uptake values (SUVR) as measured by PET in multiple region of interests (ROIs) with autoradiographic signal in matching ROIs at postmortem. Those results are also going to be correlated to quantitative Tau measurements as burden of Tau aggregates in immunostained tissue and measurements of different soluble Tau species in whole tissue homogenates and synaptic/cytosolic enriched fractions as detected by Western Blot and ELISA.

It has been demonstrated that [¹⁸F]-AV-1451 has a significantly higher affinity for Tau aggregates in the form of NFTs in AD compared to Tau aggregates in other tauopathies non-AD (Lowe et al., 2016; Marquie et al., 2015; 2017; Sander et al., 2016). This justifies the closer look by autoradiography of CTE cases to have a better understanding of the usefulness of these radioligands for the detection of Tau burden in this pathology.

Tau tracers in CTE

The development of novel neuroimaging biomarkers potentially capable of improving the diagnosis of CTE and monitoring the progression of the disease would be highly beneficial (Sundman et al., 2015; Zetterberg et al., 2016). While Tau PET tracer [¹⁸F]-AV-1451 has recently shown great potential in AD with binding to NFTs with PHF conformation, the utility of this ligand in assessing the Tau burden in CTE remains uncertain.

We have examined the postmortem binding patterns with phosphor screens autoradiography of [¹⁸F]-AV-1451 in multiple ROIs from autopsy-confirmed CTE cases. Our results showed negligible binding of [¹⁸F]-AV-1451 in brain regions with a high burden of Tau lesions. In contrast, AD brains included here as positive control,

exhibited strong [¹⁸F]-AV-1451 binding signal as previously reported (Xia et al., 2013; Lowe et al., 2016; Marquie et al., 2015; 2017; Sander et al., 2016;).

In addition with these findings, our research groups have performed some high resolution nuclear emulsion autoradiography experiments showing no detectable silver grain accumulation overlapping with CTE Tau aggregates seeing in immunohistochemistry. Also, they have demonstrated that the pathological Tau burden in these CTE cases, quantified by immunostaining, significantly correlated with the levels of soluble Tau phosphorylated (Western blotting), and with Tau seeding activity in the same ROIs (Marique et al., 2019) (Annexe 2).

These observations suggest that *in vivo* neuroimaging [¹⁸F]-AV-1451 may not have sufficient sensitivity for detecting and quantifying Tau pathology in CTE.

We also studied by phosphor screen autoradiography, the binding patterns of the two novel PET tracers [¹⁸F]-MK-6240 and [¹⁸F]-PI-2620 for CTE in post-mortem. Our results confirmed that [¹⁸F]-MK-6240 and [¹⁸F]-PI-2620 avidly bound with significantly stronger affinity and selectivity to Tau aggregates containing all six isoforms of Tau (3R and 4R) with PHF ultrastructure in AD slices, they did not bind to Tau aggregates containing all six isoforms of Tau (3R and 4R) in CTE slices. These findings strongly suggest that Tau in tangles of AD has a unique conformation that is recognized by these radioligands which are behaving similarly than AV-1451.

The overall utility of these tracers as an *in vivo* biomarker in CTE can seem very limited from these *in vitro* results. Despite Tau aggregates in CTE and AD are both containing 3 and 4 repeat isoforms of Tau, our results suggest that [¹⁸F]-AV-1451 differs in its affinity for Tau burden from these two diseases. In accordance with this hypothesis, recent studies demonstrated that Tau filament structures in CTE are distinct from those of AD (Falcon et al., 2018; 2019) with a conformation of the β -helix region creating a hydrophobic cavity that is absent in AD Tau filaments. Nonetheless, it has been also demonstrated that the filaments structures *in vivo* are distinct from those formed *in vitro* (Falcon et al., 2019). Another limitation in this study is that *in vitro* autoradiography of human brain tissue is a reliable method to assess the binding selectivity of radioligands however, the non physiological assay conditions could affect the results by changing the native conformation of target and non-target proteins. In order to conclude on the usefulness of p-Tau PET imaging

with those tracers in CTE, further investigations are required. Now that the conformation of the p-Tau protein in CTE has been well defined, a new generation of p-Tau PET tracer specifically made to recognise this conformation could be helpful.

Tau tracers and off-target binding

[¹⁸F]-AV-1451 have shown a strong affinity to PHF-tau aggregates in AD brains, and those that form as a function of age. However this compound show limited affinity for some isoforms of Tau and also suffers from off-target binding that can lead to a misinterpretation of imaging data.

[¹⁸F]-AV-1451 exhibits *in vivo* strong off-target binding to neuromelanin (in pigmented brainstem regions), melanin (in leptomeninges), calcifications in choroid plexus, iron-associated regions as basal ganglia and to intraparenchymal hemorrhage (Okamura et al., 2018; Lowe et al., 2016; Ikonovic et al., 2016). The former of these affinities explains the nearly universal elevated *in vivo* retention observed in the substantia nigra of elderly individuals regardless of their pathological diagnosis (Marquie et al., 2015). In post-mortem our research groups previously identified AV-1451 off-target binding to neuromelanin- and melanin-containing cells, to choroid plexus and to brain hemorrhagic lesions (Marquie et al., 2015). These observations justify the investigation of the off-target binding patterns of newly developed Tau PET radio tracers.

With phosphor screen autoradiography experiments we have noticed a strong binding of [¹⁸F]-MK-6240 and [¹⁸F]-PI-2620 to neuromelanin- and melanin-containing cells including pigmented neurons in the substantia nigra (regardless of the presence or absence of nigral Tau pathology), leptomeningeal melanocytes, metastatic melanoma and retinal pigment epithelium. We have seen some weaker off-target binding to brain hemorrhages as well. This is relevant for the correct interpretation of *in vivo* imaging as for example on the relative abundance and distribution of leptomeningeal melanocytes across different individuals (Goldgeier et al., 1984) or the presence of brain hemorrhagic lesions in parallel with the lesions of the pathology. *In vivo* it has been demonstrated by others that [¹⁸F]-MK-6240 doesn't follow the same behaviour than [¹⁸F]-AV-1451 (Choi et al., 2018) for the off-

target on the basal ganglia and choroid plexus (Betthausen et al., 2019). We observed the same post-mortem binding pattern with a lack of signal in the basal ganglia for [¹⁸F]-MK-6240 and [¹⁸F]-PI-2620. We still need to have a closer look at the choroid plexus with those tracers to complete this off-target binding characterization.

In addition, one of the first generation Tau PET tracers, THK-5351, has been recently found to demonstrate high binding affinity to MAO-B (Monoamine Oxydase B) (Harada et al., 2016; Ng et al., 2017), seriously compromising its value as a Tau-specific tracer and increasing the need for alternative Tau-specific imaging agents. To date, our own observations and some of other groups about a potential non-specific binding of AV-1451 to MAO enzymes have demonstrated conflicting results (Aguero et al., 2019, Annexe 1; Hansen et al., 2018; Vermeiren et al., 2018). We are going to run tritium autoradiography with [³H]deprenyl (imaging MAOB) and [³H]clorgyline (imaging MAOA) to figure out if some signal is due to an off-target binding of those agents to Tau.

The two novel Tau PET tracers of second generation showed some slight improvement about the off-targets, but there are still many others off-target too close to the pathologic lesions, making the interpretation of the images difficult. We need a new generation of Tau PET tracers free from these gaps of selectivity to improve the imaging of the protein Tau *in vivo*.

In conclusion this autoradiographic characterization allowed to confirm the potential utility of Tau PET tracers for the reliable detection/quantification of Tau aggregates and disease-progression tracking in AD.

In the next part of this work, we will see *in vivo* if that selective p-Tau imaging could be used as a follow-up tool for monitoring the efficacy of a treatment.

**PART 3: Tau PET imaging in AD : Effect of
modulating gamma oscillations by
transcranial alternating current stimulation
on brain structure in humans**

PROBLEM STATEMENT

AD is the leading cause of dementia and the sixth leading cause of death in the United States in 2013 (James et al., 2014). The therapeutic options are very limited, with some pharmacologic interventions that transiently improve cognitive functions but with no treatments that avoid the progression of the disease.

AD is characterized by diffuse A β and p-Tau aggregates as well as widespread neurodegeneration (Villain et al. 2012, Villemagne et al. 2013). Apart from protein deposition, a consistent finding in patients with AD is a relative attenuation of brain fast oscillatory activity in the 30-80 Hz range, known as “gamma” activity (Babiloni et al., 2015). More recently, it has been demonstrated that exogenously-induced 40 Hz gamma oscillations reduce A β levels *via* microglia activation, and may also reduce p-Tau levels in a mouse model of AD (Iaccarino et al., 2016). The same authors have also determined that in presymptomatic AD mice, induction of gamma activity prevents subsequent neurodegeneration and behavioral impairments, suggesting that gamma induction may represent a novel and powerful therapeutic approach for AD.

Recent studies in the field of non-invasive brain stimulation suggest the feasibility of interacting with brain oscillations by transcranial alternating current stimulation (tACS), where low intensity (max 2mA) alternating sinusoidal currents are applied via scalp electrodes. Due to the safety of the procedure (Rossini et al., 2015), the stimulation frequency and the controllability of the target stimulated, tACS have been promoted as one of the most promising techniques to modulate the healthy and pathological brain (Tatti et al., 2016). In humans, the effects have been documented at the behavioral level for sensorimotor (Santarnechi et al., 2017; Feurra et al., 2011; 2013), visual (Kanai et al., 2008), somatosensory (Feurra et al., 2011) and higher-order cognitive domains (Santarnechi et al., 2013; 2016), with effects lasting for up to 70 minutes after stimulation (Kasten et al., 2016).

In our study each participant underwent 4 weeks (20 sessions of one hour) of tACS in bi-temporal brain areas. tACS uses low amplitude alternating currents *via* externally applied electrodes to modulate brain activity and cortical rhythmic activity gamma oscillations.

In AD patient with amyloid-positive PET scores we look at the p-Tau distribution after tACS stimulation sessions. The present study, done in collaboration with the Berenson-Allen Center for Non-Invasive Brain Stimulation (CNBS) at Beth Israel Deaconess Medical Center (BIDMC), will investigate the impact of a novel transcranial electrical stimulation therapeutic intervention on PET markers of AD as hyperphosphorylated Tau protein distribution.

The purpose of this study is to determine the ability of Tau PET imaging to establish the viability of a new potential treatment. A β and Tau will be measured using [^{11}C]-PiB and [^{18}F]-AV-1451 in PET imaging. These scans have been done before the 20 tACS treatments and then done again after the tACS treatment to assess the difference in the cerebral Tau burden occurring after the treatment.

MATERIALS AND METHODS

1. Subject selection

We recruited 5 subjects for a pilot study. The patients must have had a diagnosis of mild to moderate AD and be over 65 years old.

All subjects underwent at least one comprehensive medical and neurological evaluation using tests such as the Mini-Mental State Examination (MMSE) and/or the Clinical Dementia Rating (CDR) scale.

The study has been approved by the institutional review board at Massachusetts General Hospital (MGH), and all subjects signed an informed consent form.

2. Data acquisition

All enrolled subjects underwent separate PET and MRI procedures. The [^{11}C]-PiB and [^{18}F]-AV-1451 tracers were synthesized and administered onsite.

Structural MRI was performed for anatomical reference. A 3-dimensional structural T1-weighted BRAVO sequence was acquired using a 3 T GE MRI. The 3D acquisitions used the following parameters: repetition time = 8240 ms; echo time = 3.24 ms; inversion time = 450 ms; flip angle = 12° ; voxel size = $0.94 \times 0.94 \times 1 \text{ mm}^3$ and matrix size = 256×256 . MRI data were used to define regions of interest for image analysis.

Five participants (S1-S5) were scanned on a Discovery MI (GE Healthcare) PET/CT scanner. The full width at half maximum (FWHM) spatial resolutions measured at the center of the axial field of view (radial position = 1 cm) were 4.3 mm and 5.1 mm in transverse and axial direction respectively. 50 min after the injection of a 15mCi (555MBq) intravenous bolus of [^{11}C]-PiB, static data were acquired during 20 min (McNamee et al., 2009). Following a 10mCi (370 MBq) bolus injection of [^{18}F]-AV-1451, static data were measured 75 min after injection, for a duration of 30 min

(Baker et al., 2017). An X-ray CT scan was performed right before each PET segment for attenuation correction and was obtained using standard acquisition parameters with the GE MI Discovery PET/CT scanner.

All 2 PET/CT scans were completed within 3 weeks following the final tACS study visit.

3. Image reconstruction and processing

PET data acquired on the Discovery MI (GE Healthcare) PET/CT scanner were reconstructed using a validated fully 3D time-of-flight iterative reconstruction algorithm using five iterations and 16 subsets while applying corrections for scatter, attenuation, deadtime, random coincident events and scanner normalization. Final reconstructed images had voxel dimensions of $256 \times 256 \times 89$ and voxel sizes of $1.17 \times 1.17 \times 2.8 \text{ mm}^3$.

PET images were motion corrected frame-by-frame through rigid body registration of adjacent frames using a least-squares algorithm with Levenberg–Marquardt optimization (Alpert et al., 1996). All MR and PET images were registered into the standard Montreal Neurological Institute (MNI) space following the procedure described in Wooten et al. (2017). The first 10 min of the PET images were summed and rigidly co-registered to the structural MRI image, itself transformed into the MNI space using a 12-parameter affine transformation followed by nonlinear warping (FMRIB’s Linear Image Registration Tool [FLIRT] and FMRIB’s Non-Linear Image Registration Tool [FNIRT] in the FMRIB Software Library [FSL] (Jenkinson et al., 2012)). The transformation matrices were combined and applied inversely on MNI and Harvard–Oxford atlases (available in FSL) in order to warp the atlas based regions of interest into the native PET images for extraction of radioactivity time–activity curves. The regions of interest surveyed in this work included the frontal cortex, parietal cortex, occipital cortex, temporal cortex, mesial temporal cortex (MTC), precuneus, cerebellum gray no vermis, cingulate gyrus posterior, gray matter, white matter, amygdala, caudate, hippocampus, pallidum, putamen and thalamus.

4. Biostatistical Analysis

PET A β and p-Tau levels across brain regions were quantified using relative SUVR (Lopresti et al., 2005). Reference region based analyses of [^{11}C]-PiB uptake were performed using the cerebellum (excluding the vermis) as a reference tissue (McNamee et al., 2009) and for [^{18}F]-AV-1451 we used the white matter (Hanseeuw et al., 2019; Baker et al., 2019) providing more stable estimates for longitudinal studies. Subjects were defined as amyloid positive if the global (across frontal, occipital, parietal and temporal regions) cortical to cerebellar SUV ratio is greater than or equal to 1.4 (Bullich et al., 2017).

Studies have suggested that the test-retest reliability of amyloid-PET measurement is high, with an intraclass correlation of 0.99, and a relative measurement error of 3% for PiB and AV-1451 PET imaging. Test-retest analyses demonstrated low variability in [^{11}C]-PiB and [^{18}F]-AV-1451 SUVR (C. R. Jack et al., 2013; Devous et al., 2017). The annual rate of change in the global and regional A β and p-Tau ratio is generally either nonsignificant or positive, typically on the order of 0.05 units/year, and asymptotes in patients with cognitive deficits and high A β and p-Tau levels (C. R. Jack et al., 2013; 2019; Villain et al., 2012; Villemagne et al., 2013). This suggests that major changes are unlikely over the short time period between baseline and post-tACS testing. Furthermore, significant decreases in A β or p-Tau (> 0.05 units/year) are rare, particularly in patients with AD (C. R. Jack et al., 2013), suggesting that decreases above this magnitude would represent a reliable measure of tACS effect.

RESULTS

Longitudinal changes in A β and p-Tau deposition are measured by [^{11}C]-PiB-PET and [^{18}F]-AV-1451-PET in patients with mild to moderate AD, after 20 daily sessions of tACS.

1. A β imaging

15 mCi (555 MBq) of the radiotracer [^{11}C]-PiB, an agent that binds specifically to A β , was infused as a slow bolus over 60 seconds *via* intravenous line placed prior to the scan. PET data were acquired in static mode at 50-70 minutes post-injection.

All the subjects are amyloid positive (Table 1).

Subjects	Mean SUVR
S1	2.12
S2	2.07
S3	2.49
S4	1.87
S5	1.41

Table 1: A β scores for each subject. This score has been calculated from the SUVR values in the frontal, occipital, parietal and temporal cortex. The subjects are considered amyloid positive if the ratio is superior or equal to 1.4.

SUVR (50-70 min) maps, before and after tACS treatment, generated using the cerebellum no vermis as a reference region are shown in Figure 15 for the 5 subjects. Also displayed is the subjects BRAVO image in standardised space of the same slice for localisation. From these parametric images we can see that the A β distribution is very spread out in the brain of each subject.

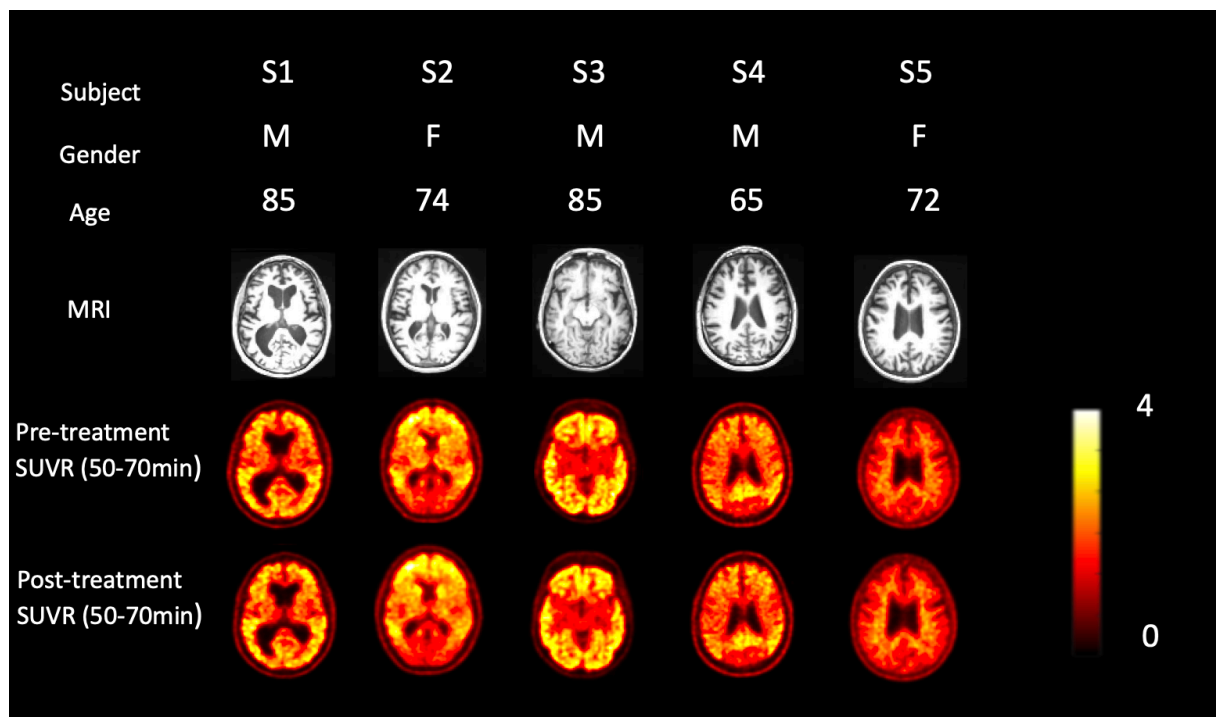


Figure 15: SUVR parametric images of [¹¹C]-PiB for all subjects using the cerebellum no vermis as reference region. First row shows the corresponding individual BRAVO images for anatomical reference, the second row the PET images before the tACS treatment and the last row the PET images after the tACS treatment.

We looked closer at the temporal lobe, the region of the brain targeted and stimulated by tACS for each subject. We calculated the dSUVR between the two scans as follow : $(\text{SUVR}_{\text{post-tACS}} / \text{SUVR}_{\text{pre-tCAS}}) * 100 - 100$.

[¹¹C]-PiB binding generally decreased after the tACS treatment in that population (Figure 16). However, PET analysis studies have suggested that the relative measurement error of the test-retest of amyloid-PET can reach 3%. The decrease of [¹¹C]-PiB binding observed in that study is not significant because it doesn't reach that threshold. To conclude about the findings and see if the declining trend of A β deposition represented by the decrease of [¹¹C]-PiB binding after a tCAS treatment is significant we need to study a larger population with a longer TACs treatment.

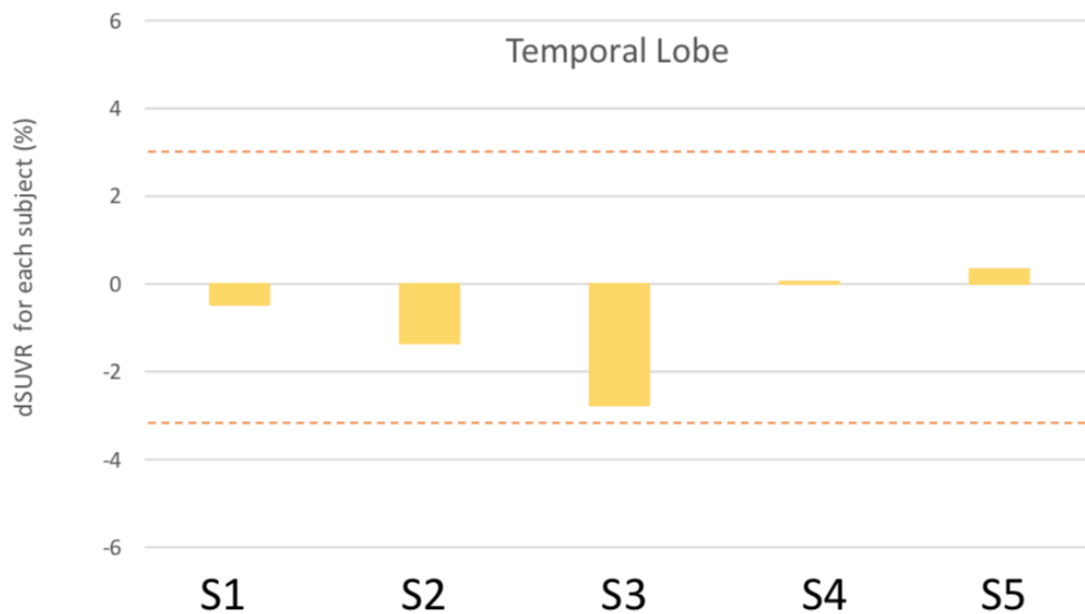


Figure 16: Change in [11C]-PiB binding across the 5 subjects in the temporal lobe. The mean dSUVR obtained from the scans pre and post tCAS doesn't show any significant effect of the treatment on the [11C]-PiB binding at the temporal lobe.

2. Hyperphosphorylated Tau imaging

[18F]-AV-1451 binds with high affinity and selectivity to aggregated Tau pathology in *ex-vivo* human brain sections. 10 mCi (370 MBq) of [18F]-AV-1451 were infused as a slow bolus over 60 seconds *via* intravenous line placed prior to the scan. PET data were acquired in static mode at 75-105 minutes post-injection.

SUVR (75-105 min) maps, before and after tACS treatment, generated using the white matter as a reference region are shown in Figure 17 for the 5 subjects. Also displayed is the subjects BRAVO image in standardised space of the same slice for localisation. From these parametric images we can see that all the subjects showed p-Tau depositions in the brain. The temporal lobe of these subjects is reached by p-Tau, that means they are all at least in Braak stage IV (MCI). Also they all have p-Tau present in other region of interest related to AD as frontal cortex (S2, S4), parietal

cortex (S1-S4), occipital cortex (S1-S5), MTC (S2-S5), precuneus (S1-S4), cingulate gyrus posterior (S1-S4), amygdala (S1-S5), caudate (S5), hippocampus (S3-S5), pallidum (S1-S5), putamen (S1-S5) and thalamus (S1-S5). Our results demonstrate that Tau-PET imaging is helpful to improve the AD diagnosis of these patients.

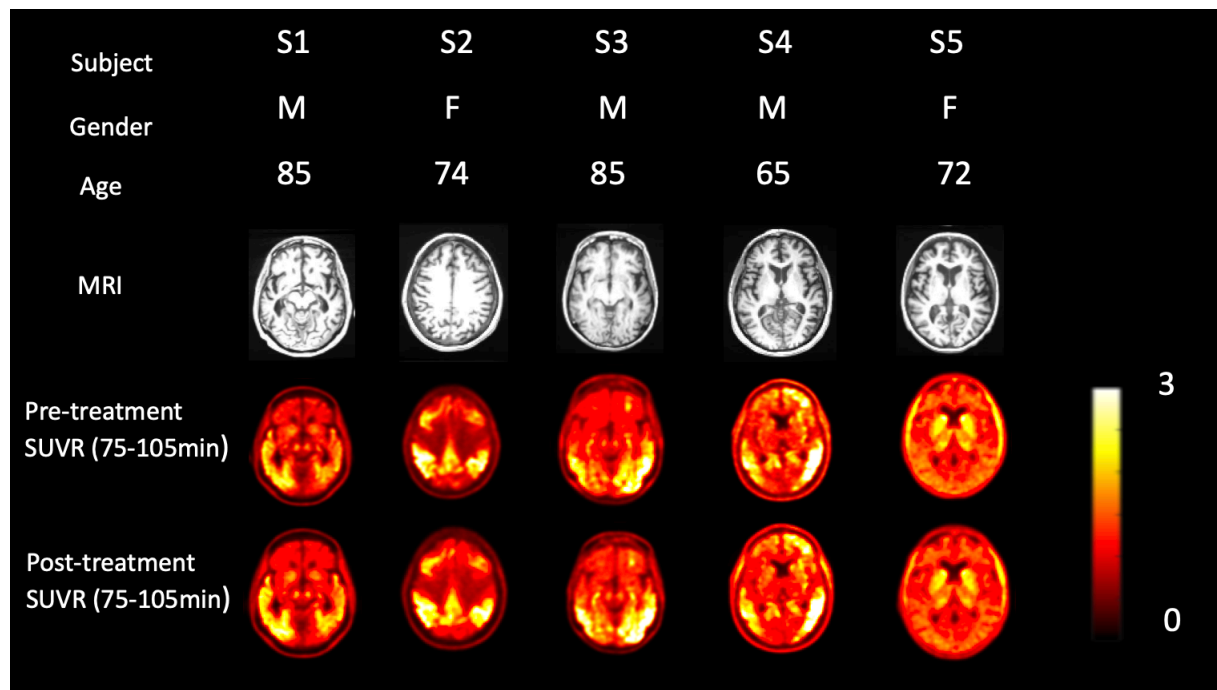


Figure 17: SUVR parametric images of $[^{18}\text{F}]\text{-AV-1451}$ for all subjects using the white matter as reference region. SUVR (75-105min) maps before after tACS treatment are shown for all subjects studied in this work, as well the corresponding MRI slices for anatomical reference.

We looked closer at the temporal lobe (Figure 18), the targeted region of the brain by tACS for each subject and in other regions of interest related to AD (Figure 19). $[^{18}\text{F}]\text{-AV-1451}$ binding generally decreased after the tACS treatment in that population.

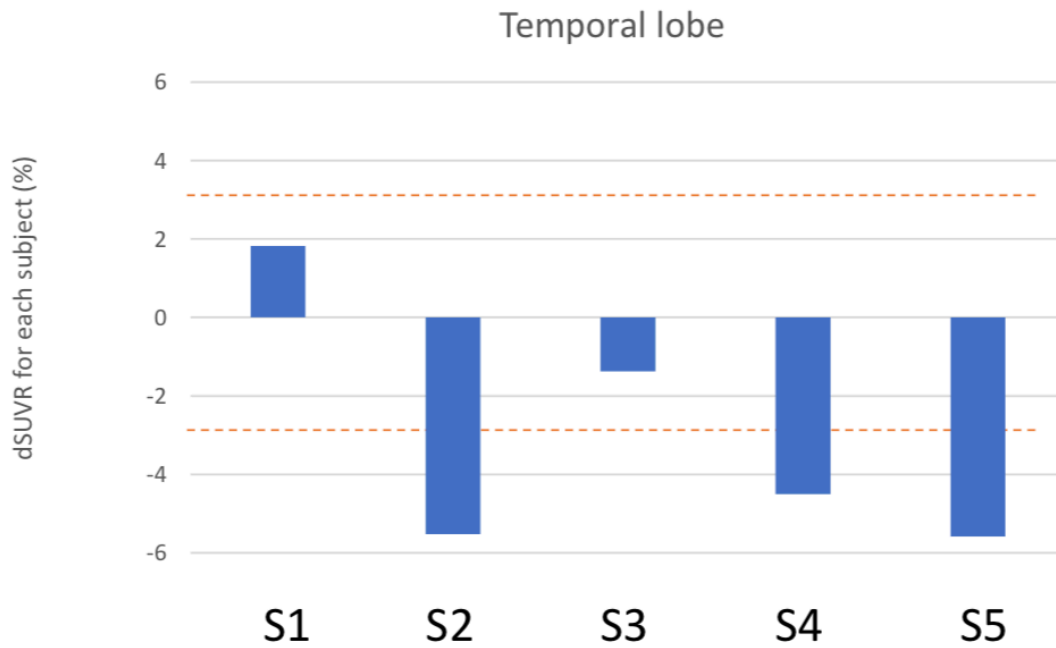


Figure 18: Change in [18F]-AV-1451 binding across the 5 subjects in the Temporal Lobe. PET analysis studies have suggested that the relative measurement error of the test-retest of Tau-PET can reach 3%. Three subjects (S2, S4 and S5) show a decrease of [18F]-AV-1451 binding (over 3%) after the tCAS treatment at the temporal lobe.

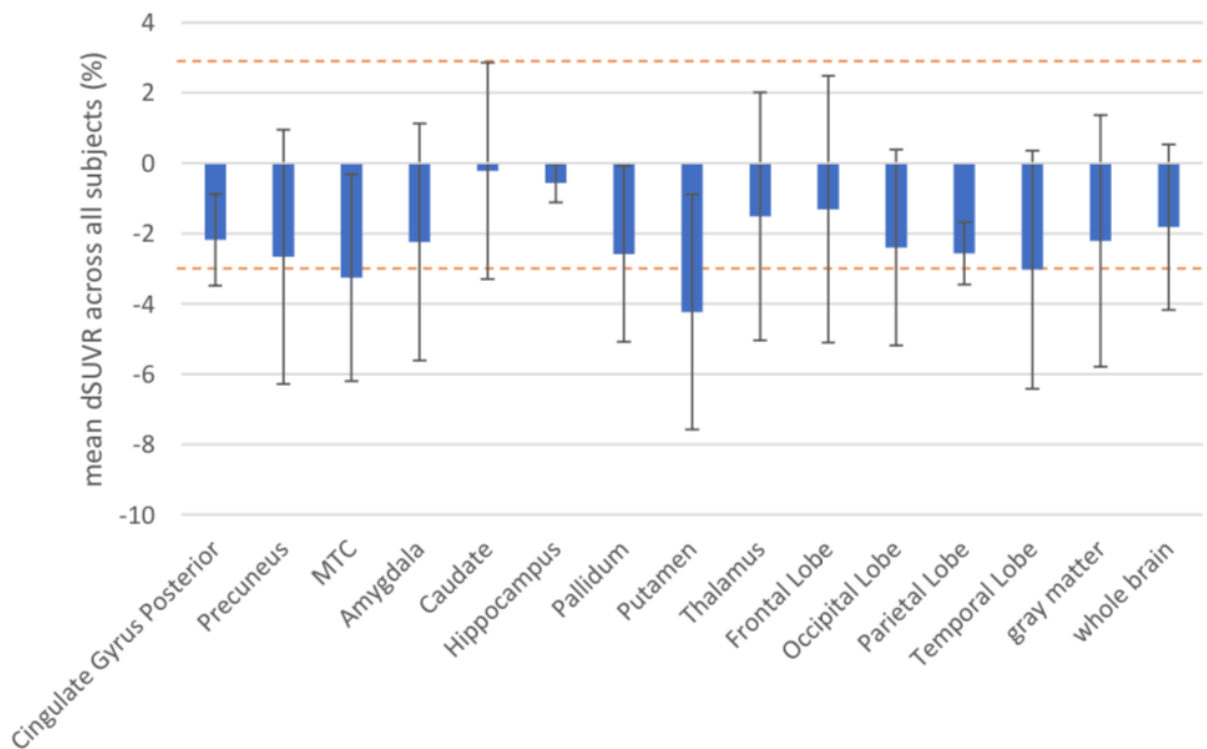


Figure 19: Change in [¹⁸F]-AV-1451 binding across the 5 subjects in regions of interest. A global decrease in [¹⁸F]-AV-1451 binding is observed after the tACS treatment. To confirm these results and avoid high variabilities, an investigation on a larger population is necessary.

DISCUSSION

The neurotracers [¹⁸F]-AV-1451 and [¹¹C]-PIB allow to image by PET the tissue concentration of the p-Tau protein (Mishra et al., 2017) and A β (Klunk et al., 2004) respectively.

We observed on 5 subjects a general decrease of the intracerebral Tau burden following the tACS. These 5 subjects are amyloid positive as demonstrated with the [¹¹C]-PIB scan but the amount of A β didn't seem to be influenced by tACS. The p-Tau PET scan was useful to determine the viability of this novel treatment and allowed a more accurate diagnosis of AD (Braak stage) by accessing the pattern of distribution of Tau protein.

Our hypothesis is that a tACS treatment entraining gamma oscillations on humans with diagnosed AD would decrease cerebral p-Tau aggregates by microglial activation. It is evident that neuroinflammation plays a critical role in the pathophysiology of AD (Cagnin et al., 2001; Edison et al., 2008; Nuzzo et al., 2014). Under physiological conditions, microglia, immune cells of the brain, is neuroprotective (Nimmerjahn et al., 2005). In AD, microglia plays a dual role. Acute microglial activation increases clearance mechanisms against misfolded proteins as p-Tau and in contrast, chronic activation of microglia contributes to neurotoxicity with prolonged inflammation and liberation of proteolytic enzymes damaging the extracellular matrix (Liddel et al., 2017).

Changes in gamma oscillations have been observed in neurodegenerative diseases. *In vivo* studies on mice have demonstrated that gamma oscillations can polarize microglia toward a beneficial activation state by increasing clearance mechanisms without activating the pro-inflammatory response (Iaccarino et al., 2017).

In order to verify the mechanism in our human study, PET imaging of inflammation biomarkers could be necessary. A potent TSPO antagonist, PBR28, has been [¹¹C]-labelled and demonstrated a good correlation between activated microglia and AD pathology (Kreisl et al., 2013). Our group tried to image some of these subjects for TSPO at the same time point used for PiB and AV-1451 scans. However, we couldn't see any binding of the tracer and there was no significant change showing the

microglial activation after the tACS treatment. This scan has been cancelled for the rest of the study. Nevertheless, the lack of signal could have been explained by a wrong time-point of observation for the inflammation. Indeed, the time-course and progression of neuroinflammation is a really important parameter (Hamelin et al., 2016) suggesting that the microglial activation may have an earlier role and could be observed upstream of the effects on the Tau burden.

This study has a limitation with the relative measurement error of the test-retest in PET imaging avoiding the detection of small effect inferior to 3%. In addition, we have some limitations because of the off-target binding of this p-Tau tracer at the choroid plexus, leading to some difficulties to interpret the signal around the hippocampus area (important region of interest in AD).

We need to have a larger population in order to conclude on the effect of the treatment about the progression of AD. Also, all these subjects underwent cognitive tests before and after treatments to see if they got some cognitive improvements. These results will be correlated with the PET imaging findings when the number of subjects will be higher. The future work following this preliminary study will include a TACs treatment of three months instead of one. That could maybe allow us to see a bigger impact of the TACs treatment on the A β and p-Tau aggregates. Also we will look at the effect of this treatment on a control group with subjects free from neurodegenerative diseases.

In conclusion, p-Tau PET imaging with [18 F]-AV-1451 was useful in the diagnostic and follow-up of patients with AD ensuing a tCAS treatment. Those results suggest that [18 F]-AV-1451 could be used to examine changes in Tau burden over time. In the next part of this work, we are going to evaluate the value of *in vivo* p-Tau PET imaging in a tauopathie with similar Tau aggregates : CTE.

**PART 4: Tau PET Imaging in CTE in athletes:
a sequela of TBI**

PROBLEM STATEMENT

Several studies have suggested an association between TBI and the risk of developing dementia later in life. For instance, a meta-analysis of 15 case-control studies reported an association between head injury and the risk of Alzheimer disease (Fleminger et al, 2003). Another study has shown an association with CTE (Mckee et al, 2013). TBIs appear to trigger and exacerbate some of the pathological processes involved in these diseases such as the formation and accumulation of misfolded Tau protein aggregates (Edwards et al, 2016). Preliminary research indicates that iron deposits due to haemorrhaging, following TBIs, may increase Tau pathology (Yoshiyama et al., 2005).

CTE is a neurodegenerative disease that has been associated with a history of repetitive head impacts, including those that may associated with concussion symptoms in American football players. At this time, CTE can only be diagnosed after death by a neuropathological examination. Like AD, CTE has been suggested to be associated with a progressive loss of brain cells. In contrast to AD, the diagnosis of CTE is based in part on the pattern of Tau deposition and a relative lack of amyloid plaques.

In our protocol each participant underwent A β and p-Tau PET imaging measured by [¹¹C]-PiB and [¹⁸F]-AV-1451.

The aim of this football players study is to determine the ability of p-Tau PET imaging to detect early stages of CTE in a population at risk of developing this disease. Also, this study could advance our understanding in the complex mechanism that underlies the development of player-related illnesses and disability.

MATERIALS AND METHODS

1. Subject selection

In total, we plan to recruit and enroll up to 150 study participants. We recruited 10 subjects so far between 34 to 56 years old. To be included in the cohort, a participant must be a former professional football player who played in the American or National Football League from 1960 to present. This includes former players of all races, ages and geographic locations nationally. Women are not included in this group, as the National Football League is historically and currently a male-only entity.

Prior to arrival all participants are pre-screened over the phone for cognitive impairment using the Telephone Montreal Cognitive Assessment (T-MoCA). If impairment is suspected, additional tools are employed to further assess the potential participant's functioning as the Alzheimer's Disease Cooperative Study (ADCS-ADL), and the Neuropsychiatric Inventory–Questionnaire (NPI-Q). These assessments are conducted by study staff members who have been specifically trained by a licensed neurologist or neuropsychologist. The purpose of this assessment is to provide a mechanism to identify if the potential participant should be excluded from the study due to severity of cognitive impairment and to identify the need to have a study partner accompany the participant to Boston for the study. This is necessary to assure that a participant with cognitive impairment has someone to participate in the informed consent process if needed.

At the first in-person visit, the participant performs the MMSE. The purpose of administering the MMSE is to serve as an additional measure of cognitive functioning and when combined with known medical history, medications and T-MoCA score from the screening, is used to determine the participant's ability to provide consent.

All subjects signed an informed consent form, and the study was approved by the institutional review board at MGH.

2. Data acquisition

All enrolled subjects underwent separate PET and MRI procedures.

Structural MRI was performed for anatomical reference. A 3-dimensional structural T1-weighted magnetization-prepared rapid gradient-echo (MPRAGE) was acquired using a 3 T Tim Trio (Siemens Medical Systems). The MPRAGE acquisitions parameters were as follows: repetition time/echo time/inversion time, 2530/1.69/1100 ms; 7° flip angle; 1 mm slice thickness and matrix size 256 × 256. MRI data were used to define regions of interest for image analysis.

Ten participants (S1-S10) were scanned on a Discovery MI (GE Healthcare) PET/CT scanner. The FWHM spatial resolutions measured at the center of the axial field of view (radial position = 1 cm) were 4.3 mm and 5.1 mm in transverse and axial direction respectively. 40 min after the injection of a 15mCi (555 MBq) intravenous bolus of [¹¹C]-PiB, static data were acquired during 20 min (McNamee et al., 2009). Following a 10mCi (370 MBq) bolus injection of [¹⁸F]-AV-1451, static data were measured 75 min after injection, for a duration of 30 min (Baker et al., 2017). An X-ray CT scan was performed at the start of each emission scan for the purpose of attenuation correction and was obtained using standard acquisition parameters with the GE MI Discovery PET/CT scanner.

3. Image reconstruction and processing

PET data acquired on the Discovery MI (GE Healthcare) PET/CT scanner were reconstructed using a validated fully 3D time-of-flight iterative reconstruction algorithm using five iterations and 16 subsets while applying corrections for attenuation, scatter, random coincidences, normalization, and deadtime. Final reconstructed images had matrix sizes of 256 × 256 × 89 and voxel sizes of 1.17 × 1.17 × 2.8 mm³.

PET images were motion corrected frame-by-frame through rigid body registration of adjacent frames using a least-squares algorithm with Levenberg–Marquardt optimization (Alpert et al., 1996). All MR and PET images were registered into the

standard Montreal Neurological Institute (MNI) space following the procedure described in Wooten et al. (2017). The first 10 min of the PET images were summed and rigidly co-registered to the structural MRI image, itself transformed into the MNI space using a 12-parameter affine transformation followed by nonlinear warping (FMRIB's Linear Image Registration Tool [FLIRT] and FMRIB's Non-Linear Image Registration Tool [FNIRT] in the FMRIB Software Library [FSL] (Jenkinson et al., 2012)). The transformation matrices were combined and applied inversely on MNI and Harvard–Oxford atlases (available in FSL) in order to warp the atlas based regions of interest into the native PET images for extraction of radioactivity time–activity curves. The regions of interest surveyed in this work included the frontal cortex, parietal cortex, occipital cortex, temporal cortex, MTC, precuneus, cerebellum gray no vermis, cingulate gyrus posterior, gray matter, white matter, amygdala, caudate, hippocampus, pallidum, putamen and thalamus.

4. Biostatistical Analysis

PET A β and p-Tau levels across brain regions were quantified using relative SUVR (Lopresti et al., 2005). Reference region based analyses of [^{11}C]-PiB and [^{18}F]-AV-1451 uptake were performed using the cerebellum (excluding the vermis) as a reference tissue (McNamee et al., 2009; Wooten et al., 2017) providing more stable estimates for transversal studies. Subjects were defined as amyloid positive if the global (across frontal, occipital, parietal and temporal regions) cortical to cerebellar SUV ratio is greater than or equal to 1.4 (Bullich et al., 2017).

RESULTS

A β and p-Tau deposition are measured by [^{11}C]-PiB-PET and [^{18}F]-AV-1451-PET in a population of American Football players.

SUVR maps for [^{11}C]-PiB and [^{18}F]-AV-1451, generated using the cerebellum no vermis as a reference region, are shown in Figure 20 for the 10 subjects. Also displayed is the subjects MPRAGE image in standardised space of the same slice for localisation. From these parametric images we can see that all the subjects show [^{11}C]-PiB binding in their brain, mostly around the central gray nucleus. About [^{18}F]-AV-1451, the pallidum seems to be an area with high affinity (S1-S10). Other areas have a high signal as the hippocampus (S2, S6-S10), amygdala (S2-S5, S7, S9), putamen (S2-S4, S6-S9) and thalamus (S2-S10). Also we can see some off-target binding of [^{18}F]-AV-1451 as the substantia nigra (S1-S10) and the choroid plexus (S1, S2, S4, S6, S7, S8, S9, S10).

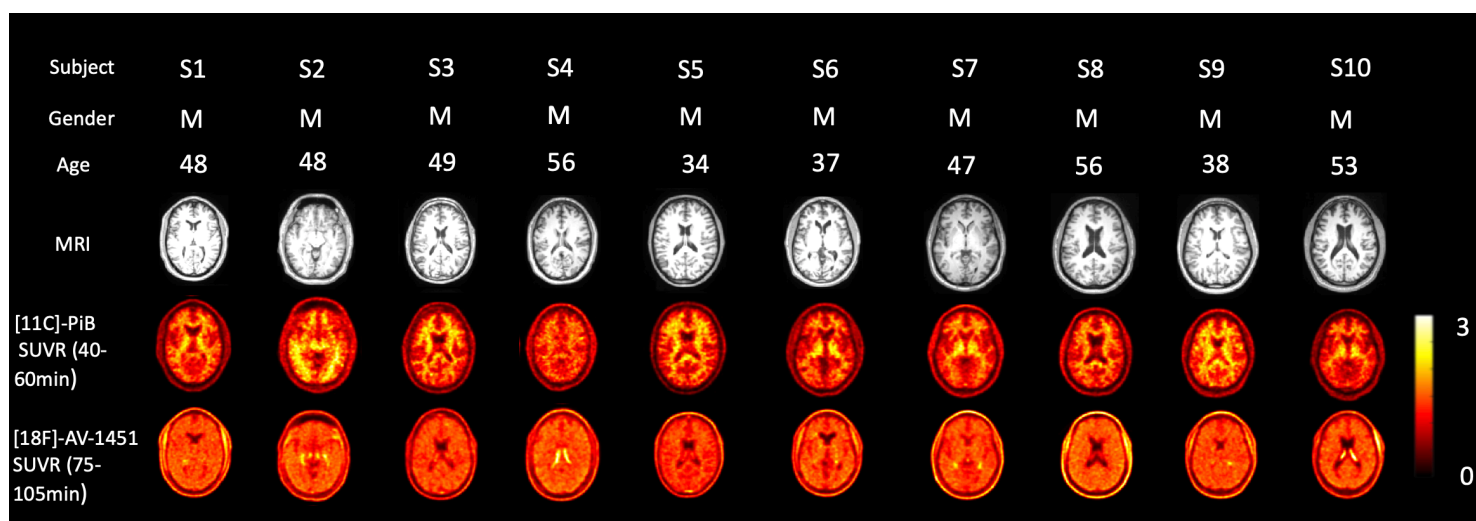


Figure 20: SUVR parametric images of [^{11}C]-PiB and [^{18}F]-AV-1451 for all subjects. First row shows the corresponding individual MPRAGE images for anatomical reference, the second row the PET images with [^{11}C]-PiB and the last row the [^{18}F]-AV-1451 PET images. The Subjects seem to all have some A β aggregates represented by the binding of [^{11}C]-PiB. The tracer [^{18}F]-AV-1451 shows mainly some

binding in pallidum, hippocampus, amygdala, putamen, thalamus, substantia nigra and choroid plexus.

1. A β imaging

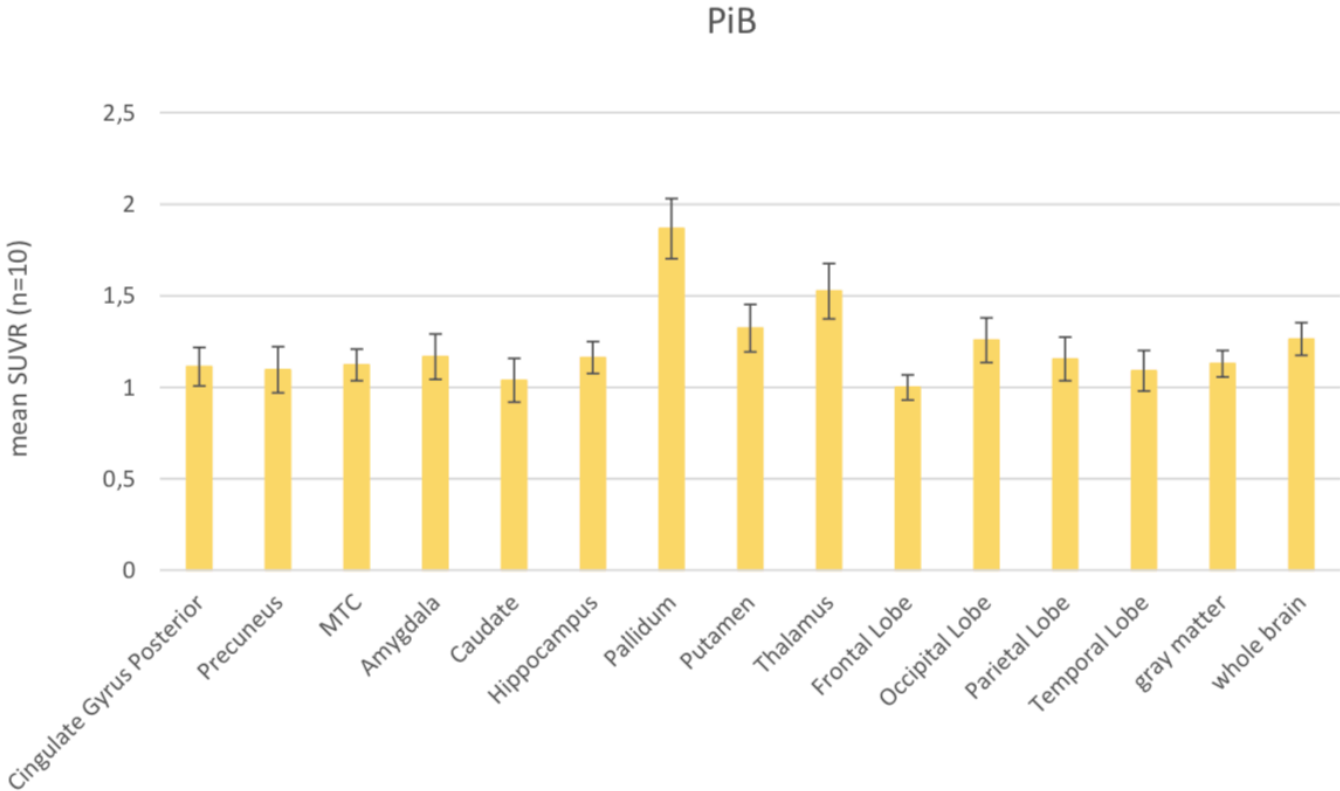
15 mCi (555 MBq) of the radiotracer [^{11}C]-PiB, an agent that binds specifically to A β , was infused as a slow bolus over 60 seconds *via* intravenous line placed prior to the scan. PET data were acquired in static mode at 40-60 minutes post-injection.

All the subjects show some A β in their brain but they are not considered amyloid positive, except for subject 5 (Table 2).

Subjects	Mean SUVR
S1	1.13
S2	1.37
S3	1.16
S4	1.11
S5	1.41
S6	1.03
S7	1.10
S8	1.02
S9	1.18
S10	1.06

Table 2: A β scores for each subject. This score has been calculated from the SUVR values in the frontal, occipital, parietal and temporal cortex. The subjects are considered amyloid positive if the ratio is superior or equal to 1.4.

We looked closer at the [¹¹C]-PiB binding pattern in other regions of interest (Figure 21) across all the subjects. [¹¹C]-PiB seems to show a higher affinity in areas as the



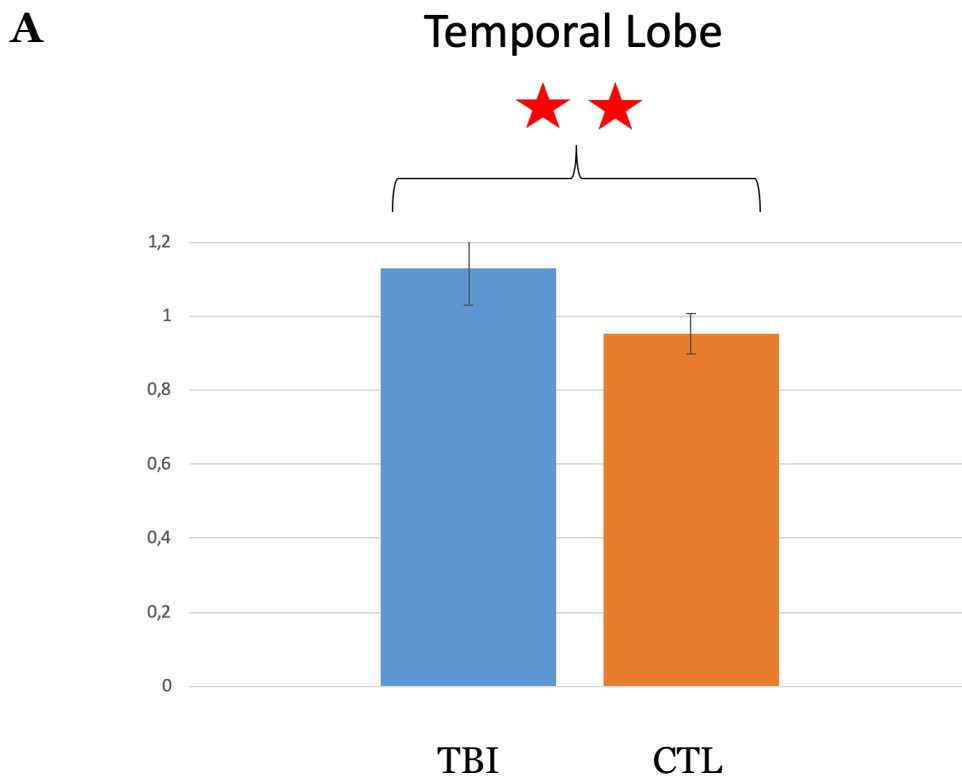
pallidum and the thalamus in that population.

Figure 21: Mean SUVR values for [¹¹C]-PiB across 10 subjects in the regions of interest. In the central gray nucleus and the thalamus, [¹¹C]-PiB has a stronger binding in that population of American football players.

2. Hyperphosphorylated Tau imaging

10 mCi (370 MBq) of [¹⁸F]-AV-1451 were infused as a slow bolus over 60 seconds *via* intravenous line placed prior to the scan. PET data were acquired in static mode at 75-105 minutes post-injection.

We compared the SUVR results of the temporal lobe (Figure 22) of this TBI population with 4 gender and age-matched control subjects, without known history of mild TBI, scanned in our Center. We used the temporal lobe for this comparison because it is an area commonly affected in focal TBI (Werner et al., 2007). We also looked at the pallidum to confirm if the signal observed represent a non specific binding of the tracer. These two populations showed significant differences in the binding of the tracer in the temporal lobe (TBI subjects SUVR : $1,13 \pm 0,09$; control group SUVR : $0,95 \pm 0,05$) and in the pallidum (TBI subjects SUVR : $1,3 \pm 0,13$; control group SUVR : $0,95 \pm 0,09$).



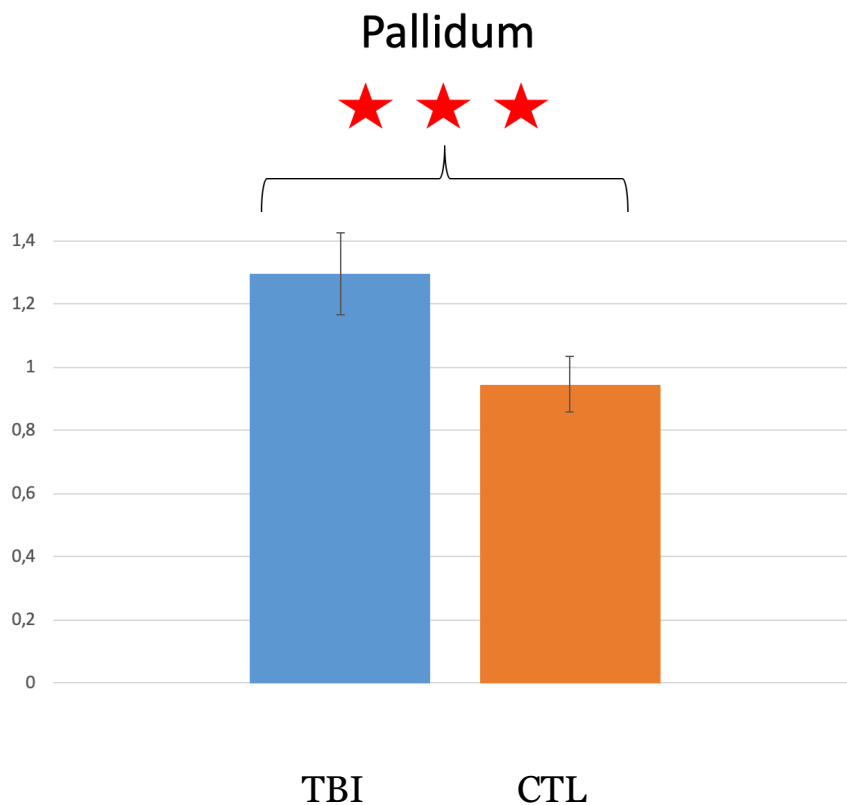
B

Figure 22: [¹⁸F]AV-1451 binding in temporal lobe and pallidum of TBI and control subjects. This figure shows the mean \pm SD SUVR of [¹⁸F]AV-1451 in the temporal lobe and the pallidum for TBI subjects (n=10) and controls (n=4) which were grouped together only for this comparison. Statistically significant difference was observed between the two groups for the temporal lobe (panel A) and for the pallidum (panel B) (Test T Student, bilateral value $<0,01$ and $<0,001$ respectively).

We looked closer at the [¹⁸F]-AV-1451 binding pattern in other regions of interest (Figure 23) across all the subjects. In that population, [¹⁸F]-AV-1451 seems to present a high affinity in MTC, amygdala, hippocampus, putamen, thalamus, occipital lobe, temporal lobe, white matter and a positive tracer uptake (SUVR >1.3 ; Ossenkoppele et al., 2018) in the pallidum.

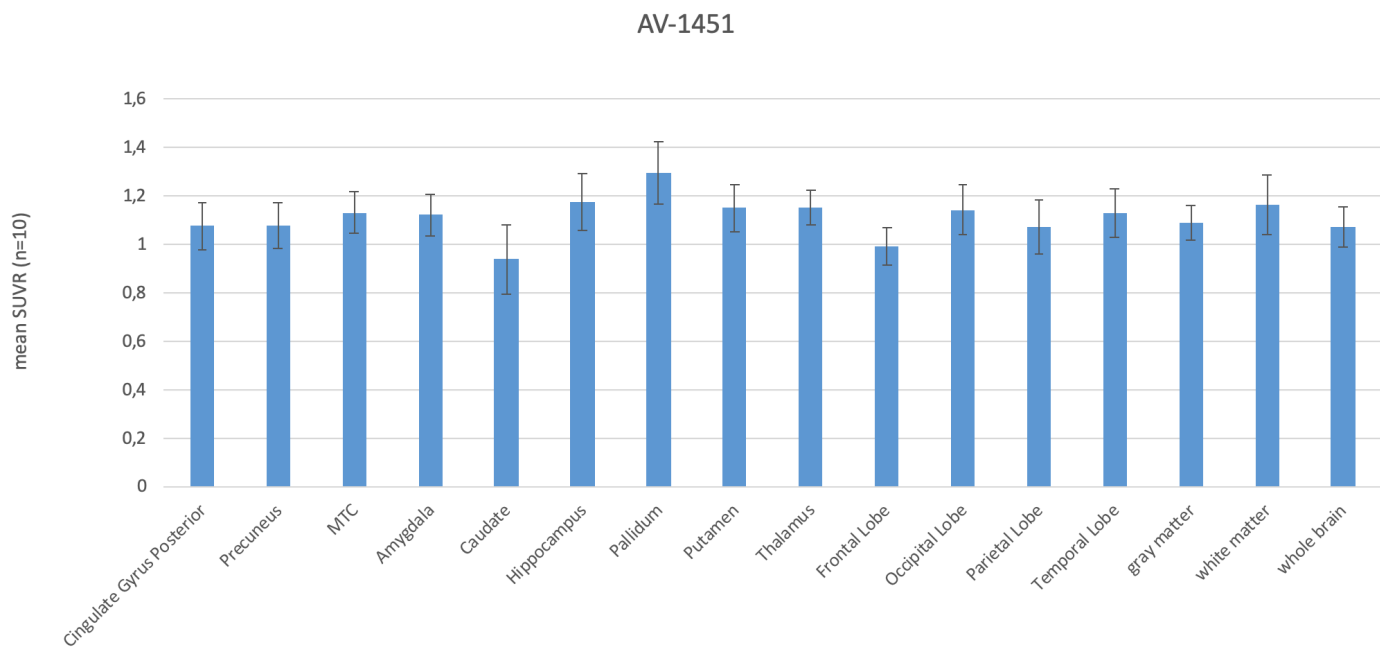


Figure 23: Mean SUVR values for [18F]-AV-1451 across the 10 subjects in the regions of interest. [18F]-AV-1451 has a high affinity in MTC, amygdala, hippocampus, putamen, thalamus, occipital lobe, temporal lobe, white matter and a higher affinity in the pallidum.

DISCUSSION

Several tau PET tracers with a high binding affinity and selectivity have been developed (Okamura et al, 2016). Tau PET is currently being evaluated in AD and has shown promise in monitoring the development of Tau pathology and improving the understanding of the pathophysiology (Villemagne et al, 2015). However, no clinical studies using Tau PET in patients with TBIs or clinically suspected CTE have been performed on a large population. There is a great interest in developing novel biomarkers for CTE to estimate the prevalence of this disorder, improve diagnostic accuracy, allow the tracking of the disease progression and evaluate the effect of a potential treatment. Indeed, for now the diagnostic of CTE is possible only in post-mortem.

In a population of American football player mostly amyloid negative of 34 to 56 years old, we investigated the binding pattern of [¹⁸F]-AV-1451. We observed a high binding of this p-Tau PET tracer in MTC, amygdala, hippocampus, putamen, thalamus, occipital lobe, temporal lobe, substantia nigra, choroid plexus, white matter and a higher affinity in the pallidum. Also, the subjects have a stronger binding of [¹¹C]-PiB in the area of central gray nucleus, showing significant concomitant amyloid deposition with the [¹⁸F]-AV-1451 binding in the pallidum, putamen and thalamus. The relationship between axonal injury and A β accumulation has already been demonstrated, suggesting a direct relationship between [¹¹C]PiB binding and white matter damage in connected tracts (Scott et al., 2016).

We compared the binding of [¹⁸F]-AV-1451 in the temporal lobe and the pallidum of our TBI group with the binding of the same tracer in a group of control subjects, showing significative differences. The signal observed in the substantia nigra and the choroid plexus seem to correspond to an off-target binding of this tracer (Okamura et al., 2018; Lowe et al., 2016; Ikonomic et al., 2016)

This p-Tau pattern have been reported in few other studies as a 71-year old retired NFL football player who had experienced multiple concussions and presented progressive cognitive impairment (Mitsis et al., 2014). Another 39-year old retired NFL football player with a history of multiple concussions who experienced cognitive decline, irritability and emotional lability (Dickstein et al, 2016) has been studied.

[¹⁸F]-AV-1451 showed increased retention in midbrain, globus pallidus and hippocampus, and also at gray-white matter junctions in multiple cortical areas. This distribution is similar to the postmortem distribution of CTE Tau lesions. These results show similarities with the atrophy of pallidum, putamen and thalamus observed by MRI in a population of TBI patients (Gooijers et al., 2016). Very recently, another study has reported a significantly higher [¹⁸F]-AV-1451 *in vivo* retention in three brain regions (bilateral superior frontal, bilateral medial temporal, and left parietal) in a cohort of 26 former NFL players with cognitive and neuropsychiatric symptoms compared to 31 control subjects (Stern et al., 2019). This last study showed a binding pattern in frontal and parietal lobes not seen in our population. This difference could be explained by our smaller group and probably by a different CTE stage of our subjects compared to theirs. This part will be clarified when we will have a larger group and access to the cognitive assessments of our population allowing us to assume the stage of the disease.

The limitation of this study is the off-target and non specific binding of the tracer [¹⁸F]-AV-1451. The non specific binding in basal ganglia seems to be concomitant with the areas reached by CTE, as the pallidum and may complicate image interpretation. Iron load (quantified using MRI R2*) has been revealed to correlate with [¹⁸F]-AV-1451 binding in the basal ganglia (Choi et al., 2018). A solution to have a better understanding of this binding in the pallidum for these TBI subjects could be to scan the same subjects with [¹⁸F]-MK-6240 to verify that the binding in the pallidum is due to p-Tau protein and not from a non specific binding of [¹⁸F]-AV-1451. The [¹⁸F]-MK-6240 doesn't show this non specific binding in the basal ganglia (Betthausen et al., 2019). Also, the off-target signal in choroid plexus make quantification of hippocampus SUVR challenging.

Each subject of our study will undergo anatomic and functional MRI data in order to access to high level structural sensitivity and changes in functional connectivity. There is growing interest in the potential of combined PET and MRI to shed light on the underlying cellular and molecular processes involved in TBIs. The two modalities are complementary. PET offers uneven sensitivity at a molecular level, while MRI offers excellent soft tissue contrast as well as a number of additional information such as areas of cerebral activation in functional MRI and a mapping of the structural

changes following brain injury. DTI is the most widely used MRI technique for the detection of axonal injury (Niogi et al, 2010). Functional MRI (fMRI) can also reveal functional alterations to the brain after TBIs, such as areas of either reduced or increased activation and altered connectivity (Irimia et al, 2015). We plan to make these correlations between PET and MRI data, and we expect that the deposition rate of the p-Tau protein seen with PET will be correlated to degenerative markers on DTI and synchronization changes in functional connectivity measured with resting-state fMRI, as well as behavioral and psychiatric assessments. These correlations have already been observed in a previous work in our Center on TBIs (Wooten et al, 2019). These findings have demonstrated that synergistic neurobiological information may be gained by interpreting the neuroimaging modalities together instead of separately. Given that TBIs affects 1.5 million people in the United States each year, our multimodal approach will help our comprehension of the full spectrum of TBIs to at last customize diagnostic and therapeutic efforts.

Also, all these subjects of this population at risk of developing this disease underwent cognitive tests. These results will be correlated with the PET imaging findings when the number of subjects will be higher. In the future of this project we will have subjects with different stages of cognitive impairments. This will allows us to observe the different stages of CTE among that TBI population.

In conclusion, p-Tau PET imaging with [¹⁸F]-AV-1451 seem useful in the diagnostic of TBI patients for possible early stages of CTE but still need further investigations. In fact, the non specific binding and off-target of this tracer are overlapping with the areas reached by the pathology. The study on a larger population is required as the noise in the [¹⁸F]-AV-1451 measurement could pose challenges when studying early Tau accumulation.

CONCLUSION AND PERSPECTIVES

In general conclusion of this work, we have demonstrated the potential utility of Tau PET tracers as [¹⁸F]-AV-1451 for the reliable detection/quantification of p-Tau aggregates and disease-progression tracking in AD, while we showed it was still a work in progress for CTE.

We have established that p-Tau PET imaging with [¹⁸F]-AV-1451 was useful in the diagnostic and able to detect the beneficial effect of a non-invasive brain stimulation, called transcranial alternating current stimulation in people with AD. We confirmed our *in vivo* assessments of the binding of this tracer in AD by autoradiography post mortem. The perspective of this work is to study a larger population with cognitive assessments and longer TACs treatments. Also, we will make the comparison of the binding pattern of this PET tracer between images acquired *in vivo* and in post mortem from the same subject. To go further in the characterization of p-Tau PET tracers we will evaluate the pharmacokinetic modeling strategies *in vivo* of PI-2620 as we have already achieved in our Center for AV-1451 (Wooten et al., 2017) and MK-6240 (Guehl et al., 2019).

In addition, in a population of American football players we observed some promise that [¹⁸F]-AV-1451 can detect early stages of CTE but with some lack of efficiency because of the non specific and off target binding of this tracer. These findings don't seem to match the [¹⁸F]-AV-1451 post mortem binding pattern we demonstrated in CTE for this tracer. In perspective of this work, we will study a larger population with different stages of cognitive impairments and we will compare the PET data with cognitive and MRI data from the same subjects to assess a better understanding of this condition. Also it could be useful to perform the same work than with the AD subjects, as the comparison of *in vivo* retention with post mortem binding signal from the same subjects.

This doctoral work has been done in collaboration with :

The Gordon Center for Medical Imaging at Massachusetts General Hospital (MGH) and Harvard Medical School



Laboratoire d'Imagerie Médicale Paris at UPMC Sorbonne University



Acknowledgments

First of all, I would like to thank my thesis director, Mr Georges El Fakhri, for welcoming me to his team, for choosing me for this project and for trusting me throughout these three years. I am also grateful to him for the time he has given me, his sympathy and support, I learned a lot from him and I thank him for all that.

I warmly thank my supervisor, Mr Marc Normandin, for his constant attention to my work, for his sound advice and his listening which have been preponderant for the successful completion of this thesis. His energy, his pedagogical and scientific qualities, his kindness have been a driving force for me. I enjoyed working with him.

I would like to thank the reviewers and the jury members of this thesis, Mme. Aurélie Kas, my co-director for this doctoral work, M. Georges El Fakhri, Mme. Marie-Odile Habert, M. Alain Prigent, M. Vincent Lebon and M. Damien Galanaud.

Of course, achieving these goals would not have been possible without the help of all my co-workers, since I started to work in a lab, I thank all of them and I am really grateful to have worked with each of them.

I wanted to thank M. Nicolas Guehl, Mme. Cinthya Aguero, Mme. Teresa Gomez, M. Sung-Hyun Moon, Mme. Amal Tiss, M. Ramesh Neelamegam, M. Dustin Wooten, Mme. Marina Macdonald-Soccorso, M. Steve Weise, M. Peter Rice, M. Yoann Petibon, M. Emiliano Santarnecchi, Mme. Marion Baillet, Mme. Sandra Chanraud, Mme. Gwenaelle Catheline for their help, mentoring and support in all of these projects.

I wish to thank my parents and my sister especially for their support, love and patience and all my family and friends, they are so many to be there for me that is not possible to enumerate them but I have a thought for each of them.

THANK YOU

References

- Alpert, N. M., D. Berdichevsky, Z. Levin, E. D. Morris, and A. J. Fischman. 1996. "Improved Methods for Image Registration." *NeuroImage*. <https://doi.org/10.1006/ning.1996.0002>.
- Anand, S. S., H. Singh, and A. K. Dash. 2009. "Clinical Applications of PET and PET-CT." *Medical Journal Armed Forces India*. [https://doi.org/10.1016/S0377-1237\(09\)80099-3](https://doi.org/10.1016/S0377-1237(09)80099-3).
- Arima, Kunimasa. 2006. "Ultrastructural Characteristics of Tau Filaments in Tauopathies: Immuno-Electron Microscopic Demonstration of Tau Filaments in Tauopathies." In *Neuropathology*. <https://doi.org/10.1111/j.1440-1789.2006.00669.x>.
- Ariza, Manuela, Hartmuth C. Kolb, Dieder Moechars, Frederik Rombouts, and José Ignacio Andrés. 2015. "Tau Positron Emission Tomography (PET) Imaging: Past, Present, and Future." *Journal of Medicinal Chemistry*. <https://doi.org/10.1021/jm5017544>.
- Arnold, Steven E., Bradley T. Hyman, Jill Flory, Antonio R. Damasio, and Gary W. Van Hoesen. 1991. "The Topographical and Neuroanatomical Distribution of Neurofibrillary Tangles and Neuritic Plaques in the Cerebral Cortex of Patients with Alzheimer's Disease." *Cerebral Cortex*. <https://doi.org/10.1093/cercor/1.1.103>.
- Babiloni, Claudio, Roberta Lizio, Nicola Marzano, Paolo Capotosto, Andrea Soricelli, Antonio Ivano Triggiani, Susanna Cordone, Loreto Gesualdo, and Claudio Del Percio. 2016. "Brain Neural Synchronization and Functional Coupling in Alzheimer's Disease as Revealed by Resting State EEG Rhythms." *International Journal of Psychophysiology*. <https://doi.org/10.1016/j.ijpsycho.2015.02.008>.
- Bailey, Dale L., Felicia Zito, Maria Carla Gilardi, Anna Rita Savi, Ferruccio Fazio, and Terry Jones. 1994. "Performance Comparison of a State-of-the-Art Neuro-SPET Scanner and a Dedicated Neuro-PET Scanner." *European Journal of Nuclear Medicine*. <https://doi.org/10.1007/BF00171411>.
- Bailey, Townsend, Valk. 2006. "Positron emission tomography. Basic sciences." *J. Neuroradiol.*, vol. 33, no. 4, p. 265.
- Baker, Suzanne L., Samuel N. Lockhart, Julie C. Price, Mark He, Ronald H. Huesman, Daniel Schonhaut, Jamie Faria, Gil Rabinovici, and William J. Jagust. 2017. "Reference Tissue-Based Kinetic Evaluation of 18F-AV-1451 for Tau Imaging." *Journal of Nuclear Medicine*. <https://doi.org/10.2967/jnumed.116.175273>.
- Baker, Suzanne L., Theresa M. Harrison, Anne Maass, Renaud La Joie, and William J. Jagust. 2019. "Effect of Off-Target Binding on 18F-Flortaucipir Variability in Healthy Controls across the Life Span." *Journal of Nuclear Medicine*. <https://doi.org/10.2967/jnumed.118.224113>.
- Ballatore, Carlo, Virginia M.Y. Lee, and John Q. Trojanowski. 2007. "Tau-Mediated Neurodegeneration in Alzheimer's Disease and Related Disorders." *Nature Reviews Neuroscience*. <https://doi.org/10.1038/nrn2194>.

- Barrachina, Marta, and Isidre Ferrer. 2009. "DNA Methylation of Alzheimer Disease and Tauopathy-Related Genes in Postmortem Brain." *Journal of Neuropathology and Experimental Neurology*. <https://doi.org/10.1097/NEN.0b013e3181af2e46>.
- Beththausen, Tobey J., Karly A. Cody, Matthew D. Zammit, Dhanabalan Murali, Alexander K. Converse, Todd E. Barnhart, Charles K. Stone, Howard A. Rowley, Sterling C. Johnson, and Bradley T. Christian. 2019. "In Vivo Characterization and Quantification of Neurofibrillary Tau PET Radioligand 18 F-MK-6240 in Humans from Alzheimer Disease Dementia to Young Controls." *Journal of Nuclear Medicine*. <https://doi.org/10.2967/jnumed.118.209650>.
- Binder, Lester I., Anthony Frankfurter, and Lionel I. Rebhun. 1985. "The Distribution of Tau in the Mammalian Central Nervous Central Nervous." *Journal of Cell Biology*. <https://doi.org/10.1083/jcb.101.4.1371>.
- Braak, H., and E. Braak. 1991. "Neuropathological Staging of Alzheimer-Related Changes." *Acta Neuropathologica*. <https://doi.org/10.1007/BF00308809>.
- Braak, Heiko, Irina Alafuzoff, Thomas Arzberger, Hans Kretschmar, and Kelly Tredici. 2006. "Staging of Alzheimer Disease-Associated Neurofibrillary Pathology Using Paraffin Sections and Immunocytochemistry." *Acta Neuropathologica*. <https://doi.org/10.1007/s00401-006-0127-z>.
- Brier, MR; Gordon, B; Friedrichsen, K; McCarthy, J; Stern, A; Christensen, J; Owen, C; Aldea, P; Su, Y; Hassenstab, J; Cairns, NJ; Holtzman, DM; Fagan, AM; Morris, JC; Benzinger, TLS; Ances, BM. 2016. « Tau and Ab imaging, CSF measures, and cognition in Alzheimer's disease .» *Sci Transl Med*, 8: 1-9.
- Brion, J. P., P. van den Bosch de Aguilar, and J. Flament-Durand. 1985. "Senile Dementia of the Alzheimer Type: Morphological and Immunocytochemical Studies." In . https://doi.org/10.1007/978-3-642-70644-8_13.
- Buée-Scherrer, V., P. R. Hof, L. Buée, B. Leveugle, P. Vermersch, D. P. Perl, C. W. Olanow, and A. Delacourte. 1996. "Hyperphosphorylated Tau Proteins Differentiate Corticobasal Degeneration and Pick's Disease." *Acta Neuropathologica*. <https://doi.org/10.1007/s004010050436>.
- Buée, Luc, Thierry Bussière, Valérie Buée-Scherrer, André Delacourte, and Patrick R. Hof. 2000. "Tau Protein Isoforms, Phosphorylation and Role in Neurodegenerative Disorders." *Brain Research Reviews*. [https://doi.org/10.1016/S0165-0173\(00\)00019-9](https://doi.org/10.1016/S0165-0173(00)00019-9).
- Bullich, Santiago, John Seibyl, Ana M. Catafau, Aleksandar Jovalekic, Norman Koglin, Henryk Barthel, Osama Sabri, and Susan De Santi. 2017. "Optimized Classification Of 18F-Florbetaben PET Scans as Positive and Negative Using an SUVR Quantitative Approach and Comparison to Visual Assessment." *NeuroImage: Clinical*. <https://doi.org/10.1016/j.nicl.2017.04.025>.
- Butner, K. A., and M. W. Kirschner. 1991. "Tau Protein Binds to Microtubules through a Flexible Array of Distributed Weak Sites." *Journal of Cell Biology*. <https://doi.org/10.1083/jcb.115.3.717>.

- Cacabelos, R., B. Rodríguez, C. Carrera, J. Caamaño, K. Beyer, J. I. Lao, and M. A. Sellers. 1996. "APOE-Related Frequency of Cognitive and Noncognitive Symptoms in Dementia." *Methods and Findings in Experimental and Clinical Pharmacology*.
- Cagnin, Annachiara, David J. Brooks, Angus M. Kennedy, Roger N. Gunn, R. Myers, Federico E. Turkheimer, Terry Jones, and Richard B. Banati. 2001. "In-Vivo Measurement of Activated Microglia in Dementia." *Lancet*. [https://doi.org/10.1016/S0140-6736\(01\)05625-2](https://doi.org/10.1016/S0140-6736(01)05625-2).
- Chassoux, F., S. Rodrigo, F. Semah, F. Beuvon, E. Landre, B. Devaux, B. Turak, et al. 2010. "FDG-PET Improves Surgical Outcome in Negative MRI Taylor-Type Focal Cortical Dysplasias." *Neurology*. <https://doi.org/10.1212/WNL.0b013e31820203a9>.
- Chen, J., Y. Kanai, N. J. Cowan, and N. Hirokawa. 1992. "Projection Domains of MAP2 and Tau Determine Spacings between Microtubules in Dendrites and Axons." *Nature*. <https://doi.org/10.1038/360674a0>.
- Cherry, Sorenson, and Phelps, *Physics in Nuclear Medicine*. 2012.
- Cho, Hanna, Jae Yong Choi, Mi Song Hwang, You Jin Kim, Hye Mi Lee, Hye Sun Lee, Jae Hoon Lee, Young Hoon Ryu, Myung Sik Lee, and Chul Hyoung Lyoo. 2016. "In Vivo Cortical Spreading Pattern of Tau and Amyloid in the Alzheimer Disease Spectrum." *Annals of Neurology*. <https://doi.org/10.1002/ana.24711>.
- Cho, Jae Hyeon, and Gail V.W. Johnson. 2004. "Glycogen Synthase Kinase 3 β Induces Caspase-Cleaved Tau Aggregation in Situ." *Journal of Biological Chemistry*. <https://doi.org/10.1074/jbc.M403364200>.
- Cho, Jae Hyeon, and Gail V.W. Johnson. 2003. "Glycogen Synthase Kinase 3 β Phosphorylates Tau at Both Primed and Unprimed Sites: Differential Impact on Microtubule Binding." *Journal of Biological Chemistry*. <https://doi.org/10.1074/jbc.M206236200>.
- Cho, Jae-Hyeon, and Gail V. W. Johnson. 2003. "Primed Phosphorylation of Tau at Thr231 by Glycogen Synthase Kinase 3 β (GSK3 β) Plays a Critical Role in Regulating Tau's Ability to Bind and Stabilize Microtubules." *Journal of Neurochemistry*. <https://doi.org/10.1111/j.1471-4159.2004.02155.x>.
- Choi, Jae Yong, Hanna Cho, Sung Jun Ahn, Jae Hoon Lee, Young Hoon Ryu, Myung Sik Lee, and Chul Hyoung Lyoo. 2018. "Off-Target 18 F-AV-1451 Binding in the Basal Ganglia Correlates with Age-Related Iron Accumulation." *Journal of Nuclear Medicine*. <https://doi.org/10.2967/jnumed.117.195248>.
- Cleveland, Don W., Shu Ying Hwo, and Marc W. Kirschner. 1977. "Purification of Tau, a Microtubule-Associated Protein That Induces Assembly of Microtubules from Purified Tubulin." *Journal of Molecular Biology*. [https://doi.org/10.1016/0022-2836\(77\)90213-3](https://doi.org/10.1016/0022-2836(77)90213-3).
- Cleveland, Don W., Shu Ying Hwo, and Marc W. Kirschner. 1977. "Physical and Chemical Properties of Purified Tau Factor and the Role of Tau in Microtubule Assembly." *Journal of Molecular Biology*. [https://doi.org/10.1016/0022-2836\(77\)90214-5](https://doi.org/10.1016/0022-2836(77)90214-5).
- Collins-Praino, Lyndsey E., and Frances Corrigan. 2017. "Does Neuroinflammation Drive the Relationship between Tau Hyperphosphorylation and Dementia

Development Following Traumatic Brain Injury?" *Brain, Behavior, and Immunity*. <https://doi.org/10.1016/j.bbi.2016.09.027>.

Coppola, Giovanni, Subashchandrabose Chinnathambi, Jason Ji Yong Lee, Beth A. Dombroski, Matt C. Baker, Alexandra I. Soto-ortolaza, Suzee E. Lee, et al. 2012. "Evidence for a Role of the Rare p.A152T Variant in Mapt in Increasing the Risk for FTD-Spectrum and Alzheimer's Diseases." *Human Molecular Genetics*. <https://doi.org/10.1093/hmg/dds161>.

Corder, E. H., A. M. Saunders, W. J. Strittmatter, D. E. Schmechel, P. C. Gaskell, G. W. Small, A. D. Roses, J. L. Haines, and M. A. Pericak-Vance. 1993. "Gene Dose of Apolipoprotein E Type 4 Allele and the Risk of Alzheimer's Disease in Late Onset Families." *Science*. <https://doi.org/10.1126/science.8346443>.

Covassin, Tracey, Ryan Moran, and Kristyn Wilhelm. 2013. "Concussion Symptoms and Neurocognitive Performance of High School and College Athletes Who Incur Multiple Concussions." *American Journal of Sports Medicine*. <https://doi.org/10.1177/0363546513499230>.

Critchley, MacDonald. 1957. "Medical Aspects of Boxing, Particularly from a Neurological Standpoint." *British Medical Journal*. <https://doi.org/10.1136/bmj.1.5015.357>.

Davison, Christopher M., and John T. O'Brien. 2014. "A Comparison of FDG-PET and Blood Flow SPECT in the Diagnosis of Neurodegenerative Dementias: A Systematic Review." *International Journal of Geriatric Psychiatry*. <https://doi.org/10.1002/gps.4036>.

Dechow, Schreyogg, Krause, Herrmann, Buck, and Stargardt. 2010. "Economic Evaluation of PET and PET/CT in Oncology: Evidence and Methodologic Approaches." *J. Nucl. Med.*, vol. 51, no. 3, pp. 401–412.

Delacourte, A. 1994. "Pathological Tau Proteins of Alzheimer's Disease as a Biochemical Marker of Neurofibrillary Degeneration." *Biomedicine and Pharmacotherapy*. [https://doi.org/10.1016/0753-3322\(94\)90174-0](https://doi.org/10.1016/0753-3322(94)90174-0).

Delacourte, A., J. P. David, N. Sergeant, L. Buée, A. Wattez, P. Vermersch, F. Ghzali, et al. 1999. "The Biochemical Pathway of Neurofibrillary Degeneration in Aging and Alzheimer's Disease." *Neurology*. <https://doi.org/10.1212/WNL.54.2.538>.

Delacourte, André, Yves Robitaille, Nicolas Sergeant, Luc Buée, Patrick R. Hof, Annick Wattez, Andrée Laroche-Cholette, Jean Mathieu, Pierre Chagnon, and Denis Gauvreau. 1996. "Specific Pathological Tau Protein Variants Characterize Pick's Disease." *Journal of Neuropathology and Experimental Neurology*. <https://doi.org/10.1097/00005072-199602000-00004>.

Devous, Michael D., Abhinay D. Joshi, Michael Navitsky, Sudeepti Southekal, Michael J. Pontecorvo, Haiqing Shen, Ming Lu, et al. 2018. "Test–Retest Reproducibility for the Tau PET Imaging Agent Flortaucipir F 18." *Journal of Nuclear Medicine*. <https://doi.org/10.2967/jnumed.117.200691>.

Dickstein, D. L., M. Y. Pullman, C. Fernandez, J. A. Short, L. Kostakoglu, K. Knesaurek, L. Soleimani, et al. 2016. "Cerebral [18 F]T807/AV1451 Retention

Pattern in Clinically Probable CTE Resembles Pathognomonic Distribution of CTE Tauopathy.” *Translational Psychiatry*. <https://doi.org/10.1038/tp.2016.175>.

Dixit, Ram, Jennifer L. Ross, Yale E. Goldman, and Erika L.F. Holzbaur. 2008. “Differential Regulation of Dynein and Kinesin Motor Proteins by Tau.” *Science*. <https://doi.org/10.1126/science.1152993>.

Dotti, C. G., G. A. Banker, and L. I. Binder. 1987. “The Expression and Distribution of the Microtubule-Associated Proteins Tau and Microtubule-Associated Protein 2 in Hippocampal Neurons in the Rat in Situ and in Cell Culture.” *Neuroscience*. [https://doi.org/10.1016/0306-4522\(87\)90276-4](https://doi.org/10.1016/0306-4522(87)90276-4).

Driessen, Raijmakers, Stuijzand, and Knaapen. 2017. “Myocardial perfusion imaging with PET.” *Int. J. Cardiovasc. Imaging*, vol. 33, no. 7, pp. 1021–1031.

Drubin, David, Summer Kobayashi, and Marc Kirschner. 1986. “Association of Tau Protein with Microtubules in Living Cells.” *Annals of the New York Academy of Sciences*. <https://doi.org/10.1111/j.1749-6632.1986.tb38398.x>.

Dujardin, Simon, Katia Lécolle, Raphaëlle Caillierez, Séverine Bégard, Nadège Zommer, Cédric Lachaud, Sébastien Carrier, et al. 2014. “Neuron-to-Neuron Wild-Type Tau Protein Transfer through a Trans-Synaptic Mechanism: Relevance to Sporadic Tauopathies.” *Acta Neuropathologica Communications*. <https://doi.org/10.1186/2051-5960-2-14>.

Dunker, A. Keith, Christopher J. Oldfield, Jingwei Meng, Pedro Romero, Jack Y. Yang, Jessica Walton Chen, Vladimir Vacic, Zoran Obradovic, and Vladimir N. Uversky. 2008. “The Unfoldomics Decade: An Update on Intrinsically Disordered Proteins.” In *BMC Genomics*. <https://doi.org/10.1186/1471-2164-9-S2-S1>.

Dunker, A. Keith, Israel Silman, Vladimir N. Uversky, and Joel L. Sussman. 2008. “Function and Structure of Inherently Disordered Proteins.” *Current Opinion in Structural Biology*. <https://doi.org/10.1016/j.sbi.2008.10.002>.

Ebneth, A., R. Godemann, K. Stamer, S. Illenberger, B. Trinczek, E. M. Mandelkow, and E. Mandelkow. 1998. “Overexpression of Tau Protein Inhibits Kinesin-Dependent Trafficking of Vesicles, Mitochondria, and Endoplasmic Reticulum: Implications for Alzheimer’s Disease.” *Journal of Cell Biology*. <https://doi.org/10.1083/jcb.143.3.777>.

Edison, Paul, Hilary A. Archer, Alexander Gerhard, Rainer Hinz, Nicola Pavese, Federico E. Turkheimer, Alexander Hammers, et al. 2008. “Microglia, Amyloid, and Cognition in Alzheimer’s Disease: An [¹¹C](R)PK11195-PET and [¹¹C]PIB-PET Study.” *Neurobiology of Disease*. <https://doi.org/10.1016/j.nbd.2008.08.001>.

Edwards, George, Ines Moreno-Gonzalez, and Claudio Soto. 2017. “Amyloid-Beta and Tau Pathology Following Repetitive Mild Traumatic Brain Injury.” *Biochemical and Biophysical Research Communications*. <https://doi.org/10.1016/j.bbrc.2016.07.123>.

Ennulat, D. J., R. K.H. Liem, G. A. Hashim, and M. L. Shelanski. 1989. “Two Separate 18-Amino Acid Domains of Tau Promote the Polymerization of Tubulin.” *Journal of Biological Chemistry*.

Falcon B, Zhang W, Schweighauser M, Murzin AG, Vidal R, Garringer HJ, Ghetti B, Scheres SHW, Goedert M. 2018. «Tau filaments from multiple cases of sporadic and

inherited Alzheimer's disease adopt a common fold. » *Acta Neuropathol.* 136(5):699-708. doi: 10.1007/s00401-018-1914-z.

Falcon B, Zivanov J, Zhang W, Murzin AG, Garringer HJ, Vidal R, Crowther RA, Newell KL, Ghetti B, Goedert M, Scheres SHW. 2019. « Novel tau filament fold in chronic traumatic encephalopathy encloses hydrophobic molecules. » *Nature.* 568(7752):420-423. doi: 10.1038/s41586-019-1026-5.

Farrer, Lindsay A., L. Adrienne Cupples, Jonathan L. Haines, Bradley Hyman, Walter A. Kukull, Richard Mayeux, Richard H. Myers, Margaret A. Pericak-Vance, Neil Risch, and Cornelia M. Van Duijn. 1997. "Effects of Age, Sex, and Ethnicity on the Association between Apolipoprotein E Genotype and Alzheimer Disease: A Meta-Analysis." *Journal of the American Medical Association.* <https://doi.org/10.1001/jama.278.16.1349>.

Ferrer, Isidro, Meritxell Aguiló García, Margarita Carmona, Pol Andrés-Benito, Benjamin Torrejón-Escribano, Paula Garcia-Esparcia, and José Antonio Del Rio. 2019. "Involvement of Oligodendrocytes in Tau Seeding and Spreading in Tauopathies." *Frontiers in Aging Neuroscience.* <https://doi.org/10.3389/fnagi.2019.00112>.

Feurra, Matteo, Giovanni Bianco, Emiliano Santarnecchi, Massimiliano del Testa, Alessandro Rossi, and Simone Rossi. 2011. "Frequency-Dependent Tuning of the Human Motor System Induced by Transcranial Oscillatory Potentials." *Journal of Neuroscience.* <https://doi.org/10.1523/JNEUROSCI.0978-11.2011>.

Feurra, Matteo, Patrizio Pasqualetti, Giovanni Bianco, Emiliano Santarnecchi, Alessandro Rossi, and Simone Rossi. 2013. "State-Dependent Effects of Transcranial Oscillatory Currents on the Motor System: What You Think Matters." *Journal of Neuroscience.* <https://doi.org/10.1523/JNEUROSCI.1414-13.2013>.

Feurra, Matteo, Walter Paulus, Vincent Walsh, and Ryota Kanai. 2011. "Frequency Specific Modulation of Human Somatosensory: Cortex." *Frontiers in Psychology.* <https://doi.org/10.3389/fpsyg.2011.00013>.

Filippi, Luca, Agostino Chiaravalloti, Oreste Bagni, and Orazio Schillaci. 2018. "18F-Labeled Radiopharmaceuticals for the Molecular Neuroimaging of Amyloid Plaques in Alzheimer's Disease." *American Journal of Nuclear Medicine and Molecular Imaging.*

Fischer, Daniela, Marco D. Mukrasch, Jacek Biernat, Stefan Bibow, Martin Blackledge, Christian Griesinger, Eckhard Mandelkow, and Markus Zweckstetter. 2009. "Conformational Changes Specific for Pseudophosphorylation at Serine 262 Selectively Impair Binding of Tau to Microtubules." *Biochemistry.* <https://doi.org/10.1021/bi901090m>.

Fleminger, S., D. L. Oliver, S. Lovestone, S. Rabe-Hesketh, and A. Giora. 2003. "Head Injury as a Risk Factor for Alzheimer's Disease: The Evidence 10 Years on; a Partial Replication." *Journal of Neurology Neurosurgery and Psychiatry.* <https://doi.org/10.1136/jnnp.74.7.857>.

Foster, Norman L., Angela Y. Wang, Tolga Tasdizen, P. Thomas Fletcher, John M. Hoffman, and Robert A. Koeppe. 2008. "Realizing the Potential of Positron Emission Tomography with 18F-Fluorodeoxyglucose to Improve the Treatment of Alzheimer's

Disease.” *Alzheimer’s and Dementia*, 2008. <https://doi.org/10.1016/j.jalz.2007.10.004>.

Fratiglioni, L, L J Launer, K Andersen, M M Breteler, J R Copeland, J F Dartigues, A Lobo, J Martinez-Lage, H Soininen, and A Hofman. 2000. “Incidence of Dementia and Major Subtypes in Europe: A Collaborative Study of Population-Based Cohorts. Neurologic Diseases in the Elderly Research Group.” *Neurology*.

Gao, Huabin, Zhaoli Han, Ruoqing Bai, Shan Huang, Xintong Ge, Fanglian Chen, and Ping Lei. 2017. “The Accumulation of Brain Injury Leads to Severe Neuropathological and Neurobehavioral Changes after Repetitive Mild Traumatic Brain Injury.” *Brain Research*. <https://doi.org/10.1016/j.brainres.2016.11.028>.

Gavett, Brandon E., Robert A. Stern, Robert C. Cantu, Christopher J. Nowinski, and Ann C. McKee. 2010. “Mild Traumatic Brain Injury: A Risk Factor for Neurodegeneration.” *Alzheimer’s Research and Therapy*. <https://doi.org/10.1186/alzrt42>.

Gavett, Brandon E., Robert A. Stern, and Ann C. McKee. 2011. “Chronic Traumatic Encephalopathy: A Potential Late Effect of Sport-Related Concussive and Subconcussive Head Trauma.” *Clinics in Sports Medicine*. <https://doi.org/10.1016/j.csm.2010.09.007>.

Gilman S, Koeppe RA, Little R, An H, Junck L, Giordani B, Persad C, Heumann M, Wernette K. 2005. « Differentiation of Alzheimer's disease from dementia with Lewy bodies utilizing positron emission tomography with [18F]fluorodeoxyglucose and neuropsychological testing. » *Exp Neurol*. 191 Suppl 1:S95-S103.

Goedert, M., and R. Jakes. 1990. “Expression of Separate Isoforms of Human Tau Protein: Correlation with the Tau Pattern in Brain and Effects on Tubulin Polymerization.” *The EMBO Journal*. <https://doi.org/10.1002/j.1460-2075.1990.tb07870.x>.

Goedert, M., M. G. Spillantini, R. Jakes, D. Rutherford, and R. A. Crowther. 1989. “Multiple Isoforms of Human Microtubule-Associated Protein Tau: Sequences and Localization in Neurofibrillary Tangles of Alzheimer’s Disease.” *Neuron*. [https://doi.org/10.1016/0896-6273\(89\)90210-9](https://doi.org/10.1016/0896-6273(89)90210-9).

Goedert, M., M. G. Spillantini, M. C. Potier, J. Ulrich, and R. A. Crowther. 1989. “Cloning and Sequencing of the cDNA Encoding an Isoform of Microtubule-Associated Protein Tau Containing Four Tandem Repeats: Differential Expression of Tau Protein MRNAs in Human Brain.” *The EMBO Journal*. <https://doi.org/10.1002/j.1460-2075.1989.tb03390.x>.

Goedert, Michel, Masami Masuda-Suzukake, and Benjamin Falcon. 2017. “Like Prions: The Propagation of Aggregated Tau and α -Synuclein in Neurodegeneration.” *Brain*. <https://doi.org/10.1093/brain/aww230>.

Goedert, M., C. M. Wischik, R. A. Crowther, J. E. Walker, and A. Klug. 1988. “Cloning and Sequencing of the cDNA Encoding a Core Protein of the Paired Helical Filament of Alzheimer Disease: Identification as the Microtubule-Associated Protein Tau.” *Proceedings of the National Academy of Sciences of the United States of America*. <https://doi.org/10.1073/pnas.85.11.4051>.

Goldgeier, M. H., L. E. Klein, and S. Klein-Angerer. 1984. "The Distribution of Melanocytes in the Leptomeninges of the Human Brain." *Journal of Investigative Dermatology*. <https://doi.org/10.1111/1523-1747.ep12260111>.

Gooijers, Jolien, Sima Chalavi, Kurt Beeckmans, Karla Michiels, Christophe Lafosse, Stefan Sunaert, and Stephan P. Swinnen. 2016. "Subcortical Volume Loss in the Thalamus, Putamen, and Pallidum, Induced by Traumatic Brain Injury, Is Associated with Motor Performance Deficits." *Neurorehabilitation and Neural Repair*. <https://doi.org/10.1177/1545968315613448>.

Grüner, Paamand, Højgaard, and Law. 2011. "Brain perfusion CT compared with ^{15}O - H_2O -PET in healthy subjects," *EJNMMI Res.*, vol. 1, no. 1, p. 28.

Guehl N., Wooten D., Yokell D., Moon SY, Dhaynaut M., Katz S., Moody K., Gharagouzloo C., Kas A., Johnson K., El Fakhri G., Normandin M. 2019. "Evaluation of pharmacokinetic modeling strategies for in-vivo quantification of tau with the radiotracer ^{18}F -MK6240 in human subjects". *Eur J Nucl Med Mol Imaging*.

Gulyás, B., and C. Halldin. 2012. "New PET Radiopharmaceuticals beyond FDG for Brain Tumor Imaging." *Quarterly Journal of Nuclear Medicine and Molecular Imaging*.

Hamelin, Lorraine, Julien Lagarde, Guillaume Dorothée, Claire Leroy, Mickael Labit, Robert A. Comley, Leonardo Cruz De Souza, et al. 2016. "Early and Protective Microglial Activation in Alzheimer's Disease: A Prospective Study Using ^{18}F -DPA-714 PET Imaging." *Brain*. <https://doi.org/10.1093/brain/aww017>.

Hammers A, Koeppe MJ, Hurlemann R. 2002. « Abnormalities of grey and white matter ^{11}C flumazenil binding in temporal lobe epilepsy with normal MRI. » *Brain*; 125:2257–2271.

Hanseuw, Bernard J., Rebecca A. Betensky, Heidi I.L. Jacobs, Aaron P. Schultz, Jorge Sepulcre, J. Alex Becker, Danielle M. Orozco Cosio, et al. 2019. "Association of Amyloid and Tau with Cognition in Preclinical Alzheimer Disease: A Longitudinal Study." *JAMA Neurology*. <https://doi.org/10.1001/jamaneurol.2019.1424>.

Hansen, Allan K., David J. Brooks, and Per Borghammer. 2018. "MAO-B Inhibitors Do Not Block In Vivo Flortaucipir(^{18}F -AV-1451) Binding." *Molecular Imaging and Biology*. <https://doi.org/10.1007/s11307-017-1143-1>.

Harada, Ryuichi, Aiko Ishiki, Hideaki Kai, Naomi Sato, Katsutoshi Furukawa, Shozo Furumoto, Tetsuro Tago, et al. 2018. "Correlations of ^{18}F -THK5351 PET with Postmortem Burden of Tau and Astrogliosis in Alzheimer Disease." *Journal of Nuclear Medicine*. <https://doi.org/10.2967/jnumed.117.197426>.

Harada, Ryuichi, Nobuyuki Okamura, Shozo Furumoto, Katsutoshi Furukawa, Aiko Ishiki, Naoki Tomita, Tetsuro Tago, et al. 2016. " ^{18}F -THK5351: A Novel PET Radiotracer for Imaging Neurofibrillary Pathology in Alzheimer Disease." *Journal of Nuclear Medicine*. <https://doi.org/10.2967/jnumed.115.164848>.

Hebert, Liesi E., Jennifer Weuve, Paul A. Scherr, and Denis A. Evans. 2013. "Alzheimer Disease in the United States (2010-2050) Estimated Using the 2010 Census." *Neurology*. <https://doi.org/10.1212/WNL.ob013e31828726f5>.

- Heiss, W. D. 2000. "Ischemic Penumbra: Evidence from Functional Imaging in Man." *Journal of Cerebral Blood Flow and Metabolism*. <https://doi.org/10.1097/00004647-200009000-00002>.
- Herholz, Karl. 2017. "Brain Tumors: An Update on Clinical PET Research in Gliomas." *Seminars in Nuclear Medicine*. <https://doi.org/10.1053/j.semnuclmed.2016.09.004>.
- Himmler, A, D Drechsel, M W Kirschner, and D W Martin. 1989. "Tau Consists of a Set of Proteins with Repeated C-Terminal Microtubule-Binding Domains and Variable N-Terminal Domains." *Molecular and Cellular Biology*. <https://doi.org/10.1128/mcb.9.4.1381>.
- Hof, P. R., C. Bouras, L. Buée, A. Delacourte, D. P. Perl, and J. H. Morrison. 1992. "Differential Distribution of Neurofibrillary Tangles in the Cerebral Cortex of Dementia Pugilistica and Alzheimer's Disease Cases." *Acta Neuropathologica*. <https://doi.org/10.1007/BF00304630>.
- Hof, Patrick R., Constantin Bouras, Daniel P. Perl, D. Larry Sparks, Nehal Mehta, and John H. Morrison. 1995. "Age-Related Distribution of Neuropathologic Changes in the Cerebral Cortex of Patients with Down's Syndrome: Quantitative Regional Analysis and Comparison with Alzheimer's Disease." *Archives of Neurology*. <https://doi.org/10.1001/archneur.1995.00540280065020>.
- Hoffman, J. M., K. A. Welsh-Bohmer, M. Hanson, B. Crain, C. Hulette, N. Earl, and R. E. Coleman. 2000. "FDG PET Imaging in Patients with Pathologically Verified Dementia." *Journal of Nuclear Medicine*.
- Hooli, B. V., Z. M. Kovacs-Vajna, K. Mullin, M. A. Blumenthal, M. Mattheisen, C. Zhang, C. Lange, G. Mohapatra, L. Bertram, and R. E. Tanzi. 2014. "Rare Autosomal Copy Number Variations in Early-Onset Familial Alzheimer's Disease." *Molecular Psychiatry*. <https://doi.org/10.1038/mp.2013.77>.
- Howell, David R., Louis R. Osternig, and Li Shan Chou. 2013. "Dual-Task Effect on Gait Balance Control in Adolescents with Concussion." *Archives of Physical Medicine and Rehabilitation*. <https://doi.org/10.1016/j.apmr.2013.04.015>.
- Howell, David, Louis Osternig, Paul Van Donkelaar, Ulrich Mayr, and Li Shan Chou. 2013. "Effects of Concussion on Attention and Executive Function in Adolescents." *Medicine and Science in Sports and Exercise*. <https://doi.org/10.1249/MSS.ob013e3182814595>.
- Hwang, Sung Il, Jae Hyoung Kim, Sun Won Park, Moon Hee Han, In Kyu Yu, Sang Hyun Lee, Dong Soo Lee, Sang Kun Lee, Chun Kee Chung, and Kee Hyun Chang. 2001. "Comparative Analysis of MR Imaging, Positron Emission Tomography, and Ictal Single-Photon Emission CT in Patients with Neocortical Epilepsy." *American Journal of Neuroradiology*.
- Hyder, Adnan A., Colleen A. Wunderlich, Prasanthi Puvanachandra, G. Gururaj, and Olive C. Kobusingye. 2007. "The Impact of Traumatic Brain Injuries: A Global Perspective." *NeuroRehabilitation*.
- Iaccarino, Hannah F., Annabelle C. Singer, Anthony J. Martorell, Andrii Rudenko, Fan Gao, Tyler Z. Gillingham, Hansruedi Mathys, et al. 2016. "Gamma Frequency

Entrainment Attenuates Amyloid Load and Modifies Microglia.” *Nature*. <https://doi.org/10.1038/nature20587>.

Ibrahim, Nevein, Joanna Kusmirek, Aaron F Struck, John M Floberg, Scott B Perlman, Catherine Gallagher, and Lance T Hall. 2016. “The Sensitivity and Specificity of F-DOPA PET in a Movement Disorder Clinic.” *American Journal of Nuclear Medicine and Molecular Imaging*.

Ikonomovic, Milos D., Eric E. Abrahamson, Julie C. Price, Chester A. Mathis, and William E. Klunk. 2016. “[F-18]AV-1451 Positron Emission Tomography Retention in Choroid Plexus: More than ‘off-Target’ Binding.” *Annals of Neurology*. <https://doi.org/10.1002/ana.24706>.

Ingelsson, M., H. Fukumoto, K. L. Newell, J. H. Growdon, E. T. Hedley-Whyte, M. P. Frosch, M. S. Albert, B. T. Hyman, and M. C. Irizarry. 2004. “Early A β Accumulation and Progressive Synaptic Loss, Gliosis, and Tangle Formation in AD Brain.” *Neurology*. <https://doi.org/10.1212/01.WNL.0000115115.98960.37>.

Irimia, Andrei, and John Darrell Van Horn. 2015. “Functional Neuroimaging of Traumatic Brain Injury: Advances and Clinical Utility.” *Neuropsychiatric Disease and Treatment*. <https://doi.org/10.2147/NDT.S79174>.

Ishihara, Takeshi, Ming Hong, Bin Zhang, Yasushi Nakagawa, Michael K. Lee, John Q. Trojanowski, and Virginia M.Y. Lee. 1999. “Age-Dependent Emergence and Progression of a Tauopathy in Transgenic Mice Overexpressing the Shortest Human Tau Isoform.” *Neuron*. [https://doi.org/10.1016/S0896-6273\(00\)81127-7](https://doi.org/10.1016/S0896-6273(00)81127-7).

Ishii, K. 2014. “Pet Approaches for Diagnosis of Dementia.” *American Journal of Neuroradiology*. <https://doi.org/10.3174/ajnr.A3695>.

Ittner, Lars M., Thomas Fath, Yazı D. Ke, Mian Bi, Janet Van Eersel, Kong M. Li, Peter Gunning, and Jürgen Götz. 2008. “Parkinsonism and Impaired Axonal Transport in a Mouse Model of Frontotemporal Dementia.” *Proceedings of the National Academy of Sciences of the United States of America*. <https://doi.org/10.1073/pnas.0808084105>.

Ittner, Lars M., and Jürgen Götz. 2011. “Amyloid- β and Tau - A Toxic Pas de Deux in Alzheimer’s Disease.” *Nature Reviews Neuroscience*. <https://doi.org/10.1038/nrn2967>.

Ittner, Lars M., Yazı D. Ke, Fabien Delerue, Mian Bi, Amadeus Gladbach, Janet van Eersel, Heidrun Wölfing, et al. 2010. “Dendritic Function of Tau Mediates Amyloid- β Toxicity in Alzheimer’s Disease Mouse Models.” *Cell*. <https://doi.org/10.1016/j.cell.2010.06.036>.

Iwata, Atsushi, Kenichi Nagata, Hiroyuki Hatsuta, Hiroshi Takuma, Miki Bundo, Kazuya Iwamoto, Akira Tamaoka, Shigeo Murayama, Takaomi Saido, and Shoji Tsuji. 2014. “Altered CpG Methylation in Sporadic Alzheimer’s Disease Is Associated with APP and MAPT Dysregulation.” *Human Molecular Genetics*. <https://doi.org/10.1093/hmg/ddt451>.

Jack, Clifford R., Heather J. Wiste, Timothy G. Lesnick, Stephen D. Weigand, David S. Knopman, Prashanthi Vemuri, Vernon S. Pankratz, et al. 2013. “Brain β -Amyloid

Load Approaches a Plateau.” *Neurology*. <https://doi.org/10.1212/WNL.obo13e3182840bbe>.

Jack, Clifford R, Heather J Wiste, Hugo Botha, Stephen D Weigand, Terry M Therneau, David S Knopman, Jonathan Graff-Radford, et al. 2019. “The Bivariate Distribution of Amyloid- β and Tau: Relationship with Established Neurocognitive Clinical Syndromes.” *Brain*. <https://doi.org/10.1093/brain/awz268>.

Jack, Clifford R., Jorge R. Barrio, and Vladimir Kepe. 2013. “Cerebral Amyloid PET Imaging in Alzheimer’s Disease.” *Acta Neuropathologica*. <https://doi.org/10.1007/s00401-013-1185-7>.

James, Bryan D., Sue E. Leurgans, Liesi E. Hebert, Paul A. Scherr, Kristine Yaffe, and David A. Bennett. 2014. “Contribution of Alzheimer Disease to Mortality in the United States.” *Neurology*. <https://doi.org/10.1212/WNL.000000000000240>.

Johnson, Keith A., Aaron Schultz, Rebecca A. Betensky, J. Alex Becker, Jorge Sepulcre, Dorene Rentz, Elizabeth Mormino, et al. 2016. “Tau Positron Emission Tomographic Imaging in Aging and Early Alzheimer Disease.” *Annals of Neurology*. <https://doi.org/10.1002/ana.24546>.

Jones, Terry. 1996. “The Role of Positron Emission Tomography within the Spectrum of Medical Imaging.” *European Journal of Nuclear Medicine*. <https://doi.org/10.1007/BF01731847>.

Jones and Townsend. 2017. “History and future technical innovation in positron emission tomography.” *J. Med. Imaging*, vol. 4, no. 1, p. 011013.

Jucker, Mathias, and Lary C. Walker. 2011. “Pathogenic Protein Seeding in Alzheimer Disease and Other Neurodegenerative Disorders.” *Annals of Neurology*. <https://doi.org/10.1002/ana.22615>.

Kanai, Ryota, Leila Chaieb, Andrea Antal, Vincent Walsh, and Walter Paulus. 2008. “Frequency-Dependent Electrical Stimulation of the Visual Cortex.” *Current Biology*. <https://doi.org/10.1016/j.cub.2008.10.027>.

Killin, Lewis O.J., John M. Starr, Ivy J. Shiue, and Tom C. Russ. 2016. “Environmental Risk Factors for Dementia: A Systematic Review.” *BMC Geriatrics*. <https://doi.org/10.1186/s12877-016-0342-y>.

Klunk, William E., Henry Engler, Agneta Nordberg, Yanming Wang, Gunnar Blomqvist, Daniel P. Holt, Mats Bergström, et al. 2004. “Imaging Brain Amyloid in Alzheimer’s Disease with Pittsburgh Compound-B.” *Annals of Neurology*. <https://doi.org/10.1002/ana.20009>.

Kosik, Kenneth S., James E. Crandall, Elliott J. Mufson, and Rachael L. Neve. 1989. “Tau in Situ Hybridization in Normal and Alzheimer Brain: Localization in the Somatodendritic Compartment.” *Annals of Neurology*. <https://doi.org/10.1002/ana.410260308>.

Kreisl, William C., Chul Hyung Lyoo, Meghan McGwier, Joseph Snow, Kimberly J. Jenko, Nobuyo Kimura, Winston Corona, et al. 2013. “In Vivo Radioligand Binding to Translocator Protein Correlates with Severity of Alzheimer’s Disease.” *Brain*. <https://doi.org/10.1093/brain/awt145>.

- Kuhl DE, Metter EJ, Riege WH, Phelps ME. 1982. « Effects of human aging on patterns of local cerebral glucose utilization determined by the [18F]fluorodeoxyglucose method. » *J Cereb Blood Flow Metab.* 1982;2(2):163-71.
- Lancelot, Sophie, and Luc Zimmer. 2010. “Small-Animal Positron Emission Tomography as a Tool for Neuropharmacology.” *Trends in Pharmacological Sciences.* <https://doi.org/10.1016/j.tips.2010.06.002>.
- Lee, Gloria, Rachael L. Neve, and Kenneth S. Kosik. 1989. “The Microtubule Binding Domain of Tau Protein.” *Neuron.* [https://doi.org/10.1016/0896-6273\(89\)90050-0](https://doi.org/10.1016/0896-6273(89)90050-0).
- Lee KK, Salamon N. 2009. « [18F] fluorodeoxyglucose-positron-emission tomography and MR imaging coregistration for presurgical evaluation of medically refractory epilepsy. » *AJNR Am J Neuroradiol.* 30(10):1811-6. doi: 10.3174/ajnr.A1637.
- Levy-Lahad, Ephrat, Wilma Wasco, Parvoneh Poorkaj, Donna M. Romano, Junko Oshima, Warren H. Pettingell, Chang En Yu, et al. 1995. “Candidate Gene for the Chromosome 1 Familial Alzheimer’s Disease Locus.” *Science.* <https://doi.org/10.1126/science.7638622>.
- Levy-Lahad, Ephrat, Ellen M. Wijsman, Ellen Nemens, Leojean Anderson, Katrina A.B. Goddard, James L. Weber, Thomas D. Bird, and Gerard D. Schellenberg. 1995. “A Familial Alzheimer’s Disease Locus on Chromosome I.” *Science.* <https://doi.org/10.1126/science.7638621>.
- Lewis, D. A., M. J. Campbell, R. D. Terry, and J. H. Morrison. 1987. “Laminar and Regional Distributions of Neurofibrillary Tangles and Neuritic Plaques in Alzheimer’s Disease: A Quantitative Study of Visual and Auditory Cortices.” *Journal of Neuroscience.* <https://doi.org/10.1523/jneurosci.07-06-01799.1987>.
- Liddelow, Shane A., Kevin A. Guttenplan, Laura E. Clarke, Frederick C. Bennett, Christopher J. Bohlen, Lucas Schirmer, Mariko L. Bennett, et al. 2017. “Neurotoxic Reactive Astrocytes Are Induced by Activated Microglia.” *Nature.* <https://doi.org/10.1038/nature21029>.
- Liu, Chang, and Jürgen Götz. 2013. “Profiling Murine Tau with 0N, 1N and 2N Isoform-Specific Antibodies in Brain and Peripheral Organs Reveals Distinct Subcellular Localization, with the 1N Isoform Being Enriched in the Nucleus.” *PLoS ONE.* <https://doi.org/10.1371/journal.pone.0084849>.
- Liu, Fei, Bin Li, E. Jan Tung, Inge Grundke-Iqbal, Khalid Iqbal, and Cheng Xin Gong. 2007. “Site-Specific Effects of Tau Phosphorylation on Its Microtubule Assembly Activity and Self-Aggregation.” *European Journal of Neuroscience.* <https://doi.org/10.1111/j.1460-9568.2007.05955.x>.
- Lois, Cristina, Ivan Gonzalez, Keith A. Johnson, and Julie C. Price. 2019. “PET Imaging of Tau Protein Targets: A Methodology Perspective.” *Brain Imaging and Behavior.* <https://doi.org/10.1007/s11682-018-9847-7>.
- Lopresti, Brian J., William E. Klunk, Chester A. Mathis, Jessica A. Hoge, Scott K. Ziolko, Xueling Lu, Carolyn C. Meltzer, et al. 2005. “Simplified Quantification of Pittsburgh Compound B Amyloid Imaging PET Studies: A Comparative Analysis.” *Journal of Nuclear Medicine.*

Lopresti, Patrizia, Sara Szuchet, Sozos Ch Papasozomenos, Raymond P. Zinkowski, and Lester I. Binder. 1995. "Functional Implications for the Microtubule-Associated Protein Tau: Localization in Oligodendrocytes." *Proceedings of the National Academy of Sciences of the United States of America*. <https://doi.org/10.1073/pnas.92.22.10369>.

Love, Seth, Leslie R. Bridges, and C. Patrick Case. 1995. "Neurofibrillary Tangles in Niemann - Pick Disease Type C." *Brain*. <https://doi.org/10.1093/brain/118.1.119>.

Lowe, Val J., Geoffrey Curran, Ping Fang, Amanda M. Liesinger, Keith A. Josephs, Joseph E. Parisi, Kejal Kantarci, et al. 2016. "An Autoradiographic Evaluation of AV-1451 Tau PET in Dementia." *Acta Neuropathologica Communications*. <https://doi.org/10.1186/s40478-016-0315-6>.

Maas, Thorsten, Jochen Eidenmüller, and Roland Brandt. 2000. "Interaction of Tau with the Neural Membrane Cortex Is Regulated by Phosphorylation at Sites That Are Modified in Paired Helical Filaments." *Journal of Biological Chemistry*. <https://doi.org/10.1074/jbc.M000389200>.

Mandelkow, Eva Maria, E. Thies, and E. Mandelkow. 2007. "Tau and Axonal Transport." In *Alzheimer's Disease: Advances in Genetics, Molecular and Cellular Biology*. https://doi.org/10.1007/978-0-387-35135-3_14.

Mandelkow, Eva Maria, and Eckhard Mandelkow. 2011. "Biochemistry and Cell Biology of Tau Protein in Neurofibrillary Degeneration." *Cold Spring Harbor Perspectives in Biology*. <https://doi.org/10.1101/cshperspect.a006247>.

Marquié M, Normandin MD, Vanderburg CR, Costantino IM, Bien EA, Rycyna LG, Klunk WE, Mathis CA, Ikonomic MD, Debnath ML, Vasdev N, Dickerson BC, Gomperts SN, Growdon JH, Johnson KA, Frosch MP, Hyman BT, Gómez-Isla T. 2015. « Validating novel tau positron emission tomography tracer [F-18]-AV-1451 (T807) on postmortem brain tissue. » *Ann Neurol*. Nov;78(5):787-800. doi: 10.1002/ana.24517.

Marquié M, Verwer EE, Meltzer AC, Kim SJW, Agüero C, Gonzalez J, Makaretz SJ, Siao Tick Chong M, Ramanan P, Amaral AC, Normandin MD, Vanderburg CR, Gomperts SN, Johnson KA, Frosch MP, Gómez-Isla T. 2017. « Lessons learned about [F-18]-AV-1451 off-target binding from an autopsy-confirmed Parkinson's case. » *Acta Neuropathol Commun*. 19;5(1):75. doi: 10.1186/s40478-017-0482-0.

Marquié M, Normandin MD, Meltzer AC, Siao Tick Chong M, Andrea NV, Antón-Fernández A, Klunk WE, Mathis CA, Ikonomic MD, Debnath M, Bien EA, Vanderburg CR, Costantino I, Makaretz S, DeVos SL, Oakley DH, Gomperts SN, Growdon JH, Domoto-Reilly K, Lucente D, Dickerson BC, Frosch MP, Hyman BT, Johnson KA, Gómez-Isla T. 2017. « Pathological correlations of [F-18]-AV-1451 imaging in non-alzheimer tauopathies. » *Ann Neurol*. 81(1):117-128. doi: 10.1002/ana.24844.

Marquié M, Siao Tick Chong M, Antón-Fernández A, Verwer EE, Sáez-Calveras N, Meltzer AC, Ramanan P, Amaral AC, Gonzalez J, Normandin MD, Frosch MP, Gómez-Isla T. 2017. « [F-18]-AV-1451 binding correlates with postmortem neurofibrillary tangle Braak staging. » *Acta Neuropathol*. 134(4):619-628. doi: 10.1007/s00401-017-1740-8.

- McCrorry, Paul. 2013. "Traumatic Brain Injury: Revisiting the AAN Guidelines on Sport-Related Concussion." *Nature Reviews Neurology*. <https://doi.org/10.1038/nrneurol.2013.88>.
- McKee, Ann C., Michael L. Alosco, and Bertrand R. Huber. 2016. "Repetitive Head Impacts and Chronic Traumatic Encephalopathy." *Neurosurgery Clinics of North America*. <https://doi.org/10.1016/j.nec.2016.05.009>.
- McKee, Ann C., Robert C. Cantu, Christopher J. Nowinski, E. Tessa Hedley-Whyte, Brandon E. Gavett, Andrew E. Budson, Veronica E. Santini, Hyo Soon Lee, Caroline A. Kubitius, and Robert A. Stern. 2009. "Chronic Traumatic Encephalopathy in Athletes: Progressive Tauopathy after Repetitive Head Injury." *Journal of Neuropathology and Experimental Neurology*. <https://doi.org/10.1097/NEN.0b013e3181a9d503>.
- McKee, Ann C., Thor D. Stein, Christopher J. Nowinski, Robert A. Stern, Daniel H. Daneshvar, Victor E. Alvarez, Hyo Soon Lee, et al. 2013. "The Spectrum of Disease in Chronic Traumatic Encephalopathy." *Brain*. <https://doi.org/10.1093/brain/aws307>.
- McKhann, Guy M., David S. Knopman, Howard Chertkow, Bradley T. Hyman, Clifford R. Jack, Claudia H. Kawas, William E. Klunk, et al. 2011. "The Diagnosis of Dementia Due to Alzheimer's Disease: Recommendations from the National Institute on Aging-Alzheimer's Association Workgroups on Diagnostic Guidelines for Alzheimer's Disease." *Alzheimer's and Dementia*. <https://doi.org/10.1016/j.jalz.2011.03.005>.
- Menamee, Rebecca L., Seong Hwan Yee, Julie C. Price, William E. Klunk, Bedda Rosario, Lisa Weissfeld, Scott Ziolko, et al. 2009. "Consideration of Optimal Time Window for Pittsburgh Compound B PET Summed Uptake Measurements." *Journal of Nuclear Medicine*. <https://doi.org/10.2967/jnumed.108.057612>.
- Minoshima, Satoshi, Norman L. Foster, Anders A.F. Sima, Kirk A. Frey, Roger L. Albin, and David E. Kuhl. 2001. "Alzheimer's Disease versus Dementia with Lewy Bodies: Cerebral Metabolic Distinction with Autopsy Confirmation." *Annals of Neurology*. <https://doi.org/10.1002/ana.1133>.
- Mishra, Shruti, Brian A. Gordon, Yi Su, Jon Christensen, Karl Friedrichsen, Kelley Jackson, Russ Hornbeck, et al. 2017. "AV-1451 PET Imaging of Tau Pathology in Preclinical Alzheimer Disease: Defining a Summary Measure." *NeuroImage*. <https://doi.org/10.1016/j.neuroimage.2017.07.050>.
- Mitsis, E. M., S. Riggio, L. Kostakoglu, D. L. Dickstein, J. Machac, B. Delman, M. Goldstein, et al. 2014. "Tauopathy PET and Amyloid PET in the Diagnosis of Chronic Traumatic Encephalopathies: Studies of a Retired NFL Player and of a Man with FTD and a Severe Head Injury." *Translational Psychiatry*. <https://doi.org/10.1038/tp.2014.91>.
- Mondragón-Rodríguez, Siddhartha, Emilie Trillaud-Doppia, Anthony Dudilot, Catherine Bourgeois, Michel Lauzon, Nicole Leclerc, and Jannic Boehm. 2012. "Interaction of Endogenous Tau Protein with Synaptic Proteins Is Regulated by N-Methyl-D-Aspartate Receptor-Dependent Tau Phosphorylation." *Journal of Biological Chemistry*. <https://doi.org/10.1074/jbc.M112.401240>.

- Mosconi, Lisa, Susan De Santi, Yi Li, Juan Li, Jiong Zhan, Hon Tsui Wai, Madhu Boppana, Alberto Pupi, and Mony J. De Leon. 2006. "Visual Rating of Medial Temporal Lobe Metabolism in Mild Cognitive Impairment and Alzheimer's Disease Using FDG-PET." *European Journal of Nuclear Medicine and Molecular Imaging*. <https://doi.org/10.1007/s00259-005-1956-z>.
- Mukrasch, Marco D., Stefan Bibow, Jegannath Korukottu, Sadasivam Jeganathan, Jacek Biernat, Christian Griesinger, Eckhard Mandelkow, and Markus Zweckstetter. 2009. "Structural Polymorphism of 441-Residue Tau at Single Residue Resolution." *PLoS Biology*. <https://doi.org/10.1371/journal.pbio.1000034>.
- Myers, A. J., M. Kaleem, L. Marlowe, A. M. Pittman, A. J. Lees, H. C. Fung, J. Duckworth, et al. 2005. "The H1c Haplotype at the MAPT Locus Is Associated with Alzheimer's Disease." *Human Molecular Genetics*. <https://doi.org/10.1093/hmg/ddi241>.
- Myers, Amanda J., Alan M. Pittman, Alice S. Zhao, Kristen Rohrer, Mona Kaleem, Lauren Marlowe, Andrew Lees, et al. 2007. "The MAPT H1c Risk Haplotype Is Associated with Increased Expression of Tau and Especially of 4 Repeat Containing Transcripts." *Neurobiology of Disease*. <https://doi.org/10.1016/j.nbd.2006.10.018>.
- Mylonas, Efstratios, Antje Hascher, Pau Bernadó, Martin Blackledge, Eckhard Mandelkow, and Dmitri I. Svergun. 2008. "Domain Conformation of Tau Protein Studied by Solution Small-Angle X-Ray Scattering." *Biochemistry*. <https://doi.org/10.1021/bi800900d>.
- Namjoshi, Dhananjay R., Craig Good, Wai Hang Cheng, William Panenka, Darrin Richards, Peter A. Cripton, and Cheryl L. Wellington. 2013. "Towards Clinical Management of Traumatic Brain Injury: A Review of Models and Mechanisms from a Biomechanical Perspective." *DMM Disease Models and Mechanisms*. <https://doi.org/10.1242/dmm.011320>.
- Neve, Rachael L., Peter Harris, Kenneth S. Kosik, David M. Kurnit, and Timothy A. Donlon. 1986. "Identification of cDNA Clones for the Human Microtubule-Associated Protein Tau and Chromosomal Localization of the Genes for Tau and Microtubule-Associated Protein 2." *Molecular Brain Research*. [https://doi.org/10.1016/0169-328X\(86\)90033-1](https://doi.org/10.1016/0169-328X(86)90033-1).
- Ng, Kok Pin, Tharick A. Pascoal, Sulantha Mathotaarachchi, Joseph Therriault, Min Su Kang, Monica Shin, Marie Christine Guiot, et al. 2017. "Monoamine Oxidase B Inhibitor, Selegiline, Reduces 18F-THK5351 Uptake in the Human Brain." *Alzheimer's Research and Therapy*. <https://doi.org/10.1186/s13195-017-0253-y>.
- Nimmerjahn, Axel, Frank Kirchhoff, and Fritjof Helmchen. 2005. "Neuroscience: Resting Microglial Cells Are Highly Dynamic Surveillants of Brain Parenchyma in Vivo." *Science*. <https://doi.org/10.1126/science.1110647>.
- Niogi, Sumit, Pratik Mukherjee, Jamshid Ghajar, and Bruce D. McCandliss. 2010. "Individual Differences in Distinct Components of Attention Are Linked to Anatomical Variations in Distinct White Matter Tracts." *Frontiers in Neuroanatomy*. <https://doi.org/10.3389/neuro.05.002.2010>.

- Noble, Wendy, Diane P. Hanger, Christopher C.J. Miller, and Simon Lovestone. 2013. "The Importance of Tau Phosphorylation for Neurodegenerative Diseases." *Frontiers in Neurology*. <https://doi.org/10.3389/fneur.2013.00083>.
- Nuzzo, Domenico, Pasquale Picone, Luca Caruana, Sonya Vasto, Annalisa Barera, Calogero Caruso, and Marta Di Carlo. 2014. "Inflammatory Mediators as Biomarkers in Brain Disorders." *Inflammation*. <https://doi.org/10.1007/s10753-013-9780-2>.
- Okamura, Nobuyuki, Ryuichi Harada, Katsutoshi Furukawa, Shozo Furumoto, Tetsuro Tago, Kazuhiko Yanai, Hiroyuki Arai, and Yukitsuka Kudo. 2016. "Advances in the Development of Tau PET Radiotracers and Their Clinical Applications." *Ageing Research Reviews*. <https://doi.org/10.1016/j.arr.2015.12.010>.
- Okamura, Nobuyuki, Ryuichi Harada, Aiko Ishiki, Akio Kikuchi, Tadahiko Nakamura, and Yukitsuka Kudo. 2018. "The Development and Validation of Tau PET Tracers: Current Status and Future Directions." *Clinical and Translational Imaging*. <https://doi.org/10.1007/s40336-018-0290-y>.
- Ortega, Ricard L., Farida Dakterzada, Alfonso Arias, Ester Blasco, Alba Naudí, Francisco P. Garcia, and Gerard Piñol-Ripoll. 2019. "Usefulness of CSF Biomarkers in Predicting the Progression of Amnesic and Nonamnesic Mild Cognitive Impairment to Alzheimer's Disease." *Current Aging Science*. <https://doi.org/10.2174/1874609812666190112095430>.
- Ossenkoppele, Rik, Gil D. Rabinovici, Ruben Smith, Hanna Cho, Michael Scholl, Olof Strandberg, Sebastian Palmqvist, et al. 2018. "Discriminative Accuracy of [18 F]Flortaucipir Positron Emission Tomography for Alzheimer Disease vs Other Neurodegenerative Disorders." *JAMA - Journal of the American Medical Association*. <https://doi.org/10.1001/jama.2018.12917>.
- Ouyang, Yu, Martin S. Judenhofer, Jeffrey H. Walton, Jan Marik, Simon P. Williams, and Simon R. Cherry. 2015. "Simultaneous PET/MRI Imaging during Mouse Cerebral Hypoxia-Ischemia." *Journal of Visualized Experiments*. <https://doi.org/10.3791/52728>.
- Padma, M. Vasantha, S. Said, M. Jacobs, D. R. Hwang, K. Dunigan, M. Satter, B. Christian, et al. 2003. "Prediction of Pathology and Survival by FDG PET in Gliomas." *Journal of Neuro-Oncology*. <https://doi.org/10.1023/A:1025665820001>.
- Passchier, Jan, Antony Gee, Antoon Willemsen, Willem Vaalburg, and Aren Van Waarde. 2002. "Measuring Drug-Related Receptor Occupancy with Positron Emission Tomography." *Methods*. [https://doi.org/10.1016/S1046-2023\(02\)00084-1](https://doi.org/10.1016/S1046-2023(02)00084-1).
- Pellman, Elliot J., David C. Viano, Ira R. Casson, Andrew M. Tucker, Joseph F. Waeckerle, John W. Powell, Henry Feuer, et al. 2004. "Concussion in Professional Football: Repeat Injuries - Part 4." *Neurosurgery*. <https://doi.org/10.1227/01.NEU.0000137657.00146.7D>.
- Pérez, Mar, Jesús Avila, and Félix Hernández. 2019. "Propagation of Tau via Extracellular Vesicles." *Frontiers in Neuroscience*. <https://doi.org/10.3389/fnins.2019.00698>.
- Pontecorvo, Michael J., Michael D. Devous, Michael Navitsky, Ming Lu, Stephen Salloway, Frederick W. Schaerf, Danna Jennings, et al. 2017. "Relationships between

Flortaucipir PET Tau Binding and Amyloid Burden, Clinical Diagnosis, Age and Cognition.” *Brain*. <https://doi.org/10.1093/brain/aww334>.

Rabinovici, Gil D., Constantine Gatsonis, Charles Apgar, Kiran Chaudhary, Ilana Gareen, Lucy Hanna, James Hendrix, et al. 2019. “Association of Amyloid Positron Emission Tomography with Subsequent Change in Clinical Management among Medicare Beneficiaries with Mild Cognitive Impairment or Dementia.” *JAMA - Journal of the American Medical Association*. <https://doi.org/10.1001/jama.2019.2000>.

Rajendran. 2003. “[¹⁸F]FMISO and [¹⁸F]FDG PET imaging in soft tissue sarcomas: correlation of hypoxia, metabolism and VEGF expression.” *Eur. J. Nucl. Med. Mol. Imaging*, vol. 30, no. 5, pp. 695–704.

Reynolds, Bryson B., James Patrie, Erich J. Henry, Howard P. Goodkin, Donna K. Broshek, Max Wintermark, and T. Jason Druzgal. 2017. “Comparative Analysis of Head Impact in Contact and Collision Sports.” *Journal of Neurotrauma*. <https://doi.org/10.1089/neu.2015.4308>.

Reynolds, Erin, Vanessa C. Fazio, Natalie Sandel, Philip Schatz, and Luke C. Henry. 2016. “Cognitive Development and the Immediate Postconcussion Assessment and Cognitive Testing: A Case for Separate Norms in Preadolescents.” *Applied Neuropsychology: Child*. <https://doi.org/10.1080/21622965.2015.1057637>.

Rossini, P. M., D. Burke, R. Chen, L. G. Cohen, Z. Daskalakis, R. Di Iorio, V. Di Lazzaro, et al. 2015. “Non-Invasive Electrical and Magnetic Stimulation of the Brain, Spinal Cord, Roots and Peripheral Nerves: Basic Principles and Procedures for Routine Clinical and Research Application: An Updated Report from an I.F.C.N. Committee.” *Clinical Neurophysiology*. <https://doi.org/10.1016/j.clinph.2015.02.001>.

Ryman, Davis C., Natalia Acosta-Baena, Paul S. Aisen, Thomas Bird, Adrian Danek, Nick C. Fox, Alison Goate, et al. 2014. “Symptom Onset in Autosomal Dominant Alzheimer Disease: A Systematic Review and Meta-Analysis.” *Neurology*. <https://doi.org/10.1212/WNL.0000000000000596>.

Saint-Aubert, Laure, Laetitia Lemoine, Konstantinos Chiotis, Antoine Leuzy, Elena Rodriguez-Vieitez, and Agneta Nordberg. 2017. “Tau PET Imaging: Present and Future Directions.” *Molecular Neurodegeneration*. <https://doi.org/10.1186/s13024-017-0162-3>.

Sander, K; Lashley, T; Gami, P; Gendron, T; Lythgoe, MF; Rohrer, JD; Schott, JM; Revesz, T; Fox, NC; Arstad, E. 2016. « Characterization of tau positron emission tomography tracer [¹⁸F]AV-1451 binding to postmortem tissue in Alzheimer's disease, primary tauopathies, and other dementias. » *Alzheimers Dement*, 12: 1116-24.

Santaracchi, E., A. Biasella, E. Tatti, A. Rossi, D. Prattichizzo, and S. Rossi. 2017. “High-Gamma Oscillations in the Motor Cortex during Visuo-Motor Coordination: A TACS Interferential Study.” *Brain Research Bulletin*. <https://doi.org/10.1016/j.brainresbull.2017.03.006>.

Santaracchi, E., T. Muller, S. Rossi, A. Sarkar, N. R. Polizzotto, A. Rossi, and R. Cohen Kadosh. 2016. “Individual Differences and Specificity of Prefrontal Gamma

Frequency-TACS on Fluid Intelligence Capabilities.” *Cortex*. <https://doi.org/10.1016/j.cortex.2015.11.003>.

Santarneccchi, Emiliano, Nicola Riccardo Polizzotto, Marco Godone, Fabio Giovannelli, Matteo Feurra, Laura Matzen, Alessandro Rossi, and Simone Rossi. 2013. “Frequency-Dependent Enhancement of Fluid Intelligence Induced by Transcranial Oscillatory Potentials.” *Current Biology*. <https://doi.org/10.1016/j.cub.2013.06.022>.

Schellenberg, Gerard D., Thomas D. Bird, Ellen M. Wijsman, Harry T. Orr, Leojean Anderson, Ellen Nemens, June A. White, et al. 1992. “Genetic Linkage Evidence for a Familial Alzheimer’s Disease Locus on Chromosome 14.” *Science*. <https://doi.org/10.1126/science.1411576>.

Schindler, Schelbert, Quercioli, and Dilsizian. 2010. “Cardiac PET Imaging for the Detection and Monitoring of Coronary Artery Disease and Microvascular Health.” *JACC Cardiovasc. Imaging*, vol. 3, no. 6, pp. 623 LP – 640.

Schmidt, M. L., V. Zhukareva, K. L. Newell, V. M.Y. Lee, and J. Q. Trojanowski. 2001. “Tau Isoform Profile and Phosphorylation State in Dementia Pugilistica Recapitulate Alzheimer’s Disease.” *Acta Neuropathologica*. <https://doi.org/10.1007/s004010000330>.

Schöll, Michael, Samuel N. Lockhart, Daniel R. Schonhaut, James P. O’Neil, Mustafa Janabi, Rik Ossenkoppele, Suzanne L. Baker, et al. 2016. “PET Imaging of Tau Deposition in the Aging Human Brain.” *Neuron*. <https://doi.org/10.1016/j.neuron.2016.01.028>.

Scott, Gregory, Anil F. Ramackhansingh, Paul Edison, Peter Hellyer, James Cole, Mattia Veronese, Rob Leech, et al. 2016. “Amyloid Pathology and Axonal Injury after Brain Trauma.” *Neurology*. <https://doi.org/10.1212/WNL.0000000000002413>.

Sergeant, N., J. P. David, D. Lefranc, P. Vermersch, A. Watzet, and A. Delacourte. 1997. “Different Distribution of Phosphorylated Tau Protein Isoforms in Alzheimer’s and Pick’s Diseases.” *FEBS Letters*. [https://doi.org/10.1016/S0014-5793\(97\)00859-4](https://doi.org/10.1016/S0014-5793(97)00859-4).

Sergeant, N., A. Watzet, and A. Delacourte. 1999. “Neurofibrillary Degeneration in Progressive Supranuclear Palsy and Corticobasal Degeneration: Tau Pathologies with Exclusively ‘Exon 10’ Isoforms.” *Journal of Neurochemistry*. <https://doi.org/10.1046/j.1471-4159.1999.0721243.x>.

Sergeant, Nicolas, Alexis Bretteville, Malika Hamdane, Marie Laure Caillet-Boudin, Pierre Grognet, Stephanie Bombois, David Blum, et al. 2008. “Biochemistry of Tau in Alzheimer’s Disease and Related Neurological Disorders.” *Expert Review of Proteomics*. <https://doi.org/10.1586/14789450.5.2.207>.

Sergeant, Nicolas, André Delacourte, and Luc Buée. 2005. “Tau Protein as a Differential Biomarker of Tauopathies.” *Biochimica et Biophysica Acta - Molecular Basis of Disease*. <https://doi.org/10.1016/j.bbadis.2004.06.020>.

Shahpasand, Kouros, Isao Uemura, Taro Saito, Tsunaki Asano, Kenji Hata, Keitaro Shibata, Yoko Toyoshima, Masato Hasegawa, and Shin Ichi Hisanaga. 2012. “Regulation of Mitochondrial Transport and Inter-Microtubule Spacing by Tau

Phosphorylation at the Sites Hyperphosphorylated in Alzheimer's Disease." *Journal of Neuroscience*. <https://doi.org/10.1523/JNEUROSCI.5927-11.2012>.

Sharp, David J., Gregory Scott, and Robert Leech. 2014. "Network Dysfunction after Traumatic Brain Injury." *Nature Reviews Neurology*. <https://doi.org/10.1038/nrneurol.2014.15>.

Sherrington, R., E. I. Rogaev, Y. Liang, E. A. Rogaeva, G. Levesque, M. Ikeda, H. Chi, et al. 1995. "Cloning of a Gene Bearing Missense Mutations in Early-Onset Familial Alzheimer's Disease." *Nature*. <https://doi.org/10.1038/375754a0>.

Shivamurthy, Veeresh K.N., Abdel K. Tahari, Charles Marcus, and Rathan M. Subramaniam. 2015. "Brain FDG PET and the Diagnosis of Dementia." *AJR. American Journal of Roentgenology*. <https://doi.org/10.2214/AJR.13.12363>.

Sjöberg, Marcela K., Elena Shestakova, Zeyni Mansuroglu, Ricardo B. Maccioni, and Ellette Bonnefoy. 2006. "Tau Protein Binds to Pericentromeric DNA: A Putative Role for Nuclear Tau in Nucleolar Organization." *Journal of Cell Science*. <https://doi.org/10.1242/jcs.02907>.

Slart. 2006. "Prediction of functional recovery after revascularization in patients with chronic ischaemic left ventricular dysfunction: head-to-head comparison between 99mTc-sestamibi/18F-FDG DISA SPECT and 13N-ammonia/18F-FDG PET." *Eur. J. Nucl. Med. Mol. Imaging*, vol. 33, no. 6, pp. 716–723.

Smailagic, Nadja, Marco Vacante, Chris Hyde, Steven Martin, Obioha Ukoumunne, and Christos Sachpekidis. 2015. "18F-FDG PET for the Early Diagnosis of Alzheimer's Disease Dementia and Other Dementias in People with Mild Cognitive Impairment (MCI)." *Cochrane Database of Systematic Reviews*. <https://doi.org/10.1002/14651858.CD010632.pub2>.

Smith, C., S. M. Gentleman, P. D. Leclercq, L. S. Murray, W. S.T. Griffin, D. I. Graham, and J. A.R. Nicoll. 2013. "The Neuroinflammatory Response in Humans after Traumatic Brain Injury." *Neuropathology and Applied Neurobiology*. <https://doi.org/10.1111/nan.12008>.

Stamer, K., R. Vogel, E. Thies, E. Mandelkow, and E. M. Mandelkow. 2002. "Tau Blocks Traffic of Organelles, Neurofilaments, and APP Vesicles in Neurons and Enhances Oxidative Stress." *Journal of Cell Biology*. <https://doi.org/10.1083/jcb.200108057>.

Stern, Robert A., Charles H. Adler, Kewei Chen, Michael Navitsky, Ji Luo, David W. Dodick, Michael L. Alosco, et al. 2019. "Tau Positron-Emission Tomography in Former National Football League Players." *New England Journal of Medicine*. <https://doi.org/10.1056/NEJMoa1900757>.

Strittmatter, Warren J., Ann M. Saunders, Donald Schmechel, Margaret Pericak-Vance, Jan Englund, Guy S. Salvesen, and Allen D. Roses. 1993. "Apolipoprotein E: High-Avidity Binding to β -Amyloid and Increased Frequency of Type 4 Allele in Late-Onset Familial Alzheimer Disease." *Proceedings of the National Academy of Sciences of the United States of America*. <https://doi.org/10.1073/pnas.90.5.1977>.

Strittmatter, Warren J., Karl H. Weisgraber, David Y. Huang, Li Ming Dong, Guy S. Salvesen, Margaret Pericak-Vance, Donald Schmechel, Ann M. Saunders, Dmitry

- Goldgaber, and Allen D. Roses. 1993. "Binding of Human Apolipoprotein E to Synthetic Amyloid β Peptide: Isoform-Specific Effects and Implications for Late-Onset Alzheimer Disease." *Proceedings of the National Academy of Sciences of the United States of America*. <https://doi.org/10.1073/pnas.90.17.8098>.
- Sultan, Audrey, Fabrice Nessler, Marie Violet, Séverine Bégard, Anne Loyens, Smail Talahari, Zeyni Mansuroglu, et al. 2011. "Nuclear Tau, a Key Player in Neuronal DNA Protection." *Journal of Biological Chemistry*. <https://doi.org/10.1074/jbc.M110.199976>.
- Sundman, Mark, P. Murali Doraiswamy, and Rajendra A. Morey. 2015. "Neuroimaging Assessment of Early and Late Neurobiological Sequelae of Traumatic Brain Injury: Implications for CTE." *Frontiers in Neuroscience*. <https://doi.org/10.3389/fnins.2015.00334>.
- Tatti, Elisa, Simone Rossi, Iglis Innocenti, Alessandro Rossi, and Emiliano Santarnecchi. 2016. "Non-Invasive Brain Stimulation of the Aging Brain: State of the Art and Future Perspectives." *Ageing Research Reviews*. <https://doi.org/10.1016/j.arr.2016.05.006>.
- Thal, Dietmar R., Udo Rüb, Mario Orantes, and Heiko Braak. 2002. "Phases of A β -Deposition in the Human Brain and Its Relevance for the Development of AD." *Neurology*. <https://doi.org/10.1212/WNL.58.12.1791>.
- Tiepol, Solveig, Marianne Patt, Gayane Aghakhanyan, Philipp M. Meyer, Swen Hesse, Henryk Barthel, and Osama Sabri. 2019. "Current Radiotracers to Image Neurodegenerative Diseases." *EJNMMI Radiopharmacy and Chemistry*. <https://doi.org/10.1186/s41181-019-0070-7>.
- Tolnay, Markus, Nicholas Sergeant, Antonie Ghestem, Sonia Chalbot, Rob A.I. de Vos, Ernst N.H. Jansen Steur, Alphonse Probst, and André Delacourte. 2002. "Argyrophilic Grain Disease and Alzheimer's Disease Are Distinguished by Their Different Distribution of Tau Protein Isoforms." *Acta Neuropathologica*. <https://doi.org/10.1007/s00401-002-0591-z>.
- Vaquero, Juan José, and Paul Kinahan. 2015. "Positron Emission Tomography: Current Challenges and Opportunities for Technological Advances in Clinical and Preclinical Imaging Systems." *Annual Review of Biomedical Engineering*. <https://doi.org/10.1146/annurev-bioeng-071114-040723>.
- Vermeiren, Céline, Philippe Motte, Delphine Viot, Georges Mairet-Coello, Jean Philippe Courade, Martin Citron, Joël Mercier, Jonas Hannestad, and Michel Gillard. 2018. "The Tau Positron-Emission Tomography Tracer AV-1451 Binds with Similar Affinities to Tau Fibrils and Monoamine Oxidases." *Movement Disorders*. <https://doi.org/10.1002/mds.27271>.
- Vermersch, P., N. Sergeant, M. M. Ruchoux, H. Hofmann-Radvanyi, A. Wattez, H. Petit, Ph Dewailly, and A. Delacourte. 1996. "Specific Tau Variants in the Brains of Patients with Myotonic Dystrophy." *Neurology*. <https://doi.org/10.1212/WNL.47.3.711>.
- Villain, Nicolas, Gaël Chételat, Blandine Grassiot, Pierrick Bourgeat, Gareth Jones, Kathryn A. Ellis, David Ames, et al. 2012. "Regional Dynamics of Amyloid- β Deposition in Healthy Elderly, Mild Cognitive Impairment and Alzheimer's Disease:

A Voxelwise PiB-PET Longitudinal Study.” *Brain*. <https://doi.org/10.1093/brain/aws125>.

Villemagne, Victor L., Samantha Burnham, Pierrick Bourgeat, Belinda Brown, Kathryn A. Ellis, Olivier Salvado, Cassandra Szoeki, et al. 2013. “Amyloid β Deposition, Neurodegeneration, and Cognitive Decline in Sporadic Alzheimer’s Disease: A Prospective Cohort Study.” *The Lancet Neurology*. [https://doi.org/10.1016/S1474-4422\(13\)70044-9](https://doi.org/10.1016/S1474-4422(13)70044-9).

Villemagne, Victor L., Vincent Doré, Samantha C. Burnham, Colin L. Masters, and Christopher C. Rowe. 2018. “Imaging Tau and Amyloid- β Proteinopathies in Alzheimer Disease and Other Conditions.” *Nature Reviews Neurology*. <https://doi.org/10.1038/nrneurol.2018.9>.

Villemagne, Victor L., Michelle T. Fodero-Tavoletti, Colin L. Masters, and Christopher C. Rowe. 2015. “Tau Imaging: Early Progress and Future Directions.” *The Lancet Neurology*. [https://doi.org/10.1016/S1474-4422\(14\)70252-2](https://doi.org/10.1016/S1474-4422(14)70252-2).

Villemagne, Victor L., and Nobuyuki Okamura. 2016. “Tau Imaging in the Study of Ageing, Alzheimer’s Disease, and Other Neurodegenerative Conditions.” *Current Opinion in Neurobiology*. <https://doi.org/10.1016/j.conb.2015.09.002>.

Violet, Marie, Lucie Delattre, Meryem Tardivel, Audrey Sultan, Alban Chauderlier, Raphaëlle Caillierez, Smail Talahari, et al. 2014. “A Major Role for Tau in Neuronal DNA and RNA Protection in Vivo under Physiological and Hyperthermic Conditions.” *Frontiers in Cellular Neuroscience*. <https://doi.org/10.3389/fncel.2014.00084>.

Wang, Yipeng, Varun Balaji, Senthivelrajan Kaniyappan, Lars Krüger, Stephan Irsen, Katharina Tepper, Ramreddy Chandupatla, et al. 2017. “The Release and Trans-Synaptic Transmission of Tau via Exosomes.” *Molecular Neurodegeneration*. <https://doi.org/10.1186/s13024-016-0143-y>.

Wang, Yipeng, and Eckhard Mandelkow. 2016. “Tau in Physiology and Pathology.” *Nature Reviews Neuroscience*. <https://doi.org/10.1038/nrn.2015.1>.

Weingarten, M. D., A. H. Lockwood, S. Y. Hwo, and M. W. Kirschner. 1975. “A Protein Factor Essential for Microtubule Assembly.” *Proceedings of the National Academy of Sciences of the United States of America*. <https://doi.org/10.1073/pnas.72.5.1858>.

Werner C, Engelhard K. 2007. « Pathophysiology of traumatic brain injury. » *Br J Anaesth*. 99(1):4-9.

Wooten, Dustin W., Nicolas J. Guehl, Eline E. Verwer, Timothy M. Shoup, Daniel L. Yokell, Nevena Zubcevik, Neil Vasdev, et al. 2017. “Pharmacokinetic Evaluation of the Tau PET Radiotracer 18F-T807 (18F-AV-1451) in Human Subjects.” *Journal of Nuclear Medicine*. <https://doi.org/10.2967/jnumed.115.170910>.

Wooten, Dustin W., Laura Ortiz-Terán, Nevena Zubcevik, Xiaomeng Zhang, Chuan Huang, Jorge Sepulcre, Nazem Atassi, Keith A. Johnson, Ross D. Zafonte, and Georges El Fakhri. 2019. “Multi-Modal Signatures of Tau Pathology, Neuronal Fiber Integrity, and Functional Connectivity in Traumatic Brain Injury.” *Journal of Neurotrauma*. <https://doi.org/10.1089/neu.2018.6178>.

Xia, Chun Fang, Janna Arteaga, Gang Chen, Umesh Gangadharmath, Luis F. Gomez, Dhanalakshmi Kasi, Chung Lam, et al. 2013. “[18 F]T807, a Novel Tau Positron Emission Tomography Imaging Agent for Alzheimer’s Disease.” *Alzheimer’s and Dementia*. <https://doi.org/10.1016/j.jalz.2012.11.008>.

Yang, W. J., W. Chen, L. Chen, Y. J. Guo, J. S. Zeng, G. Y. Li, and W. S. Tong. 2017. “Involvement of Tau Phosphorylation in Traumatic Brain Injury Patients.” *Acta Neurologica Scandinavica*. <https://doi.org/10.1111/ane.12644>.

Yoshiyama, Yasumasa, Kunihiro Uryu, Makoto Higuchi, Luca Longhi, Rachel Hoover, Scott Fujimoto, Tracy McIntosh, Virginia M.Y. Lee, and John Q. Trojanowski. 2005. “Enhanced Neurofibrillary Tangle Formation, Cerebral Atrophy, and Cognitive Deficits Induced by Repetitive Mild Brain Injury in a Transgenic Tauopathy Mouse Model.” *Journal of Neurotrauma*. <https://doi.org/10.1089/neu.2005.22.1134>.

Zanier, Elisa R., Ilaria Bertani, Eliana Sammali, Francesca Pischiutta, Maria Antonietta Chiaravalloti, Gloria Vegliante, Antonio Masone, et al. 2018. “Induction of a Transmissible Tau Pathology by Traumatic Brain Injury.” *Brain*. <https://doi.org/10.1093/brain/awy193>.

Zetterberg, Henrik, and Kaj Blennow. 2016. “Fluid Biomarkers for Mild Traumatic Brain Injury and Related Conditions.” *Nature Reviews Neurology*. <https://doi.org/10.1038/nrneurol.2016.127>.

Zimmer, Luc, and André Luxen. 2012. “PET Radiotracers for Molecular Imaging in the Brain: Past, Present and Future.” *NeuroImage*. <https://doi.org/10.1016/j.neuroimage.2011.12.037>.

RESEARCH

Open Access



Autoradiography validation of novel tau PET tracer [F-18]-MK-6240 on human postmortem brain tissue

Cinthya Aguero^{1,2}, Maeva Dhaynaut^{3,4}, Marc D. Normandin³, Ana C. Amaral^{1,2}, Nicolas J. Guehl³, Ramesh Neelamegam³, Marta Marquie^{1,2}, Keith A. Johnson⁵, Georges El Fakhri³, Matthew P. Frosch^{2,6} and Teresa Gomez-Isla^{1,2*} 

Abstract

[F-18]-MK-6240, a novel tau positron emission tomography (PET) tracer recently discovered for the in vivo detection of neurofibrillary tangles, has the potential to improve diagnostic accuracy in the detection of Alzheimer disease. We have examined regional and substrate-specific binding patterns as well as possible off-target binding of this tracer on human brain tissue to advance towards its validation. We applied [F-18]-MK-6240 phosphor screen and high resolution autoradiography to postmortem samples from patients with a definite pathological diagnosis of Alzheimer disease, frontotemporal lobar degeneration-tau (Pick's disease, progressive supranuclear palsy and corticobasal degeneration), chronic traumatic encephalopathy, frontotemporal lobar degeneration-Tar DNA-binding protein 43 (TDP-43), dementia with Lewy bodies, cerebral amyloid angiopathy and elderly controls free of pathologic changes of neurodegenerative disease. We also directly compared the binding properties of [F-18]-MK-6240 and [F-18]-AV-1451 in human tissue, and examined potential nonspecific binding of both tau tracers to monoamine oxidases (MAO) by using autoradiography in the presence of selective monoamine oxidase A (MAO-A) and monoamine oxidase B (MAO-B) inhibitors. Our data indicate that MK-6240 strongly binds to neurofibrillary tangles in Alzheimer disease but does not seem to bind to a significant extent to tau aggregates in non-Alzheimer tauopathies, suggesting that it may have a limited utility for the in vivo detection of these pathologies. There is no evidence of binding to lesions containing β -amyloid, α -synuclein or TDP-43. In addition, we identified MK-6240 strong off-target binding to neuromelanin and melanin-containing cells, and some weaker binding to areas of hemorrhage. These binding patterns are nearly identical to those previously reported by our group and others for [F-18]-AV-1451. Of note, [F-18]-MK-6240 and [F-18]-AV-1451 autoradiographic binding signals were only weakly displaced by competing concentrations of selective MAO-B inhibitor deprenyl but not by MAO-A inhibitor clorgyline, suggesting that MAO enzymes do not appear to be a significant binding target of any of these two tracers. Together these novel findings provide relevant insights for the correct interpretation of in vivo [F-18]-MK-6240 PET imaging.

Introduction

The recent development of several novel positron emission tomography (PET) tracers tailored to detect tau in the brain has opened the opportunity of using them to improve diagnostic accuracy in Alzheimer disease (AD) and related tauopathies, and to allow reliable quantification of

brain tau burden and tracking of disease progression by in vivo neuroimaging [15, 35].

Emerging data from early studies -including our own- on postmortem material with the most validated thus far, [F-18]-AV-1451 (T807, Flortaucipir), have shown that this ligand binds with strong affinity to paired helical filament (PHF)-tau aggregates in AD brains and those that form as a function of age [20–22, 27, 35], closely matching the stereotypical spatiotemporal progression of neurofibrillary tangles (NFT) as described by Braak [3]. In agreement with these observations, patients

* Correspondence: tgomezisla@mgh.harvard.edu

¹Department of Neurology, Massachusetts General Hospital, WACC, Suite 715, 15th Parkman St., Boston, MA 02114, USA

²MassGeneral Institute for Neurodegenerative Disease, Charlestown, MA, USA
Full list of author information is available at the end of the article



clinically diagnosed with dementia of AD type and mild cognitive impairment (MCI) exhibit significantly higher in vivo [F-18]-AV-1451 retention than cognitively normal individuals in regions that are known to contain an elevated burden of tau lesions in AD [4, 6, 7, 11, 16, 25, 28, 33]. The overall utility of this tracer for in vivo selective and reliable detection of tau aggregates in non-AD tauopathies, however, seems very limited with the exception of certain tau mutations causing frontotemporal lobar degeneration (FTLD) characterized by tau aggregates [26] that contain all six isoforms of tau (three-repeat (3R) and four-repeat (4R)) [14] with PHF ultrastructure resembling NFT found in AD. We and others have shown that [F-18]-AV-1451 has low affinity for tau aggregates that contain primarily 4R tau with straight filament ultrastructure that predominate in tauopathies such as progressive supranuclear palsy (PSP), corticobasal degeneration (CBD), and most cases of FTLD. We also demonstrated the existence of robust [F-18]-AV-1451 off-target binding to melanin- and neuromelanin-containing cells and some weaker binding to blood components [21, 22]. Controversy exists as to whether AV-1451 may also exhibit significant nonspecific binding to MAO enzymes [12, 15, 17, 30], as it has been recently demonstrated for other tau PET tracers like THK-5351 [13, 24].

Several second-generation tau tracers have more recently been reported. The one that has garnered most attention and is largely considered to have most promise is [F-18]-MK-6240 from the Merck Translational Biomarkers team [15, 32]. To date, very limited information is available about the binding properties of this tracer. Merck's researchers performed in vitro binding screens against a wide panel of known receptor, transporter, and enzyme targets but conducted only limited autoradiography studies on AD and control brain specimens [15]. Yet, this ligand is quickly making its way into observational studies and clinical trials. Thus, a comprehensive postmortem validation of MK-6240 is critical for determining its usefulness for antemortem diagnosis and staging of AD and other tauopathies, and to understand exactly what [F-18]-MK-6240 PET positivity means in terms of neuropathological substrate. Because MK-6240 was initially screened in vitro for NFT binding affinity using AD brain homogenates rich in NFT and an amyloid plaque tracer for counterscreening [15], and seemed to bind to the same site as AV-1451 in that tissue material, we predicted that, just like AV-1451, MK-6240 would exhibit high binding affinity and selectivity for PHF-tau lesions relative to non-PHF-tau lesions, A β deposits and α -synuclein and transactive response DNA binding protein-43 (TDP-43) aggregates.

To validate the site/s of MK-6240 binding and determine whether there is off-target binding, we examined

the regional and substrate-selective autoradiographic patterns of [F-18]-MK-6240 in postmortem brain, retina and skin tissue samples. Cases with a definite pathological diagnosis of AD, FTLD-tau (PiD, PSP, CBD), chronic traumatic encephalopathy (CTE), FTLD-TDP-43, dementia with Lewy bodies (DLB), cerebral amyloid angiopathy (CAA), metastatic melanoma, brain hemorrhages, and elderly controls free of neurodegenerative diseases were studied. Most of these cases had also been included in our previous validation studies of [F-18]-AV-1451 [21, 22], giving us the opportunity to directly compare the autoradiographic binding patterns of both tracers in comparable tissue samples.

Materials and methods

Tissue samples

Postmortem brain, retina and skin tissue samples from the Massachusetts and the Boston University Alzheimer's Disease Research Centers Neuropathology cores were included in this study. Autopsies were performed according to standardized protocol [31] and tissue collection and use was approved by the local Institutional Review Boards. A summary of the demographic characteristics of the cases studied is shown in Table 1.

Histological evaluation of each case was routinely performed on a specific set of 19 blocked regions representative for a spectrum of neurodegenerative diseases. All paraffin-embedded blocks were stained with Luxol fast blue and hematoxylin and eosin (LH&E), while selected blocks were routinely stained for Bielschowsky silver stain and A β , α -synuclein, ubiquitin, TDP-43 and phospho-tau immunoreactivity. Blocks of frozen brain tissue containing hippocampal formation, entorhinal cortex (EC), frontal, parietal, temporal and occipital cortices, cerebellum, basal ganglia and midbrain were cut into sections 10 μ m-thick in a cryostat (Thermo-Shandon SME Cryostat), mounted on Histobond adhesion slides (StatLab, TX) and used for [F-18]-MK-6240 phosphor screen and nuclear emulsion high resolution autoradiography, followed by immunohistochemistry using appropriate antibodies in each case.

[F-18]-MK-6240 phosphor screen autoradiography

[F-18]-MK-6240 was synthesized as previously described [8]. Autoradiography experiments were performed using [F-18]-MK-6240 aliquots from material prepared from in vivo imaging on the same day, and following our previously published protocol [22]. In brief, 10 μ m-thick frozen brain sections were fixed in 100% methanol at room temperature for 20 min and then transferred to a bath containing high specific activity [F-18]-MK-6240 in 10 mM PBS with a radioactivity concentration of approximately 10 μ Ci/ml. Adjacent brain slices were placed in a bath that was identical in all aspects except that

Table 1 Participants' characteristics

ID#	Clinical diagnosis	Pathological diagnosis	Age at death (yrs)	Gender	PMI (hrs)	Braak & Braak (NFT)	CERAD score (neuritic plaques)	NIA-Reagan Institute criteria
#1	CTL	Normal adult brain	86	M	10	I	none	LP
#2	CTL	Normal adult brain	73	F	20	I	none	LP
#3	CTL	Normal adult brain	101	F	22	II	A	LP
#4	AD	AD	96	F	20	V	C	HP
#5	AD	AD	78	F	18	VI	C	HP
#6	AD	AD	97	F	12	VI	A	HP
#7	AD	AD	87	F	12	IV	B	IP
#8	AD	AD	60	M	24	VI	C	HP
#9	AD	AD	82	F	6	V	B	HP
#10	AD	AD	69	F	4	VI	C	HP
#11	AD	AD	70	M	6	V	C	HP
#12	AD	AD	66	F	2	VI	C	HP
#13	AD	AD	66	F	10	VI	C	HP
#14	AD	AD	97	F	24	V	C	HP
#15	AD	AD	81	M	7	IV	C	IP
#16	FTLD	AD/CAA	66	M	16	V	B	HP
#17	Memory, speech and gait difficulties, hand tremor	Diffuse CAA (D23N IowA APP mutation)	45	M	N/A	I	none	LP
#18	AD	AD/Metastatic melanoma	75	M	35	V	B	IP
#19	FTLD	PiD, type A	61	M	19	N/A	N/A	N/A
#20	FTLD	PiD	62	M	19	I	A	LP
#21	FTLD (P301L Mutation)	FTLD	71	F	4	I	none	LP
#22	FTLD	DLDH	65	M	24	I	none	LP
#23	CBD	CBD	80	M	6	I	none	LP
#24	PSP	PSP	69	M	45	II	none	LP
#25	PSP	PSP	68	M	48	II	none	LP
#26	PSP	PSP	78	M	11	II	none	LP
#27	PSP	PSP	73	M	12	II	none	LP
#28	PSP	PSP	63	F	12	II	none	LP
#29	CTE	CTE (CTE stage II-III) [23]	25	M	27	0	none	LP
#30	CTE	CTE (CTE stage III)	56	M	N/A	II	none	LP
#31	CTE	CTE (CTE stage III)	46	M	72	III	none	LP
#32	CTE	CTE (CTE stage IV)	65	M	N/A	II	A	LP
#33	CTE	CTE (CTE stage III)	58	M	N/A	III	none	LP
#34	DLB	LBD	62	M	24	N/A	none	N/A
#35	DLB	LBD, brainstem predominant	76	M	17	II	none	LP
#36	PDD	LBD (Braak stage 4/6)	83	M	9	III	none	LP
#37	MSA	MSA, cerebellar type (MSA-C)	60	F	32	II	none	LP
#38	FTLD	FTLD-TDP-43, type A	69	F	16	I	none	LP
#39	FTLD	FTLD-TDP-43	55	M	14	I	none	LP
#40	FTLD	FTLD-TDP-43	68	M	49	I	none	LP
#41	FTLD	FTLD-TDP-43	64	M	12	I	none	LP

Table 1 Participants' characteristics (Continued)

ID#	Clinical diagnosis	Pathological diagnosis	Age at death (yrs)	Gender	PMI (hrs)	Braak & Braak (NFT)	CERAD score (neuritic plaques)	NIA-Reagan Institute criteria
#42	Headache	Subarachnoid hemorrhage	92	F	N/A	IV	A	IP
#43	N/A	Parenchymal hemorrhage	75	M	N/A	I	none	LP

Abbreviations: AD Alzheimer's disease, APP amyloid precursor protein, CAA Cerebral amyloid angiopathy, CBD Corticobasal degeneration, CERAD Consortium to establish a registry for Alzheimer's disease, CTL Control subject, DLB Dementia with lewy bodies, DLDH Dementia lacking distinctive histopathology, F Female, FTL D Frontotemporal lobar degeneration, HP High probability, IP Intermediate probability, LP Low probability, M Male, MSA Multiple systemic atrophy, NFT Neurofibrillary tangles, NIA National Institute of Aging, N/A Non available, PID Pick's disease, PMI Postmortem interval, PSP Progressive supranuclear palsy, TDP-43 TAR DNA binding protein 43

unlabeled MK-6240 was added to yield 500 nM chemical concentration, a blocking condition sufficient to saturate essentially all available specific binding sites of tau [35]. Additional adjacent slices were also incubated in separate baths containing either [F-18]-MK-6240 or [F-18]-AV-1451 with a radioactivity concentration of approximately 10 μ Ci/ml and 20 μ Ci/ml respectively, and selective MAO-A (clorgyline) and MAO-B (deprenyl) inhibitors (Sigma-Aldrich) were added at a competing concentration of 1 μ M to evaluate potential displacement of [F-18]-MK-6240 and [F-18]-AV-1451 binding signals. After incubation for 60 min, racks of slides were removed from the respective radioactive solutions and briefly incubated in a series of wash baths to remove unbound radiotracer. Wash solutions and incubation times were: 10 mM PBS for 1 min, 70% ethanol/30% PBS for 2 min, 30% ethanol/70% PBS for 1 min, and lastly 100% 10 mM PBS for 1 min. Racks were removed from the final wash solution and slices were allowed to air dry before transfer of the slides to a storage phosphor screen (MultiSensitive Phosphor Screen, PerkinElmer Life and Analytic Sciences, Shelton, CT) that had been photo-bleached immediately prior by exposure on a white light box for a minimum of 15 min. The slides and phosphor screen were enclosed in an aluminum film cassette and set in a dark area away from sources of radioactivity for the duration of the overnight exposure period. Under dim lighting conditions, the cassette was opened and the slides removed from the exposed screen, which was mounted to the carousel of the digital imaging system (Cyclone Plus Storage Phosphor Scanner, PerkinElmer Life and Analytic Sciences). Scanning of screens was controlled by the manufacturer's OptiQuant software package using the highest available resolution of 600 dpi (approximately 42 μ m sampling interval). Digital images were saved in uncompressed form at full resolution and pixel depth. Images from adjacent brain slices incubated in the unblocked (high specific activity [F-18]-MK-6240 only) and blocking ([F-18]-MK-6240 plus 500 nM unlabeled MK-6240) conditions were compared to determine total and non-specific binding of [F-18]-MK-6240 in the tissue.

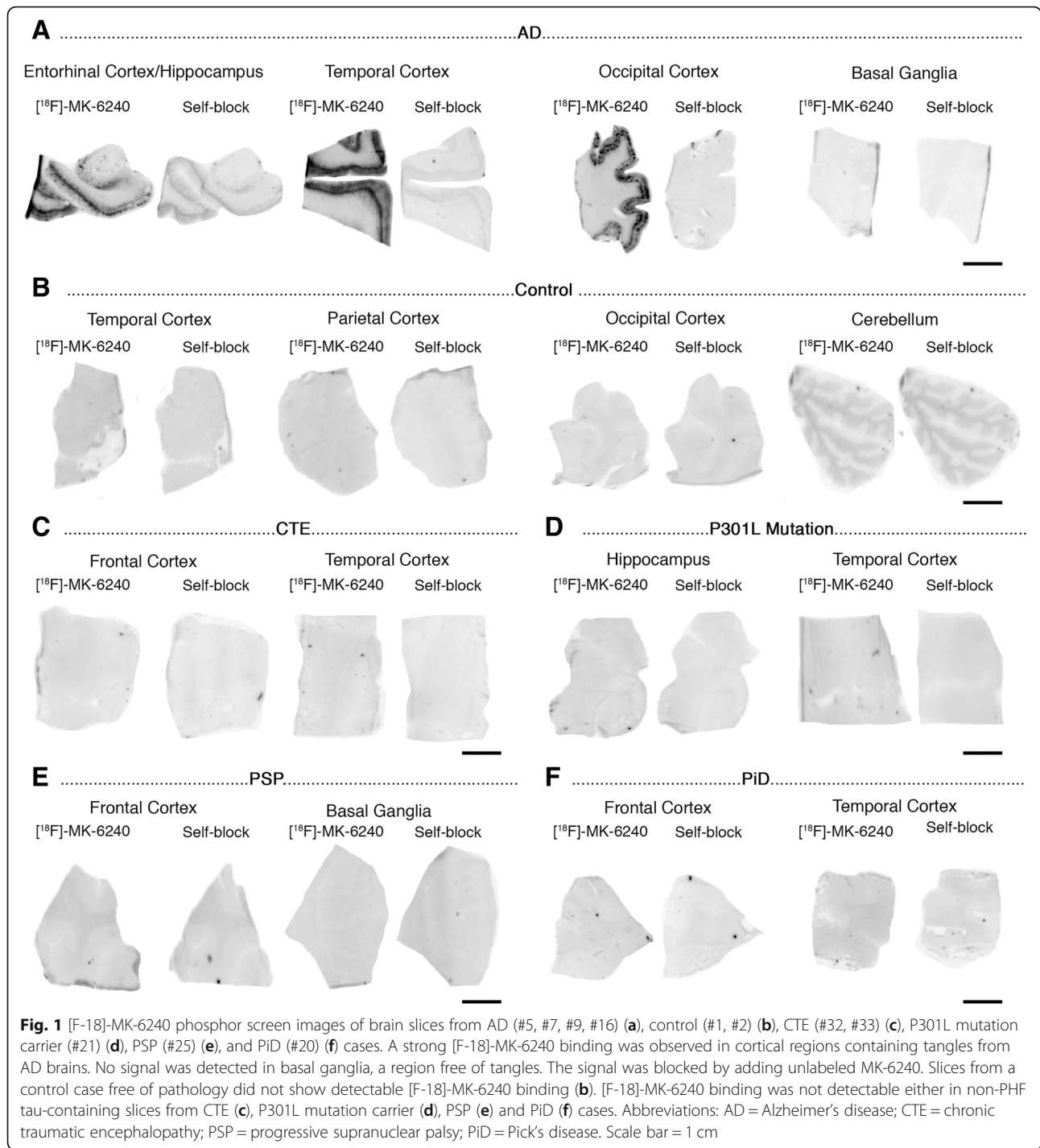
[F-18]-MK-6240 high resolution nuclear emulsion autoradiography and immunohistochemistry

To obtain autoradiographic information at the cellular resolution level, frozen cryostat sections, adjacent to those used for phosphor screen autoradiography, were coated with a liquid photographic emulsion following our previously published protocol [5, 9, 22, 34]. Immunohistochemistry was then performed on the nuclear emulsion-dipped sections. First the sections were washed for 5 min with PBS, then incubated with 2.5% normal horse blocking serum for 20 min, followed by the appropriate primary antibody - anti-tau PHF-1 (1:100, mouse, kind gift of Dr. Peter Davies), anti-A β (1:500, mouse, clone 6F/3D, Dako), anti α -synuclein (1:100, mouse, Zymed) or anti-phospho TDP-43 (pS409/410) (1:3000, mouse, Cosmo Bio CO) - for 40 min at 37 °C, washed with PBS twice for 2 min, and then incubated with the secondary antibody (ImmPRESS™ anti-mouse IgG (Vector Laboratories product MP-2400, Burlingame, CA) or ImmPRESS™ anti-rabbit Ig (Vector Laboratories product MP-7401, Burlingame, CA)) for 40 min at 37 °C. The sections were washed again with PBS twice for 2 min, and developed with DAB solution (Vector Laboratories product SK-4100). H&E was used for counterstaining. Photomicrographs were obtained on an upright Olympus BX51 (Olympus, Denmark) microscope using visible light.

Results

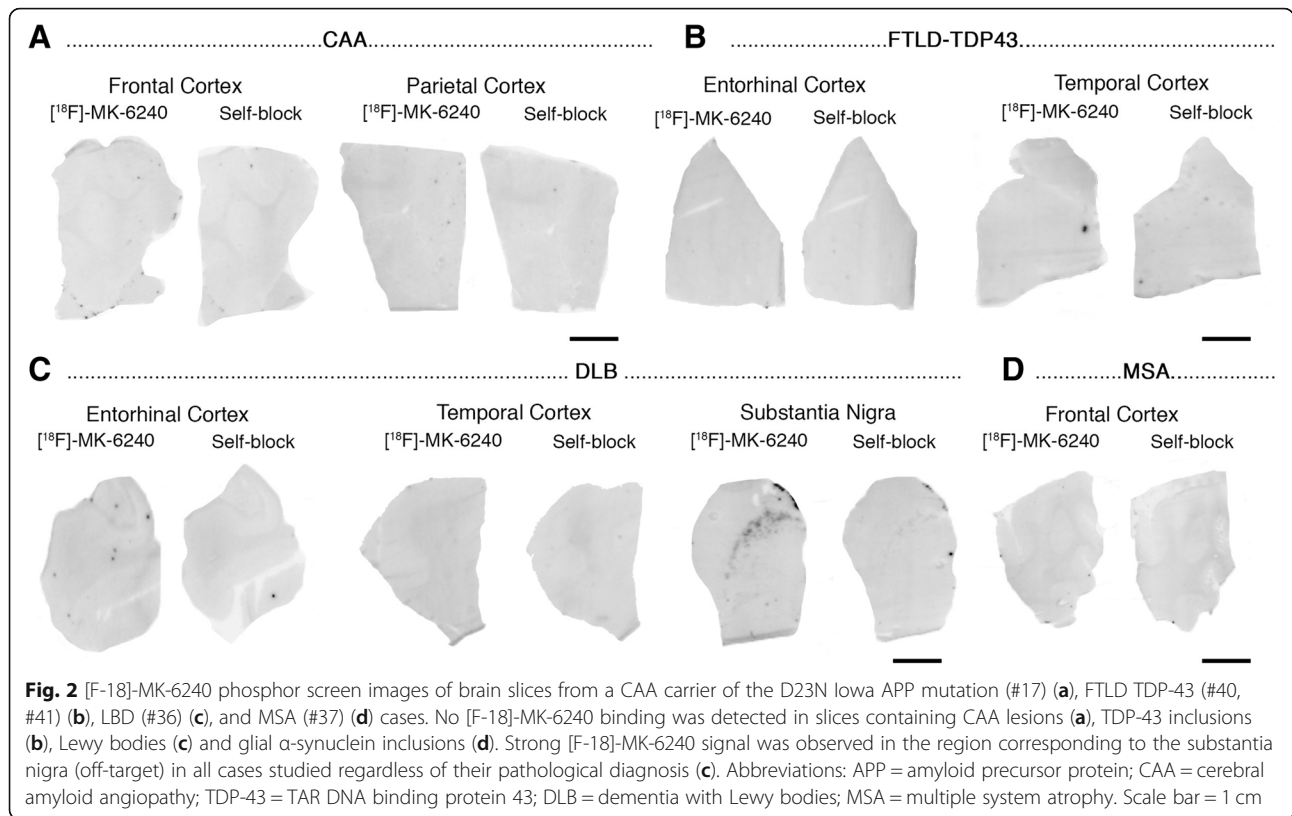
[F-18]-MK-6240 phosphor screen autoradiography

Phosphor screen autoradiography experiments revealed strong binding of [F-18]-MK-6240 in the hippocampal formation/EC and frontal, temporal, parietal and occipital cortices from brain slices containing NFT in AD cases (Fig. 1a). This binding was blocked after incubating the slides with 500 nM unlabeled MK-6240, demonstrating the selectivity of the signal. No binding was detected in non-tangle containing cortical regions or in the white matter in AD and control cases (Fig. 1b). MK-6240 binding was also absent in the cerebellum - typically used in neuroimaging studies as a reference region and lacking tangles in AD - and in the basal ganglia (Fig. 1a-f) of all



the cases studied in this series. Of note, no detectable MK-6240 binding could be observed in brain slices containing non-PHF tau aggregates from PiD, PSP, CBD and CTE cases (Fig. 1c, e-f) or in a *MAPT*P301L mutation carrier (Fig. 1d). This favors the idea that MK-6240 binds with significantly stronger affinity and selectivity to tau aggregates containing all six isoforms of tau (3R and 4R) with paired helical filament (PHF) ultrastructure

than to tau lesions primarily made of either 3R or 4R isoforms with straight filament ultrastructure. Brain slices from a D23N Iowa APP mutation carrier [29] displaying very severe CAA but no tau aggregates completely lacked [¹⁸F]-MK-6240 autoradiographic signal (Fig. 2a) and were indistinguishable from control brain slices. Brain slices containing TDP-43 inclusions in FTL-D-TDP-43 cases (Fig. 2b) and α-synuclein lesions in



DLB (Fig. 2c) and MSA (Fig. 2d) cases also lacked detectable [¹⁸F]-MK-6240 binding. A strong off-target binding of [¹⁸F]-MK-6240 was present in midbrain slices containing substantia nigra in all samples examined, regardless of the presence or absence of tau aggregates; this signal was blocked almost completely when incubating the slides with 500 nM unlabeled MK-6240 (Fig. 3a). In addition, [¹⁸F]-MK-6240 off-target binding was also noticed in retinal pigment epithelium, brain metastatic melanoma, brain slices containing parenchymal hemorrhages and extracutaneous meningeal melanocytes (Fig. 3b-f).

Overall, the [¹⁸F]-MK-6240 autoradiographic specific and off-target binding patterns described above are comparable to those exhibited by [¹⁸F]-AV-1451 that we and others have previously described in detail elsewhere [22]. Of note, [¹⁸F]-MK-6240 binding was blocked after incubating the slides with 500 nM unlabeled AV-1451 and vice versa (Fig. 4).

Importantly, when a competing concentration of 1 μM clorgyline (a selective MAO-A inhibitor) was added to the blocking solution, neither [¹⁸F]-MK-6240 nor [¹⁸F]-AV-1451 autoradiographic signal displacement could be detected (Fig. 5). [¹⁸F]-MK-6240 and [¹⁸F]-AV-1451 binding signals were only very weakly displaced (by about 20%) with 1 μM deprenyl (a selective MAO-B inhibitor) (Fig. 5), pointing to MAO-B as a low binding affinity site of these two tracers.

[¹⁸F]-MK-6240 high resolution nuclear emulsion autoradiography and immunohistochemistry

With the purpose of obtaining enough resolution at the cellular level, we dipped adjacent brain slices to those used in phosphor screen autoradiography in a photographic nuclear emulsion. Once the slides are developed, the visualization of silver grains struck by positrons emitted during [¹⁸F] nuclear decay enables precise identification of [¹⁸F]-MK-6240 labeled lesions by optical microscopy.

Using this method, we confirmed the presence of a strong and selective concentration of silver grains in tissue sections from AD cases, reflecting underlying [¹⁸F]-MK-6240 binding in the NFT-containing grey matter with negligible presence of silver grains in the white matter and following a very similar pattern to that observed with [¹⁸F]-AV-1451 (Fig. 6a-b). The silver grain distribution in the hippocampal formation/EC, and frontal, parietal, temporal and occipital cortices in AD brains closely matched the laminar distribution of tangles on adjacent slices as revealed by PHF-1 immunostaining rather than the more scattered plaque distribution pattern revealed by Aβ immunostaining (Fig. 6a-b). Silver grains were particularly abundant in layers III and V of association cortex (Fig. 6a-b) and layers II and IV in the entorhinal cortex (Fig. 6c), matching the well known laminar pattern of NFT in AD [1,

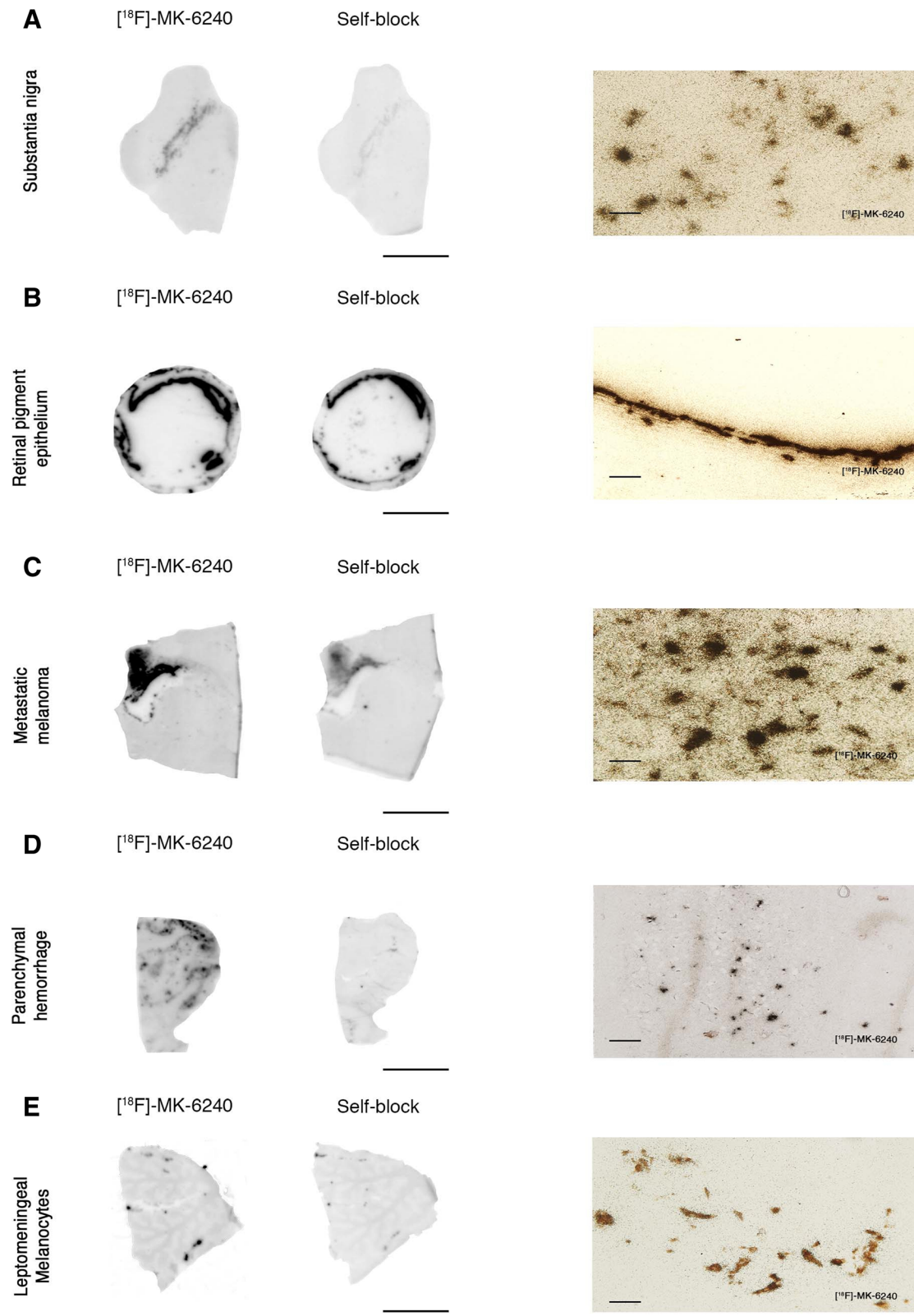


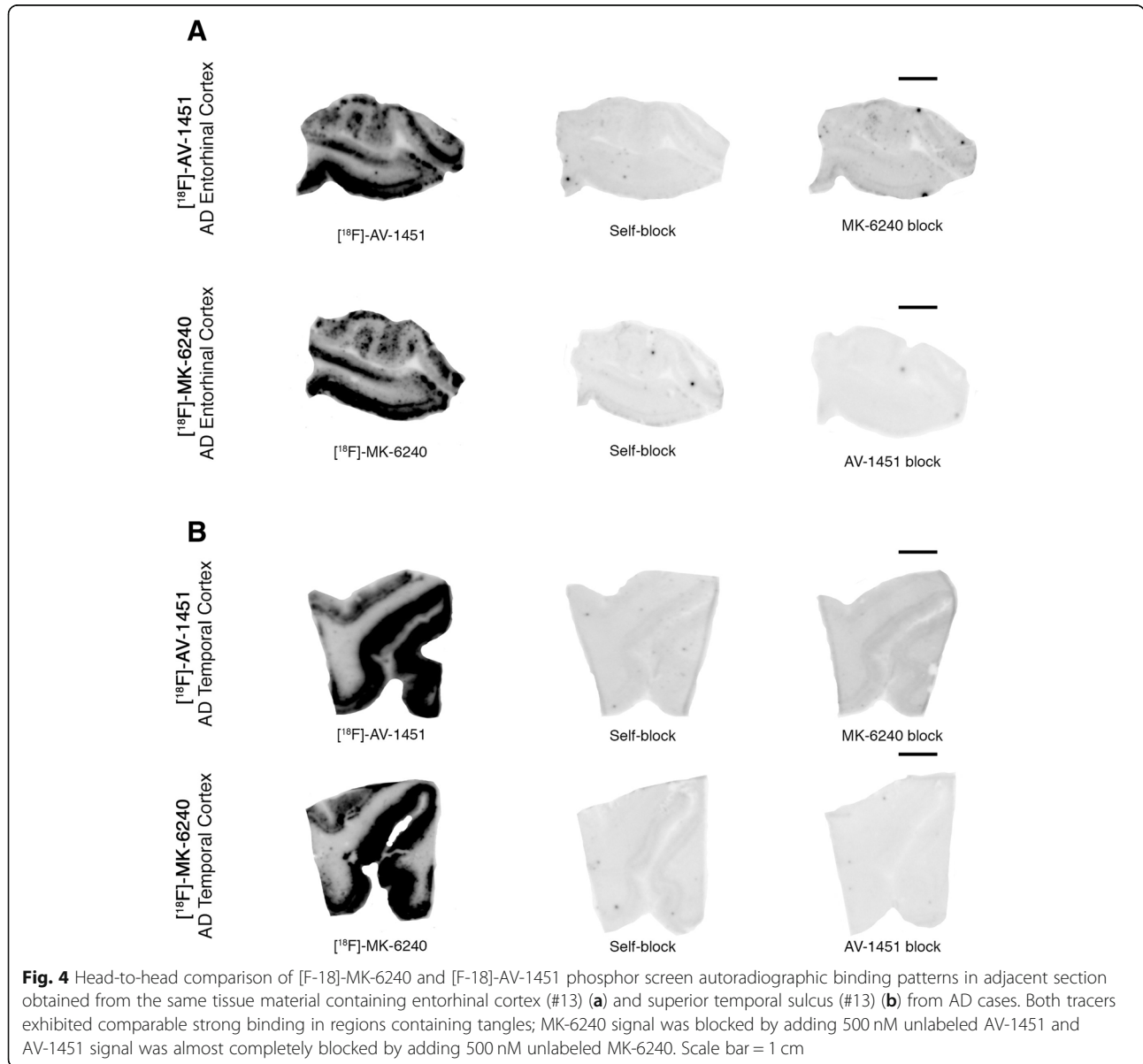
Fig. 3 (See legend on next page.)

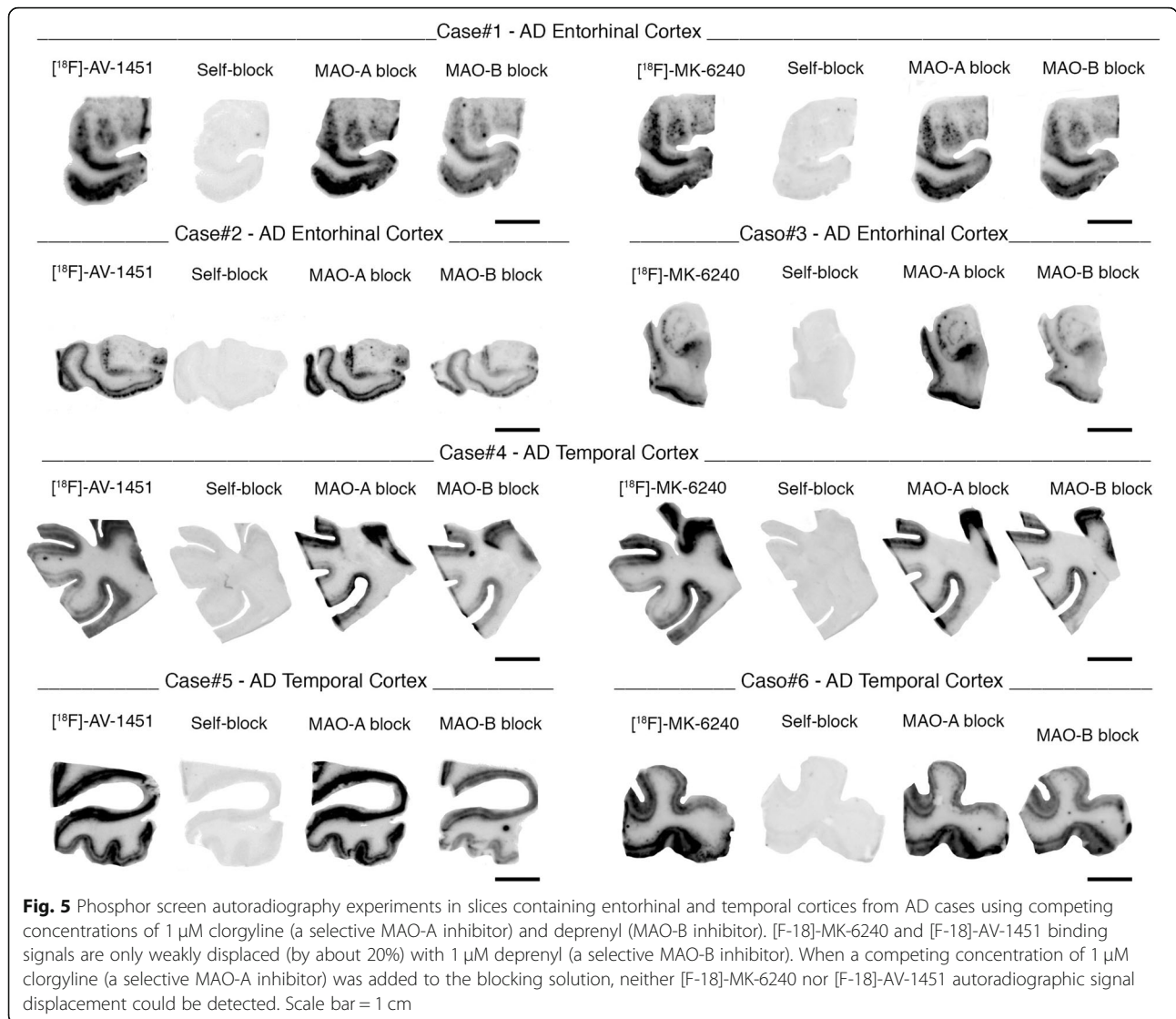
(See figure on previous page.)

Fig. 3 [F-18]-MK-6240 phosphor screen and high-resolution autoradiography images of slices containing substantia nigra in a control case (#2) (a), retinal pigment epithelium (b) in an AD case (#11), metastatic melanoma (#18) (c), parenchymal hemorrhagic lesions (#43) (d) and extracutaneous meningeal melanocytes in the cerebellum of an AD case (#8) (e). [F-18]-MK-6240 phosphor screen autoradiography images are displayed in (a-e), left and middle panels. [F-18]-MK-6240 high resolution autoradiography images are displayed in (a-e), right panel. Strong [F-18]-MK-6240 binding was observed in neuromelanin-containing neurons of the substantia nigra (a), melanin containing granules in the retinal pigment epithelium (b), malignant melanocytes from a metastatic melanoma (c), and extracutaneous meningeal melanocytes (e). [F-18]-MK-6240 binding was noticed in association with intraparenchymal hemorrhagic lesions (d). Scale bars = 1 cm (a-e left and middle panels: phosphor screen autoradiography) and 50 μm (a-e right panels; high resolution nuclear emulsion autoradiography)

18]. [F-18]-MK-6240 high resolution autoradiography followed by immunostaining with PHF-1 or Aβ antibodies on the same brain slices further confirmed that the lesions labeled by the nuclear emulsion were PHF-tau aggregates, including classic NFT and PHF-tau

containing dystrophic neurites around plaques (Fig. 7a-b), but not Aβ plaques themselves (Fig. 7c) or vessels with amyloid deposits (Fig. 7d). NFT-containing slices from AD brains dipped in the nuclear photographic emulsion omitting the incubation with





[F-18]-MK-6240 showed no silver grain accumulation and served as negative control (not shown).

Brain slices from control brains free of tau aggregates did not show accumulation of silver grains in any of regions examined (data not shown). Negligible numbers of silver grains were observed colocalizing with tau aggregates in CTE, CBD, PSP and PiD cases (Fig. 7e-h). No silver grains were observed either colocalizing with α -synuclein or TDP-43 containing inclusions (Fig. 7i-j).

Of note, neuromelanin-containing neurons in the substantia nigra pars compacta (Fig. 3a), retinal pigment epithelium (RPE) cells (Fig. 3b), tumor cells of metastatic melanoma (Fig. 3c) and leptomeningeal melanocytes (Fig. 3e), consistently demonstrated a robust concentration of silver grains confirming off-target binding of MK-6240 to neuromelanin- and melanin-containing cells. Weaker concentrations of silver grains were also observed colocalizing with parenchymal hemorrhages

(Fig. 3d), pointing to some additional [F-18]-MK-6240 off-target binding to blood components.

Discussion

Recently multiple novel PET tracers have been reported, tailored to allow detection of tau pathology in the human living brain. The status quo is largely to use PET ligands in patients carrying a particular clinical diagnosis and then simply accept, in a somewhat circular fashion, that what the scan shows is representative of the underlying disease process. However, the correct identification of biological targets of imaging agents is an essential requirement for considering them as disease-specific and progression-specific biomarkers. Validating the underlying neuropathological binding substrate/s and identifying potential off-target binding of these novel tau ligands is critical for the accurate interpretation of their in vivo PET imaging behavior. We have carefully characterized

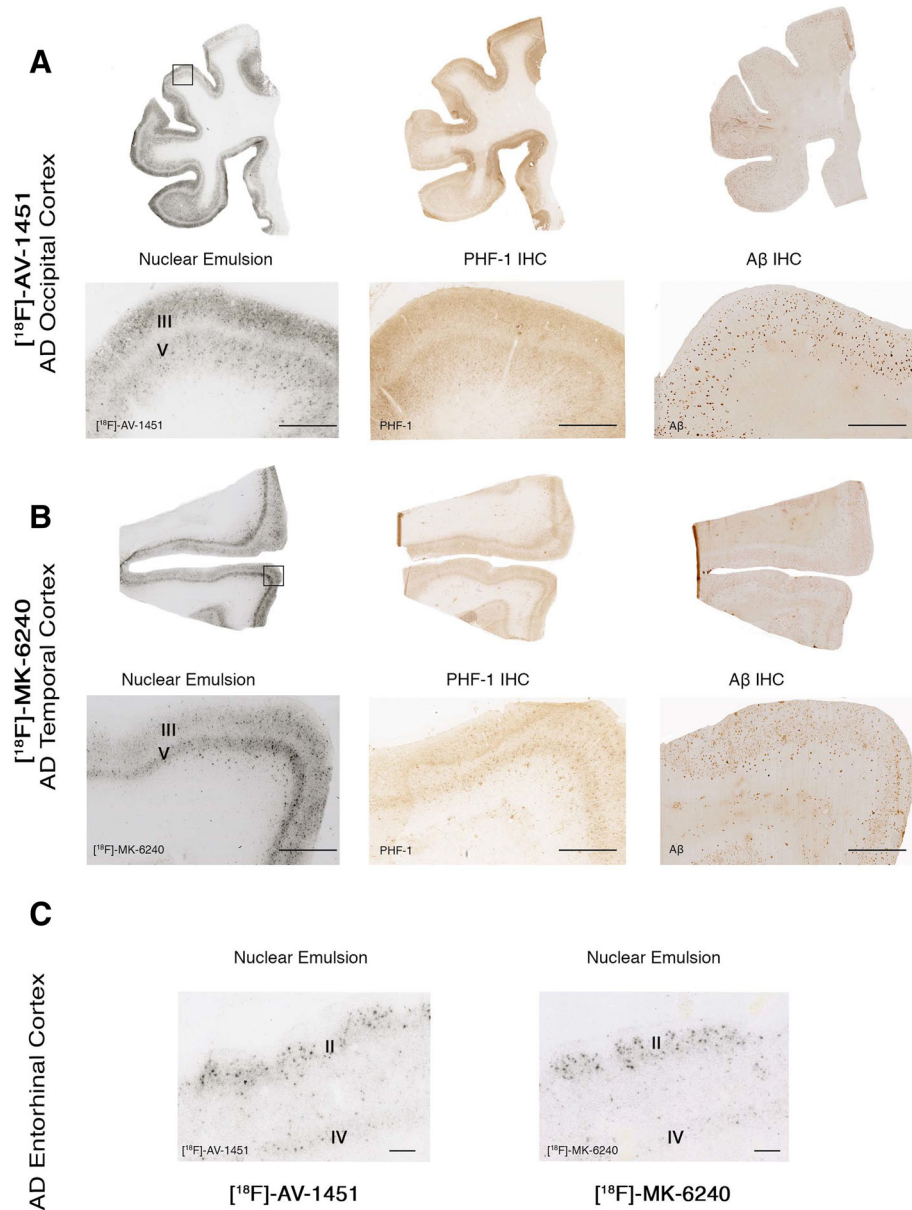


Fig. 6 [F-18]-AV-1451 and [F-18]-MK-6240 phosphor screen and high resolution autoradiography photomicrographs of brain slices containing occipital (#13) **(a)**, temporal (#9) **(b)** and entorhinal (#14) **(c)** cortices from AD cases (left panels). Middle and right panels **(a and b)** show immunostaining of adjacent sections with PHF-1 antibody (kind gift of Dr. Peter Davies) and anti-Aβ antibody (1:500, mouse, clone 6F/3D, Dako), respectively. [F-18]-AV-1451 (left panels **a and c**) and [F-18]-MK-6240 (left panel **b** and right panel **c**) high resolution nuclear emulsion autoradiography showed a strong cortical accumulation of silver grains in temporal cortical layers III and V **(a and b)**, and in layers II and IV of the entorhinal cortex **(c)** in AD brains mirroring the laminar pattern of tangles on adjacent slices as revealed by PHF-1 immunostaining (middle panels) rather than the more scattered plaque distribution pattern revealed by Aβ immunostaining (right panels). Abbreviations: AD = Alzheimer’s disease; IHC = immunohistochemistry. Scale bars = 200 μm **(a and b)** 50 μm **(c)**

the autoradiographic binding patterns of novel tau tracer [F-18]-MK-6240 in a collection of postmortem tissue samples representing a broad spectrum of neurodegenerative disorders. Our observations derived from combined [F-18]-MK-6240 sensitive autoradiography and immunohistochemistry, using this compound at similar concentrations used in vivo for PET studies, indicate that

MK-6240 has high binding affinity for tau aggregates in AD brain tissue, but does not seem to bind to a significant extent to neuronal and glial tau aggregates in non-AD tauopathies such as PiD, PSP, CBD or CTE, or to Aβ, α-synuclein or TDP-43-containing lesions. These findings strongly suggest that tau in tangles of AD has a unique conformation that is recognized by this tracer (in

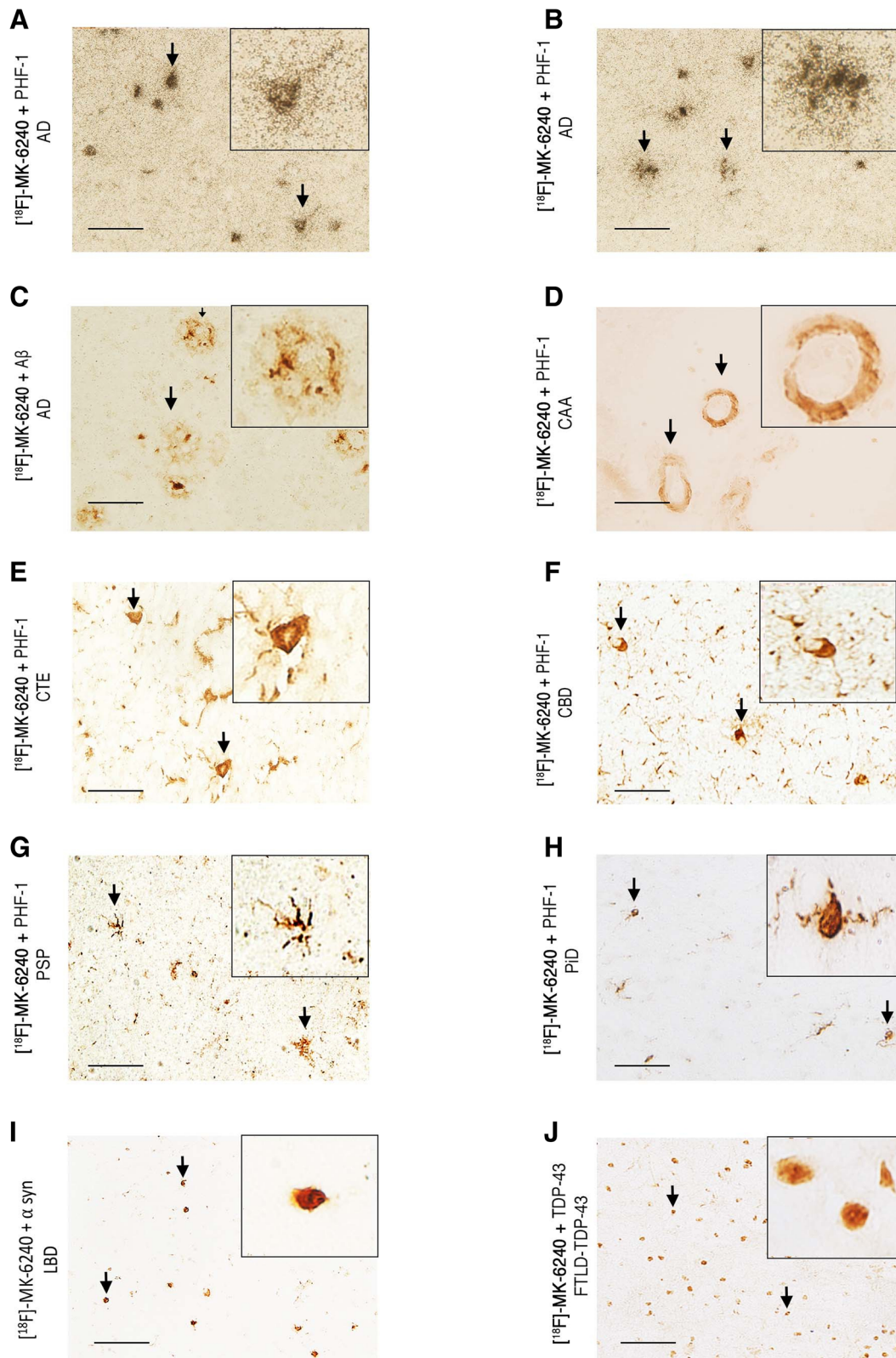


Fig. 7 (See legend on next page.)

(See figure on previous page.)

Fig. 7 Photomicrographs showing combined [F-18]-MK-6240 high-resolution nuclear emulsion autoradiography followed by immunostaining with appropriate antibodies of brain slices containing frontal and temporal cortices from AD (#10, #16) (**a-c**), CAA (#17) (**d**) CTE (#33) (**e**), CBD (#23) (**f**), PSP (#26) (**g**), PiD (#20) (**h**), LBD (#34) (**i**) and FTLD TDP-43 (#39) (**j**). Accumulation of silver grains from the nuclear emulsion colocalized with PHF-1 stained tangles and PHF-tau containing dystrophic neurites around plaques in AD. No detectable accumulations of silver grains were observed in association with A β plaques themselves or amyloid-containing vessels in CAA, tau aggregates in CTE, coiled bodies and globose tangles in CBD, astrocytic plaques in PSP, Pick bodies in PiD, Lewy bodies in LBD or TDP-43 inclusions in FTLD TDP-43. Abbreviations: AD = Alzheimer's disease; CAA = cerebral amyloid angiopathy; CTE = chronic traumatic encephalopathy; CBD = corticobasal degeneration PSP = progressive supranuclear palsy; PiD = Pick's disease; LBD = Lewy body disease; FTLD TDP-43 = frontotemporal lobar degeneration with TDP-43 inclusions. Scale bar = 50 μ m

keeping with the selection process for development of this compound as a lead imaging agent). Strong binding of [F-18]-MK-6240 to neuromelanin- and melanin-containing cells and some weaker binding to brain hemorrhagic lesions was also identified, pointing to these substrates as off-target binding sites of MK-6240. Overall, [F-18]-MK-6240 autoradiographic binding patterns closely resembled those of tau PET tracer [F-18]-AV-1451. Importantly, [F-18]-MK-6240 and [F-18]-AV-1451 binding signals were only very weakly displaced using autoradiography competition with unlabeled selective MAO-B inhibitor deprenyl, suggesting that these two tracers have low binding affinity for MAO enzymes in the human brain.

MK-6240 was identified as a potential imaging agent by screening using cortical homogenates from AD tissue rich in NFT as the binding target and an amyloid plaque tracer for counter-screen [15]. Based on this, we anticipated that MK-6240 would preferentially bind to tau lesions in the form of NFT in AD over other tau aggregates in non-AD tauopathies or lesions primarily made of A β , α -synuclein or TDP-43. To date, only very limited data from human in vivo [F-18]-MK-6240 PET imaging studies have been published [2, 19]. Results from these early studies point to a promising 2- to 3-fold higher in vivo [F-18]-MK-6240 retention in neocortical and medial temporal brain regions of AD patients compared to elderly cognitively normal individuals [19]. Because this ligand is already being incorporated into clinical trial research, validation studies such as this paper are absolutely critical to evaluate the potential usefulness of this ligand as a reliable marker of human brain tau lesions. In an attempt to advance towards that goal, we applied [F-18]-MK-6240 phosphor screen and high resolution autoradiography to the study of a series of autopsy samples from individuals with a definitive diagnosis of AD, PiD, PSP, CBD, CTE, CAA, FTLD-TDP-43, DLB, and control brains free of neurodegenerative pathology. Our results confirmed that while [F-18]-MK-6240 avidly bound to PHF-tangle containing slices from AD brains, it did not bind to a significant extent to tau-containing lesions in slices from non-AD tauopathy brains, suggesting that this tracer has higher affinity and selectivity for PHF-tau over tau aggregates

with a primarily straight filament ultrastructure, and thus raising reasonable doubts about the potential value of this ligand as a biomarker of tau pathology in non-AD tauopathies. The regional and laminar autoradiographic patterns of distribution of [F-18]-MK-6240, as revealed by the combination of autoradiography using a fine grain nuclear emulsion and immunohistochemistry, closely matched those of classic PHF-tangles in AD brains [1, 18]. Using this method, we confirmed that [F-18]-MK-6240-labeled lesions were NFT, suggesting that these lesions are the main pathological substrate of [F-18]-MK-6240 binding. The microscopic examination of diffuse plaques, CAA, α -synuclein and TDP-43 aggregates confirmed the absence of detectable [F-18]-MK-6240 binding to these lesions, favoring the relative selectivity of [F-18]-MK-6240 for NFT over β -amyloid plaques and other abnormal protein aggregates with a β -pleated sheet conformation.

Our data also establish that MK-6240 is not fully selective for PHF-tau deposits. Similarly to AV-1451, MK-6240 exhibits strong off-target binding to neuromelanin- and melanin-containing cells including pigmented neurons in the substantia nigra (regardless of the presence or absence of nigral tau pathology), leptomeningeal melanocytes, metastatic melanoma and retinal pigment epithelium, with some weaker off-target binding to brain hemorrhages as well. This is something relevant for the correct interpretation of [F-18]-MK-6240 in vivo imaging depending for example on the relative abundance and distribution of leptomeningeal melanocytes across different individuals [10], the possibility of focal artifactual increases in the density of these cells due to regional cortical atrophy, or the presence of concomitant brain hemorrhagic lesions.

One of the first generation tau PET tracers, THK-5351, has been recently found to demonstrate high binding affinity to MAO-B [13, 24], seriously compromising its value as a tau-specific tracer and increasing the need for alternative tau-specific imaging agents. To date, studies on potential non-specific binding of AV-1451 to MAO enzymes are scarce and have yielded conflicting results. A recent study by Vermeiren and colleagues suggested that H3-AV-1451 binds with similar nanomolar affinity to tau fibrils and MAO-A and B enzymes in

brain homogenates isolated from AD or PSP patients as well as those devoid of tau pathology [30]. Merck's researchers also reported high affinity displacement of 3H-AV-1451 binding, but not of 3H-MK-6240, in some non-AD brain homogenates in the presence of selective MAO-A inhibitor clorgyline. By contrary, Hansen and colleagues found that MAO-B inhibitors did not block in vivo [F-18]-AV-1451 binding in a series of 16 of 27 PD patients receiving MAO-B inhibitors at the time of scan [12]. In agreement with these results, Lemoine et al. reported that AV-1451 shows ten times lower affinity to MAO-B when compared to THK-5351 in in vitro assays [17]. Consistent with these observations, our data derived from [F-18]-MK-6240 and [F-18]-AV-1451 autoradiography experiments in the presence of selective MAO-A and MAO-B inhibitors point to a low binding affinity of both tracers for MAO enzymes. Studies using the specific enzymatic inhibitors do not exclude interaction of MK-6240 with MAO isoforms at regions removed from the active site. The discrepancies among the different studies could stem from the different techniques and isotope labeling used in each case e.g. in vitro binding assays in brain homogenates vs. autoradiography assays in tissue slices, and labeling of the tau tracer with H-3 vs. F-18. Our previous experience with H-3-AV-1451 in vitro binding assays in brain homogenates suggested that the signal-to background noise ratio when using this method was relatively low compared to [F-18]-AV-1451 autoradiographic techniques; something that could be due, at least in part, to off-target binding to sample components such as blood.

Conclusions

In conclusion, all together our results show that MK-6240 exhibits a nearly identical binding profile to AV-1451 holding promise as a potential surrogate marker for the in vivo detection of neurofibrillary tangles in AD, while still having various forms of off-target binding that need to be considered when interpreting in vivo imaging findings. The utility of MK-6240 for the reliable in vivo detection of tau aggregates in non-AD tauopathies, however, seems very limited. Both, MK-6240 and AV-1451, as opposed to other tracers like THK-5351, seem to exhibit relatively low binding affinity for MAO enzymes. Future imaging-pathological correlation studies on postmortem material from patients scanned while alive will provide additional information on the utility of these two tracers for the reliable quantification of NFT burden in AD and disease progression tracking by in vivo neuroimaging, as well as their potential usefulness when testing therapeutic approaches aimed at decreasing or halting the progression of tau aggregation in AD.

Availability of data and materials

Original slides and diagnostic material are retained. There are no novel reagents or materials for others to request.

Authors' contributions

CA participated in study design, carried out immunostaining, phosphor screen and nuclear emulsion autoradiography, data analysis and drafted the manuscript. MD carried out phosphor screen autoradiography. MDN participated in study design, analysis and interpretation of data and carried out phosphor screen autoradiography. ACA carried out immunostaining and tissue cryosectioning. NJG participated in phosphor screen autoradiography. RN carried out radiotracer synthesis and labeling. MM carried out immunostaining and tissue cryosectioning. GEF participated in study design, analysis and interpretation of data. KAJ participated in the study design. MPF carried out the neuropathologic examination and participated in the study design, analysis and interpretation of data. TGI conceived the study and participated in its design and coordination, analysis and interpretation of data and drafted the manuscript. All authors read and approved the final manuscript.

Ethics approval and consent to participate

All procedures performed in studies involving human participants were in accordance with the ethical standards of the institutional and national research committee and with the 1964 Helsinki declaration and its later amendments.

Consent for publication

Informed consent was obtained from all individual participants included in the study and according to institutional procedures for autopsy consents for post-mortem tissue.

Competing interests

Cynthia Agüero received research funding from the International Health Central America Institute, San Jose, Costa Rica. Marc D. Normandin received research funding from NIH National Institute of Neurological Disorders and Stroke (U01NS086659) and NIH National Institute of Mental Health (R01MH100350). Keith A. Johnson received research funding from NIH (grants R01 EB014894, R21 AG038994, R01 AG026484, R01 AG034556, P50 AG00513421, U19 AG10483, P01 AG036694, R13 AG042201174210, R01 AG027435 and R01 AG037497) and the Alzheimer's Association (ZEN-10-174,210 K). Keith A. Johnson has served as paid consultant for Bayer, GE Healthcare, Janssen Alzheimer's Immunotherapy, Siemens Medical Solutions, Genzyme, Novartis, Biogen, Roche, ISIS Pharma, AZTherapy, GEHC, Lundberg, and Abbvie. He is a site co-investigator for Lilly/Avid, Janssen Immunotherapy and Pfizer. Matthew P. Frosch received research funding from the Massachusetts Alzheimer's Disease Research Center (NIH AG005134). Teresa Gómez-Isla received research funding from NIH National Institute on Aging (AG005134, AG036694 and AG061206). Teresa Gómez-Isla participated as speaker in an Eli Lilly and Company sponsored educational symposium and serves in an Eli Lilly Data Monitoring Committee. Eli Lilly and Company owns Avid, the company that created AV-1451, one of the PET compounds used in this study.

Publisher's Note

Springer Nature remains neutral with regard to jurisdictional claims in published maps and institutional affiliations.

Author details

¹Department of Neurology, Massachusetts General Hospital, WACC, Suite 715, 15th Parkman St., Boston, MA 02114, USA. ²MassGeneral Institute for Neurodegenerative Disease, Charlestown, MA, USA. ³Center for Advanced Medical Imaging Sciences, Division of Nuclear Medicine and Molecular Imaging, Department of Radiology, Massachusetts General Hospital, Harvard Medical School, Boston, MA, USA. ⁴AP-HP, Department of Nuclear Medicine, Pitié-Salpêtrière Hospital, Sorbonne University, UPMC Paris 06, CNRS UMR 7371, INSERM U1146, 75013 Paris, France. ⁵Department of Radiology, Massachusetts General Hospital, Boston, MA, USA. ⁶C.S. Kubik Laboratory for Neuropathology, Massachusetts General Hospital, Boston, MA, USA.

Received: 21 February 2019 Accepted: 23 February 2019

Published online: 11 March 2019

References

1. Arnold SE, Hyman BT, Flory J, Damasio AR, Van Hoesen GW (1991) The topographical and neuroanatomical distribution of neurofibrillary tangles

- and neuritic plaques in the cerebral cortex of patients with Alzheimer's disease. *Cereb Cortex* 1:103–116
2. Betthausen TJ, Cody KA, Zammit MD, Murali D, Converse AK, Barnhart TE, Stone CK, Rowley HA, Johnson SC, Christian BT (2018) In vivo characterization and quantification of neurofibrillary tau PET radioligand [(18F)MK-6240 in humans from Alzheimer's disease dementia to young controls. *J Nucl Med*. <https://doi.org/10.2967/jnumed.118.209650>. Epub ahead of print. PubMed PMID: 29777006.
 3. Braak H, Alafuzoff I, Arzberger T, Kretschmar H, Del Tredici K (2006) Staging of Alzheimer disease-associated neurofibrillary pathology using paraffin sections and immunocytochemistry. *Acta Neuropathol* 112:389–404
 4. Brier MR, Gordon B, Friedrichsen K, McCarthy J, Stern A, Christensen J, Owen C, Aldea P, Su Y, Hassenstab J, Cairns NJ, Holtzman DM, Fagan AM, Morris JC, Benzinger TLS, Ances BM (2016) Tau and ab imaging, CSF measures, and cognition in Alzheimer's disease. *Sci Transl Med* 8:1–9
 5. Caro LG, Van Tubergen RP, Kolb JA (1962) High-resolution autoradiography. *J Cell Biol* 15:173–188
 6. Cho H, Choi JY, Hwang MS, Kim YJ, Lee HM, Lee HS, Lee JH, Ryu YH, Lee MS, Lyoo CH (2016a) In vivo cortical spreading pattern of tau and amyloid in the Alzheimer disease spectrum. *Ann Neurol* 80:247–258
 7. Cho H, Choi JY, Hwang MS, Lee JH, Kim YJ, Lee HM, Lyoo CH, Ryu YH, Lee MS (2016b) Tau PET in Alzheimer disease and mild cognitive impairment. *Neurology* 87:375–383
 8. Collier TL, Yokell DL, Livni E, Rice PA, Celen S, Serdons K, Neelamegam R, Bormans G, Harris D, Walji A, Hostetler ED, Bennacef I, Vasdev N (2017) cGMP production of the radiopharmaceutical [(18) F]MK-6240 for PET imaging of human neurofibrillary tangles. *J Labelled Comp Radiopharm* 60: 263–269
 9. Gerfen CR (2003) Basic neuroanatomical methods. *Curr Protoc Neurosci* Chapter 1:Unit 1.1
 10. Goldgeier MH, Klein LE, Klein-Angerer S, Moellmann G, Nordlund JJ (1984) The distribution of melanocytes in the Leptomeninges of the human brain. *J Invest Dermatol* 82:235–238
 11. Gordon BA, Friedrichsen K, Brier M, Blazey T, Su Y, Christensen J, Aldea P, McConathy J, Holtzman DM, Cairns NJ, Morris JC, Fagan AM, Ances BM, Benzinger TL (2016) The relationship between cerebrospinal fluid markers of Alzheimer pathology and positron emission tomography tau imaging. *Brain* 139:2249–2260
 12. Hansen AK, Brooks DJ, Borghammer P (2017) MAO-B Inhibitors Do Not Block In Vivo Flortaucipir([(18)F]-AV-1451) Binding. *Mol Imaging Biol* 20:356–360
 13. Harada R, Furumoto S, Tago T, Furukawa K, Ishiki A, Tomita N, Iwata R, Tashiro M, Arai H, Yanai K, Kudo Y, Okamura N (2016) Characterization of the radiolabeled metabolite of tau PET tracer (18)F-THK5351. *Eur J Nucl Med Mol Imaging* 43:2211–2218
 14. Hong M, Zhukareva V, Vogelsberg-Ragaglia V, Wszolek Z, Reed L, Miller BI, Geschwind DH, Bird TD, McKeel D, Goate A, Morris JC, Wilhelmsen KC, Schellenberg GD, Trojanowski JQ, Lee VM-Y (1998) Mutation-specific functional impairments in distinct tau isoforms of hereditary FTDP-17. *Science* 282:1914–1917
 15. Hostetler ED, Walji AM, Zeng Z, Miller P, Bennacef I, Salinas C, Connolly B, Gantert L, Haley H, Holahan M, Purcell M, Riffel K, Lohith TG, Coleman P, Soriano A, Ogawa A, Xu S, Zhang X, Joshi E, Della Rocca J, Hesk D, Schenk DJ, Evelhoch JL (2016) Preclinical characterization of 18F-MK-6240, a promising PET tracer for in vivo quantification of human neurofibrillary tangles. *J Nucl Med* 57:1599–1606
 16. Johnson KA, Schultz A, Betensky RA, Becker JA, Sepulcre J, Rentz D, Mormino E, Chhatwal J, Amariglio R, Papp K, Marshall G, Albers M, Mauro S, Pepin L, Alverio J, Judge K, Philiosaint M, Shoup T, Yokell D, Dickerson B, Gomez-Isla T, Hyman B, Vasdev N, Sperling R (2016) Tau positron emission tomographic imaging in aging and early Alzheimer disease. *Ann Neurol* 79: 110–119
 17. Lemoine L, Gillberg PG, Svedberg M, Stepanov V, Jia Z, Huang J, Nag S, Tian H, Ghetti B, Okamura N, Higuchi M, Halldin C, Nordberg A (2017) Comparative binding properties of the tau PET tracers THK5117, THK5351, PBB3, and T807 in postmortem Alzheimer brains. *Alzheimers Res Ther* 9:96
 18. Lewis DA, Campbell MJ, Terry RD, Morrison JH (1987) Laminar and regional distributions of neurofibrillary tangles and neuritic plaques in Alzheimer's disease: a quantitative study of visual and auditory cortices. *J Neurosci* 7: 1799–1808
 19. Lohith TG, Bennacef I, Vandenberghe R, Vandenbulcke M, Salinas-Valenzuela C, Declercq R, Reynders T, Telan-Choing F, Riffel K, Celen S, Serdons K, Bormans G, Tsai K, Walji A, Hostetler ED, Evelhoch JL, Van Laere K, Forman M, Stoch A, Sur C, Struyk A (2018) First-in-human brain imaging of Alzheimer dementia patients and elderly controls with (18)F-MK-6240, a PET tracer targeting neurofibrillary tangle pathology. *J Nucl Med*. <https://doi.org/10.2967/jnumed.118.208215> [Epub ahead of print] PubMed PMID: 29880509
 20. Lowe VJ, Curran G, Fang P, Liesinger AM, Josephs KA, Parisi JE, Kantarci K, Boeve BF, Pandey MK, Bruinsma T, Knopman DS, Jones DT, Petrucelli L, Cook CN, Graff-Radford NR, Dickson DW, Petersen RC, Jack CR Jr, Murray ME (2016) An autoradiographic evaluation of AV-1451 tau PET in dementia. *Acta Neuropathol Commun* 4:58
 21. Marquie M, Normandin MD, Meltzer AC, Siao Tick Chong M, Andrea NV, Anton-Fernandez A, Klunk WE, Mathis CA, Ikonomic MD, Debnath M, Bien EA, Vandenberg CR, Costantino I, Makarets S, DeVos SL, Oakley DH, Gomperts SN, Growdon JH, Domoto-Reilly K, Lucente D, Dickerson BC, Frosch MP, Hyman BT, Johnson KA, Gomez-Isla T (2017) Pathological correlations of [F-18]-AV-1451 imaging in non-alzheimer tauopathies. *Ann Neurol* 81:117–128
 22. Marquie M, Normandin MD, Vandenberg CR, Costantino IM, Bien EA, Rycyna LG, Klunk WE, Mathis CA, Ikonomic MD, Debnath ML, Vasdev N, Dickerson BC, Gomperts SN, Growdon JH, Johnson KA, Frosch MP, Hyman BT, Gomez-Isla T (2015) Validating novel tau positron emission tomography tracer [F-18]-AV-1451 (T807) on postmortem brain tissue. *Ann Neurol* 78:787–800
 23. McKee AC, Stern RA, Nowinski CJ, Stein TD, Alvarez VE, Daneshvar DH, Lee HS, Wojtowicz SM, Hall G, Baugh CM, Riley DO, Kubilus CA, Cormier KA, Jacobs MA, Martin BR, Abraham CR, Ikezu T, Reichard RR, Wolozin BL, Budson AE, Goldstein LE, Kowall NW, Cantu RC (2013) The spectrum of disease in chronic traumatic encephalopathy. *Brain* 136:43–64
 24. Ng KP, Pascoal TA, Mathotaarachchi S, Theriault J, Kang MS, Shin M, Guiot MC, Guo Q, Harada R, Comley RA, Massarweh G, Soucy JP, Okamura N, Gauthier S, Rosa-Neto P (2017) Monoamine oxidase B inhibitor, selegiline, reduces (18)F-THK5351 uptake in the human brain. *Alzheimers Res Ther* 9:25
 25. Pontecorvo MJ, Devous MD Sr, Navitsky M, Lu M, Salloway S, Schaerf FW, Jennings D, Arora AK, McGeehan A, Lim NC, Xiong H, Joshi AD, Siderowf A, Mintun MA (2017) Relationships between flortaucipir PET tau binding and amyloid burden, clinical diagnosis, age and cognition. *Brain* 140:748–763
 26. Reed LA, Grabowski TJ, Schmidt ML, Morris JC, Goate A, Solodkin A, Van Hoesen GW, Schelper RL, Talbot CJ, Wragg MA, Trojanowski JQ (1997) Autosomal dominant dementia with widespread neurofibrillary tangles. *Ann Neurol* 42(4):564–572
 27. Sander K, Lashley T, Gami P, Gendron T, Lythgoe MF, Rohrer JD, Schott JM, Revesz T, Fox NC, Arstad E (2016) Characterization of tau positron emission tomography tracer [(18)F]AV-1451 binding to postmortem tissue in Alzheimer's disease, primary tauopathies, and other dementias. *Alzheimers Dement* 12:1116–1124
 28. Scholl M, Lockhart SN, Schonhaut DR, O'Neil JP, Janabi M, Ossenkoppele R, Baker SL, Vogel JW, Faria J, Schwimmer HD, Rabinovici GD, Jagust WJ (2016) PET imaging of tau deposition in the aging human brain. *Neuron* 89:971–982
 29. Van Nostrand WE, Melchor JP, Cho HS, Greenberg SM, Rebeck GW (2001) Pathogenic effects of D23N Iowa mutant amyloid beta-protein. *J Biol Chem* 276: 32860–32866
 30. Vermeiren C, Motte P, Viot D, Mairet-Coello G, Courade JP, Citron M, Mercier J, Hannestad J, Gillard M (2017) The tau positron-emission tomography tracer AV-1451 binds with similar affinities to tau fibrils and monoamine oxidases. *Mov Disord* 33:273–281
 31. Vonsattel JP, Amaya Mdel P, Cortes EP, Mancevska K, Keller CE (2008) Twenty-first century brain banking: practical prerequisites and lessons from the past: the experience of New York Brain Bank, Taub Institute, Columbia University. *Cell Tissue Bank* 9:247–258
 32. Walji AM, Hostetler ED, Selnick H, Zeng Z, Miller P, Bennacef I, Salinas C, Connolly B, Gantert L, Holahan M, O'Malley S, Purcell M, Riffel K, Li J, Balsells J, O'Brien JA, Melquist S, Soriano A, Zhang X, Ogawa A, Xu S, Joshi E, Della Rocca J, Hess FJ, Schachter J, Hesk D, Schenk D, Struyk A, Babaoglu K, Lohith TG, Wang Y, Yang K, Fu J, Evelhoch JL, Coleman PJ (2016) Discovery of 6-(Fluoro-(18)F)-3-(1H-pyrrolo[2,3-c]pyridin-1-yl)isoquinolin-5-amine [(18)F]-MK-6240: a positron emission tomography (PET) imaging agent for quantification of neurofibrillary tangles (NFTs). *J Med Chem* 59:4778–4789
 33. Wang L, Benzinger TL, Su Y, Christensen J, Friedrichsen K, Aldea P, McConathy J, Cairns NJ, Fagan AM, Morris JC, Ances BM (2016) Evaluation of tau imaging in staging Alzheimer disease and revealing interactions between beta-amyloid and Tauopathy. *JAMA Neurol* 73: 1070–1077

34. Woodbury DH, Beierwaltes WH (1967) Fluorine-18 uptake and localization in soft tissue deposits of osteogenic sarcoma in rat and man. *J Nucl Med* 8: 646–651
35. Xia CF, Arteaga J, Chen G, Gangadharmath U, Gomez LF, Kasi D, Lam C, Liang Q, Liu C, Mocharla VP, Mu F, Sinha A, Su H, Szardenings AK, Walsh JC, Wang E, Yu C, Zhang W, Zhao T, Kolb HC (2013) [(18)F]T807, a novel tau positron emission tomography imaging agent for Alzheimer's disease. *Alzheimers Dement* 9:666–676

Ready to submit your research? Choose BMC and benefit from:

- fast, convenient online submission
- thorough peer review by experienced researchers in your field
- rapid publication on acceptance
- support for research data, including large and complex data types
- gold Open Access which fosters wider collaboration and increased citations
- maximum visibility for your research: over 100M website views per year

At BMC, research is always in progress.

Learn more biomedcentral.com/submissions



RESEARCH

Open Access

[¹⁸F]-AV-1451 binding profile in chronic traumatic encephalopathy: a postmortem case series



Marta Marquié^{1,2†}, Cinthya Agüero^{1,2†}, Ana C. Amaral^{1,2}, Alberto Villarejo-Galende³, Prianca Ramanan^{1,2}, Michael Siao Tick Chong^{1,2}, Nil Sáez-Calveras^{1,2}, Rachel E. Bennett^{1,2}, Eline E. Verwer⁴, Sally Ji Who Kim⁴, Maeva Dhaynaut^{4,5}, Victor E. Alvarez^{6,7,8}, Keith A. Johnson⁴, Ann C. McKee^{6,7,8}, Matthew P. Frosch^{1,2,9} and Teresa Gómez-Isla^{1,2*} 

Abstract

Introduction: Chronic traumatic encephalopathy (CTE) is a tauopathy associated to repetitive head trauma. There are no validated in vivo biomarkers of CTE and a definite diagnosis can only be made at autopsy. Recent studies have shown that positron emission tomography (PET) tracer AV-1451 (Flortaucipir) exhibits high binding affinity for paired helical filament (PHF)-tau aggregates in Alzheimer (AD) brains but relatively low affinity for tau lesions in other tauopathies like temporal lobar degeneration (FTLD)-tau, progressive supranuclear palsy (PSP) or corticobasal degeneration (CBD). Little is known, however, about the binding profile of this ligand to the tau-containing lesions of CTE.

Objective: To study the binding properties of [¹⁸F]-AV-1451 on pathologically confirmed CTE postmortem brain tissue samples.

Methods: We performed [¹⁸F]-AV-1451 phosphor screen and high resolution autoradiography, quantitative tau measurements by immunohistochemistry and Western blot and tau seeding activity assays in brain blocks containing hippocampus, superior temporal cortex, superior frontal cortex, inferior parietal cortex and occipital cortex from 5 cases of CTE, across the stages of disease: stage II-III (*n* = 1), stage III (*n* = 3), and stage IV (*n* = 1). Importantly, low or no concomitant classic AD pathology was present in these brains.

Results: Despite the presence of abundant tau aggregates in multiple regions in all CTE brains, only faint or no [¹⁸F]-AV-1451 binding signal could be detected by autoradiography. The only exception was the presence of a strong signal confined to the region of the choroid plexus and the meninges in two of the five cases. Tau immunostaining and Thioflavin-S staining ruled out the presence of tau aggregates in those regions. High resolution nuclear emulsion autoradiography revealed the presence of leptomeningeal melanocytes as the histologic source of this *off-target* binding. Levels of abnormally hyperphosphorylated tau species, as detected by Western Blotting, and tau seeding activity were both found to be lower in extracts from cases CTE when compared to AD.

Conclusion: AV-1451 may have limited utility for in vivo selective and reliable detection of tau aggregates in CTE. The existence of disease-specific tau conformations may likely explain the differential binding affinity of this tracer for tau lesions in different tauopathies.

Keywords: Chronic traumatic encephalopathy, [¹⁸F]-AV-1451, Flortaucipir, Tau, PET, Autoradiography

* Correspondence: tgomezisla@mgh.harvard.edu

†Marta Marquié and Cinthya Agüero contributed equally to this work.

¹MassGeneral Institute for Neurodegenerative Disease, Charlestown, MA, USA

²Department of Neurology, Massachusetts General Hospital, WACC Suite 715
15th Parkman St, Boston, MA 02114, USA

Full list of author information is available at the end of the article



Introduction

Chronic traumatic encephalopathy (CTE) is a neurodegenerative disorder associated with repetitive traumatic head injuries and characterized by the deposition of hyperphosphorylated tau aggregates in the brain [5, 6]. This condition, originally observed in boxers “punch drunk” [23], “dementia pugilistica” [28], has since been described in players of contact sports [13] and military personnel exposed to blast injuries [30]. The clinical picture of CTE includes progressive behavioral and cognitive changes, including irritability, aggression, depression and memory loss, with onset years or decades after brain injury [25], that can eventually progress to dementia [11, 12].

The current clinical criteria of CTE lack specificity and the definitive diagnosis of this condition can only be established by neuropathologic examination. A set of consensus neuropathological criteria for CTE were defined in 2016, which emphasize that tau-containing lesions in CTE differ from those of other tauopathies such as Alzheimer disease (AD), progressive supranuclear palsy (PSP) or corticobasal degeneration (CBD) [24]. The pathognomonic lesions for CTE consist of tau aggregates in neurons, astrocytes and cell processes around small vessels in an irregular pattern in the depths of the cortical sulci [24]. The presence of other neurodegenerative lesions such as TAR DNA binding protein 43 (TDP-43) inclusions and β -amyloid pathology (including plaques and amyloid angiopathy) is also a frequent concomitant finding in CTE [24, 26]. Four progressive stages of CTE have been described according to the abundance and distribution of tau lesions [26]. Tau aggregates in CTE contain all six isoforms with presence of both 3 (3R) and 4 (4R) repeats of the microtubule binding domain, similar to AD but distinct from most other tauopathies [34]. Despite this similarity, it has recently been demonstrated by electron cryomicroscopy (cryo-EM) that tau filament conformation in CTE differs from that of tau filaments present in classic neurofibrillary tangles (NFTs) of AD [9, 10].

There is great interest in developing novel biomarkers for CTE to estimate the prevalence of this disorder in at-risk populations, improve diagnostic accuracy, allow disease progression tracking, and assess treatment response. Several positron emission tomography (PET) tracers designed for detection of tau aggregates in the human living brain have been developed in the past few years. After a number of early failures, [^{18}F]-AV-1451 (alternatively called flortaucipir and previously [^{18}F]-T807) was reported [41] as the first promising ligand for imaging tau in AD. Increased in vivo [^{18}F]-AV-1451 uptake has been observed in AD patients compared to cognitively normal controls (CTL) in cortical regions known to contain NFTs [1, 3, 4, 14, 17, 32, 35, 39]. The

usefulness of [^{18}F]-AV-1451 as a biomarker in other tauopathies such as frontotemporal lobar degeneration (FTLD)-tau including Pick’s disease (PiD), PSP, and CBD, however, is more controversial. Some authors reported increased in vivo [^{18}F]-AV-1451 retention in patients clinically diagnosed with non-Alzheimer (non-AD) tauopathies in regions that are expected to contain tau lesions while others noticed in vivo binding patterns nearly indistinguishable from those in normal controls [1, 3, 4]. Several groups, including our own have demonstrated, using autoradiography approaches in postmortem brain tissue samples, that [^{18}F]-AV-1451 has a significantly higher affinity for tau aggregates in the form of NFTs in AD compared to tau aggregates in non-AD tauopathies [19–21, 33]. Importantly, [^{18}F]-AV-1451 also exhibits strong *off-target* binding to neuromelanin (in pigmented brainstem regions) and melanin (in leptomeninges). The former of these affinities explains the nearly universal elevated in vivo retention observed in the substantia nigra of elderly individuals regardless of their pathological diagnosis [21]. There is additional *off-target* binding in areas of intraparenchymal hemorrhage, although to a lesser degree [21]. The underlying pathology of this tracer’s in vivo uptake frequently detected in other brain regions that do not typically contain tau aggregates in AD, such as basal ganglia, is still not yet well understood.

Only a few studies using [^{18}F]-AV-1451 PET in clinically diagnosed CTE subjects have been published to date [8, 29, 36]. Results from those early reports have suggested that this tau tracer may serve as an in vivo surrogate marker for tau-containing aggregates in this condition. To date, no [^{18}F]-AV-1451 imaging-postmortem correlation studies in pathologically confirmed CTE cases have been published. The aim of our study was to investigate [^{18}F]-AV-1451 binding patterns in pathologically confirmed CTE tissue using phosphor screen and high-resolution autoradiography and correlate those findings with quantitative tau measurements as reported by immunohistochemistry, Western blotting, and tau seeding activity in the same samples. Our results show that [^{18}F]-AV-1451 exhibits relatively low binding affinity for tau aggregates in CTE suggesting that this tracer may have limited utility for the in vivo selective and reliable detection of tau aggregates which serve as the neuropathologic hallmark of this condition.

Material and methods

Brain tissue samples

Five cases from the Boston University (BU) Alzheimer’s Disease Research Center (ADRC) Brain Bank with a neuropathological diagnosis of CTE were selected for this study. Tissue collection and use were approved by the local Institutional Board. The neuropathological

processing followed the procedures previously established by the BU ADRC Brain Bank [38]. Paraffin-embedded sections were stained with Luxol fast blue, hematoxylin and eosin, Bielschowsky silver, AT8, amyloid- β (A β), α -synuclein, ubiquitin, TDP-43, SMI-31 and SMI-34 using methods described previously [25]. Diagnostic evaluation was performed in accordance with published guidelines for neurodegenerative diseases [2, 16, 27]. Neuropathological diagnoses were made by a BU ADRC Brain Bank neuropathologist without any knowledge of the subject's clinical histories and was confirmed by two other neuropathologists.

Frozen brain tissue blocks containing hippocampus (HPC), superior temporal cortex (TC), superior frontal cortex (FC), inferior parietal cortex (PC) and occipital cortex including calcarine cortex (OC) were analyzed. Demographical and neuropathological information for each case is shown in Table 1. Cases were classified according to the recently described CTE staging [26] into stages I-IV. The tissue blocks were sectioned in a freezing cryostat (Thermo-Shandon SME Cryostat) into 10- μ m-thick slices and used for immunohistochemistry (IHC) and phosphor screen and nuclear emulsion autoradiography. Fresh frozen homogenates prepared from

the same tissue blocks were used to quantify tau contents by Western Blot and to measure tau seeding activity by sensitive in vitro seeding assays. Fresh frozen homogenates containing the same regions of interest (ROIs) from 15 additional cases (including 9 pathologically-confirmed AD cases and 6 control cases free of pathology) from the Massachusetts ADRC where also included in the Western Blot and tau seeding assays for comparison.

[¹⁸F]-AV-1451 phosphor screen and high resolution autoradiography

10- μ m-thick frozen tissue sections containing the ROIs were used to perform [¹⁸F]-AV-1451 phosphor screen and high resolution autoradiography experiments following our previously published protocols [21]. In brief, sections were fixed in 100% methanol at room temperature (RT) for 20 min and transferred to a bath containing high specific activity [¹⁸F]-AV-1451 in 10 mM PBS with a radioactivity concentration of approximately 20 μ Ci/ml. Adjacent sections were placed in an identical bath except that unlabeled AV-1451 was added to yield 1 μ M chemical concentration, a blocking condition sufficient to saturate essentially all specific binding sites of tau

Table 1 Demographic and neuropathologic characteristics

Case N°	Pathological diagnosis	Age at death (years)	Gender	Braak & Braak (NFTs)	CERAD score (neuritic plaques)	NIA-Reagan Institute criteria
1	CTE (CTE stage III)	46	M	III	none	LP
2	CTE (CTE stage IV)	65	M	II	A	LP
3	CTE (CTE stage III)	56	M	II	none	LP
4	CTE (CTE stage II-III)	25	M	0	none	LP
5	CTE (CTE stage III)	58	M	III	none	LP
6	AD	87	F	V	Frequent	IP
7	AD	71	M	V	Moderate	IP
8	AD	96	F	V	Frequent	HP
9	AD	82	F	V	Moderate	HP
10	AD	79	M	V	Frequent	HP
11	AD	66	M	V	Moderate	HP
12	AD	69	F	VI	Frequent	HP
13	AD	66	F	VI	Frequent	HP
14	AD	66	F	VI	Frequent	HP
15	CTL	76	F	I	Sparse	LP
16	CTL	97	F	I	Sparse	LP
17	CTL	81	M	I	none	LP
18	CTL	59	F	I-II	Moderate	LP
19	CTL	91	M	II	none	LP
20	CTL	101	F	II	Moderate	LP

Abbreviations: CTE Chronic traumatic encephalopathy, AD Alzheimer's disease, CERAD Consortium to Establish a Registry for Alzheimer's Disease, CTL Control, F Female, HP High probability of AD, IP Intermediate probability of AD, LP Low probability of AD, M Male, NFT Neurofibrillary tangles, NIA National Institute of Ageing

[21]. After incubation for 60 min, sections were removed from radioactivity solutions and washed to remove unbound radiotracer. Wash solutions and incubation times were: 10 mM PBS for 1 min, 70% ethanol/30% PBS for 2 min, 30% ethanol/70% PBS for 1 min, and lastly 100% 10 mM PBS for 1 min. Sections were then air dried before transferring to a storage phosphor screen (Multi-Sensitive Phosphor Screen, PerkinElmer Life and Analytic Sciences, Shelton, CT) that had been photo-bleached immediately prior by exposure on a white light box for a minimum of 15 min. Sections and phosphor screen were enclosed in aluminum film cassette and set in a dark area. Under dim lighting conditions, the cassette was opened and the slides removed from the exposed screen, which was mounted to the carousel of imaging system (Cyclone Plus Storage Phosphor Scanner, PerkinElmer Life and Analytic Sciences). Scanning of screens was controlled by the manufacturer's OptiQuant software package using the highest available resolution of 600 dpi (approximately 42 μm sampling interval). Digital images were saved in uncompressed form at full resolution and pixel depth. Images from adjacent brain slices incubated in the unblocked (high specific activity [^{18}F]-AV-1451 only) and blocking [^{18}F]-AV-1451 plus 1 μM unlabeled AV-1451) conditions were compared to determine total and non-specific binding of [^{18}F]-AV-1451 in the tissue. All experiments were run in triplicate on adjacent tissue sections.

To rule out the possibility that the ethanol washing steps used in the above autoradiography protocol may have removed some weaker tracer binding, parallel experiments in comparable tissue samples incubated with [^{18}F]-AV-1451 with a radioactivity concentration of approximately 1 $\mu\text{Ci}/\text{ml}$ and avoiding the use of ethanol in the washing conditions were also conducted. All assays were done in triplicate on adjacent tissue sections.

To obtain autoradiographic information at cellular resolution level, frozen cryostat sections, adjacent to those used for phosphor screen autoradiography, were coated with liquid photographic emulsion, then immunostained using appropriate primary antibodies - anti-tau PHF1 (1:100, mouse, kind gift of Dr. Peter Davies), anti A β (1:50, rabbit, IgG Affinify Purify, IBL) or anti TDP-43 (1:100, rabbit, Protein Tech) - and counterstained with H&E following our previously published protocol [20].

Tau burden quantification by immunohistochemistry

10- μm -thick frozen tissue sections containing the five ROIs and adjacent to those used in autoradiography experiments were stained with PHF-1 antibody (1:100, mouse, kind gift of Dr. Peter Davies) and analyzed with an upright Olympus BX51 microscope (Olympus, Denmark) using the CAST software (Visiopharm, 2004, Denmark). Each ROI was drawn in the corresponding

slide at 1.25x magnification, and then a systematic random sampling was applied using the software's optical disector probe at 10x magnification (meander sampling 20%). A threshold of optical density was obtained in each microphotograph using ImageJ (National Institute of Health). Manual editing in each field eliminated artifacts. Tau pathology burden, defined as total percentage (%) of area covered by PHF-1 immunostaining, was calculated in each ROI.

Measurements of soluble tau in synaptoneurosomal fractions by Western blot

Synaptoneurosomal fractions from the five ROIs were obtained from the same tissue blocks used in immunohistochemistry and autoradiography experiments to measure soluble tau content by Western blot, following our previously published protocol [20]. Human tau (Dako, A0024) and PHF-1 (kind gift of Dr. Peter Davies) antibodies were used to assess levels of total tau and hyperphosphorylated-tau, respectively. Briefly, tissue samples were homogenized in Buffer A (25 mM HEPES 7.5, 120 mM NaCl, 5 mM KCL, 1 mM MgCl₂, 2 mM CaCl₂, 1 mM DTT) supplemented with Phosphatase Inhibitor Cocktail tablets (Roche, 04906845001) and Protease Inhibitor Cocktail tablets (Roche, 11,697,498,001). The homogenate was filtered through 2 Millipore Nylon 80 μm filters after the addition of 0.6 mL Buffer A and 200 μL of homogenate was separated. Two hundred microliter of distilled H₂O and 70 μL of 10% SDS were added to the homogenate and passed through a 27½ G needle 3 times. The remaining homogenate was filtered again through PALL Acrodisc Syringe 5 μm Filters after the addition of 1 mL Buffer A, and centrifuged at 1000 g for 10 min at 4 °C. The supernatant was then separated and ultracentrifuged at 100,000 g for 45 min, and the pellet was resuspended in 200 μL Buffer B (50 mM Tris, 1.5% SDS, 1 mM DTT). The resuspended pellet and the separated homogenate were then boiled for 5 min, centrifuged for 15 min, and the supernatants were collected as synaptoneurosomal (SNS) and total fractions, respectively.

SNS fractions from each ROI were electrophoresed in MES SDS Running Buffer (Novex, NP0002) using 4–12% Bis-Tris Novex gels (Invitrogen, #MAN0003679). Protein was then transferred onto nitrocellulose membranes and blocked for an hour at room temperature using Odyssey Blocking Buffer (LiCor, 927–40,000). Membranes were probed with human tau (Dako, A0024) and PHF-1 (kind gift of Dr. Peter Davies) antibodies to detect content of total tau and phospho-tau, respectively. GAPDH (Millipore, AB2302) was used as loading control for protein normalization. LiCor secondary antibodies (IR Dye 680RD Donkey anti-chicken 926–68,075, IR Dye 800 CW Donkey anti-rabbit 926–32,213, IR Dye 800CW Donkey anti-mouse 926–32,212) were then used

to visualize bands with the Odyssey Infrared Imaging System (V3.0). ImageStudio was used to quantify the bands of interest by drawing equal size rectangles around individual bands of interest. Background subtraction was applied by taking the median of the area three pixels to the left and right of each band of interest and subtracting that value from the measured signal.

Tau seeding assays

PBS fractions obtained from fresh frozen total homogenates from the five ROIs were used to perform tau seeding activity assays. Equivalent samples from AD ($n = 9$) and control cases free of tau pathology ($n = 6$) were also analyzed for comparison. In vitro tau seeding activity was measured as previously described elsewhere [15]. In short, HEK293 cells stably expressing TauRD^{P301S} fused with cyan fluorescent protein (CFP) and TauRD^{P301S}-yellow fluorescent protein (YFP) (Tau RD P301S FRET Biosensor (ATCC CRL^R-3275™)) were plated at 40,000 cells per well in poly-D-lysine coated black clear-bottom 96-well plates (Corning). The following day, cells were transduced with a total of 50 μ l of 2 μ g/well PBS-soluble frozen brain lysate (3,000 g) plus 7% lipofectamine 2000 transfection reagent (#11668–019, Invitrogen) in Opti-MEM (#11058–021, Life technologies), after the lysate and lipofectamine complex had incubated at room temperature for 20 min. The cells were left to incubate at 37 °C with the lysate-lipofectamine complex for 41 h. Cells were then removed from the plate using Trypsin-EDTA and transferred to a 96-well U-bottom plate (Corning) with chilled DMEM 10% FBS media. Cells were pelleted at 1,800 g using a plate spinner, fixed with 2% paraformaldehyde (PFA, #15714-S, Electron Microscopy Sciences) in the dark for 10 min at 4 °C, and pelleted again. Cells were resuspended in cold PBS and immediately run on the MACSQuant VYB flow cytometer (Miltenyi). CFP and FRET were measured on the flow cytometer by exciting the HEK293 cells with a 405 nm laser and then reading fluorescence at 405/50 nm and 525/50 nm filters, respectively. Using the MACSQuantify flow cytometry software (Miltenyi), the integrated FRET density (IFD) was calculated by multiplying the % number of FRET-positive tau aggregates by the mean fluorescence intensity of FRET-positive tau aggregates. This value was then normalized by the value for the cells that were treated only with the lipofectamine (without brain lysate), serving as a non-treated FRET-negative population. Each sample was run in triplicate. Representative images of the tau aggregates were captured using the ZOE Fluorescent Cell Imager (BioRad) in the GFP excitation and emission filters.

Statistical analysis

Correlation analyses between PHF-tau burden quantification by immunohistochemistry, measurements of

soluble tau contents as reported by Western blot, and IFD as reported by tau seeding assays were conducted using a Spearman correlation test. For non-parametric analyses, Kruskal-Wallis test was used to compare IFD in control, CTE and AD samples. Significance was set at $p < 0.05$. All statistical analysis and graphs were generated using GraphPad Prism v6.0 software (GraphPad Software Inc., La Jolla, CA).

Results

[¹⁸F]-AV-1451 phosphor screen autoradiography

As expected, strong tracer binding was detected in tangle-containing regions from AD tissue used as positive control. However, no autoradiographic signal could be detected across multiple cortical regions known to contain tau aggregates in the 5 CTE cases (Fig. 1). The exception was the presence of strong tracer binding observed in a few isolated areas in 2 cases (case #1 HPC and TC, and case #3 HCP and TC) (Fig. 1). Adjacent sections stained with PHF-1 antibody and Thio-S showed that the autoradiography signal corresponded to *off-target* binding to leptomenigeal melanocytes and not to tau aggregates. Weaker binding was also noticed in the hippocampus from case #2 (the oldest individual in the CTE group, age 65) where some classic AD NFTs were present along with abundant CTE tau aggregates (Fig. 1).

Parallel autoradiographic experiments performed on adjacent tissue slices and eliminating ethanol from the washing conditions yielded identical results (Fig. 2), ruling out the possibility that the ethanol washing steps may have removed some weaker tracer binding in these cases. A slightly higher non-specific background signal in the white matter was observed across cases when avoiding the use of ethanol in the washing steps.

[¹⁸F]-AV-1451 high resolution nuclear emulsion autoradiography

To confirm the above observations and obtain cellular resolution, we performed autoradiography with photographic nuclear emulsion on histologic sections, followed by immunohistochemistry with appropriate tau antibodies. As expected, tangle-containing sections from cases of AD exhibited a strong concentration of silver grains colocalizing with NFTs. In tissue from cases of CTE, however, there was negligible accumulation of silver grains despite the presence of robust amounts of tau aggregates in the pathognomonic pattern of the disease (Fig. 1). Of note, abundant silver grains labeled the concomitant classic NFTs present in low amounts in the hippocampus of case #2, serving as an internal positive control for our autoradiographic experiments, but not the abundant CTE tau aggregates present in the same tissue material. In agreement with the above results from phosphor screen

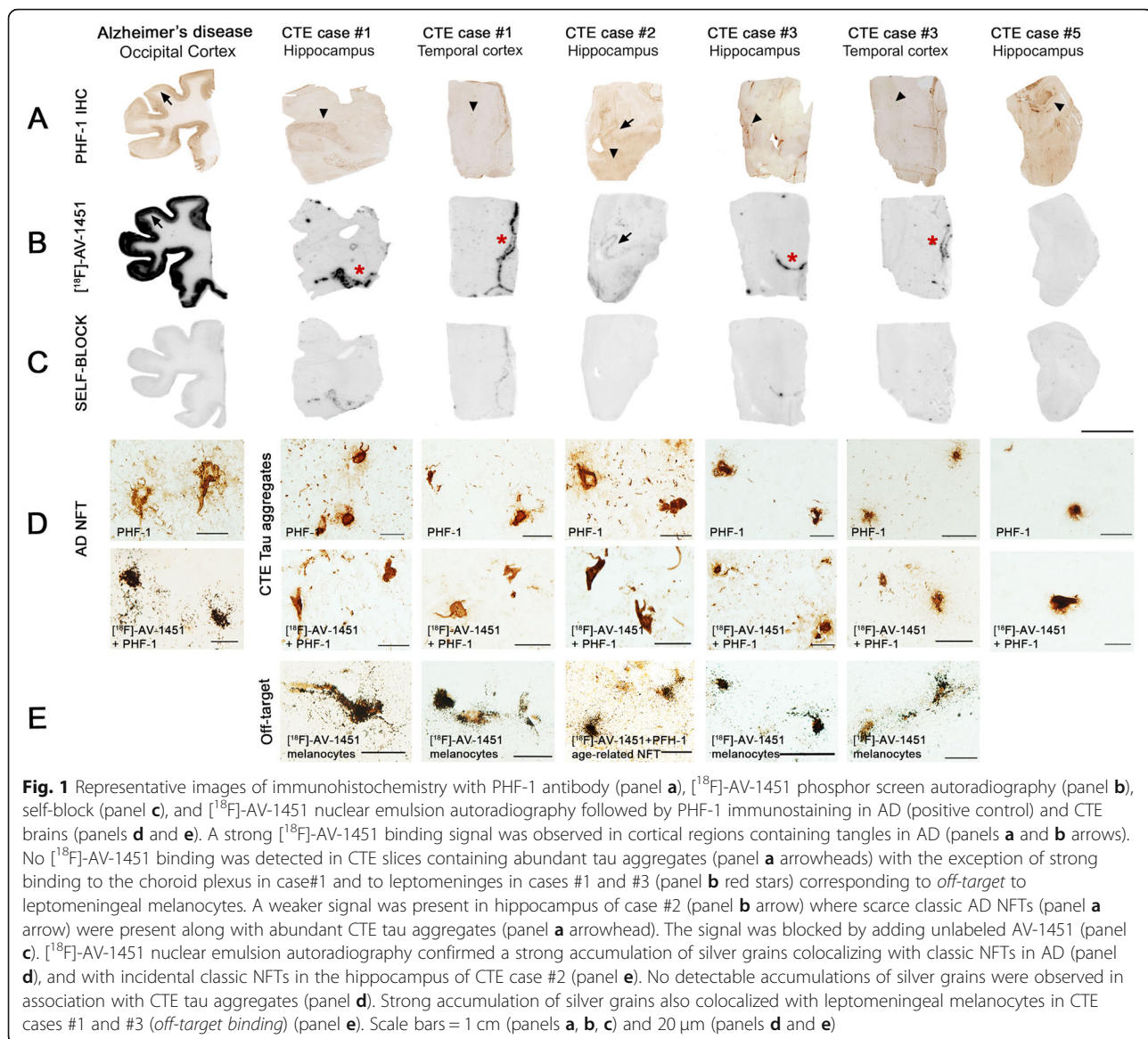


Fig. 1 Representative images of immunohistochemistry with PHF-1 antibody (panel **a**), [¹⁸F]-AV-1451 phosphor screen autoradiography (panel **b**), self-block (panel **c**), and [¹⁸F]-AV-1451 nuclear emulsion autoradiography followed by PHF-1 immunostaining in AD (positive control) and CTE brains (panels **d** and **e**). A strong [¹⁸F]-AV-1451 binding signal was observed in cortical regions containing tangles in AD (panels **a** and **b** arrows). No [¹⁸F]-AV-1451 binding was detected in CTE slices containing abundant tau aggregates (panel **a** arrowheads) with the exception of strong binding to the choroid plexus in case #1 and to leptomeninges in cases #1 and #3 (panel **b** red stars) corresponding to *off-target* to leptomeningeal melanocytes. A weaker signal was present in hippocampus of case #2 (panel **b** arrow) where scarce classic AD NFTs (panel **a** arrow) were present along with abundant CTE tau aggregates (panel **a** arrowhead). The signal was blocked by adding unlabeled AV-1451 (panel **c**). [¹⁸F]-AV-1451 nuclear emulsion autoradiography confirmed a strong accumulation of silver grains colocalizing with classic NFTs in AD (panel **d**), and with incidental classic NFTs in the hippocampus of CTE case #2 (panel **e**). No detectable accumulations of silver grains were observed in association with CTE tau aggregates (panel **d**). Strong accumulation of silver grains also colocalized with leptomeningeal melanocytes in CTE cases #1 and #3 (*off-target binding*) (panel **e**). Scale bars = 1 cm (panels **a**, **b**, **c**) and 20 μm (panels **d** and **e**)

autoradiography experiments and our previously published observations [20, 21], silver grains strongly labeled leptomeningeal melanocytes (*off target*) found in two of the five CTE cases (case #1 and case #3) (Fig. 1).

Total tau content by Western blot

Analysis of SNS fractions by Western blot revealed the presence of tau in the form of low molecular weight (monomeric) and high molecular weight (oligomeric) assemblies in CTE brains. Representative images of total tau and hyperphosphorylated tau in ROIs from CTE cases as reported by Western Blot are shown in Fig. 3a and c. Levels of hyperphosphorylated tau were significantly lower in CTE cases compared to AD cases (hippocampus CTE vs. AD: pTau monomers 0.62 ± 0.70 vs. 2.56 ± 1.95 , $p = 0.04$; pTau oligomers 0.46 ± 0.50 vs. 2.74 ± 3.41 ,

$p = 0.02$; temporal cortex CTE vs. AD: pTau monomers 0.82 ± 0.69 vs. 5.32 ± 3.74 , $p = 0.03$; pTau oligomers 0.77 ± 0.76 vs. 3.38 ± 2.82 , $p = 0.04$; occipital cortex CTE vs. AD: pTau monomers 0.02 ± 0.006 vs. 5.46 ± 5.13 , $p = 0.03$; pTau oligomers 0.01 ± 0.01 vs. 7.03 ± 7.22 , $p = 0.01$) (Fig. 3c). A significant correlation was detected between burden of tau aggregates, measured in PHF-1 immunostained ROIs, and synaptic content of total tau oligomers ($r = 0.47$, $p = 0.02$, Fig. 3b) and phospho-tau monomers and oligomers in CTE cases ($r = 0.82$, $p < 0.0001$ and $r = 0.78$, $p < 0.0001$, respectively, Fig. 3d).

Tau seeding assays

Tau seeding activity across the ROIs in CTE brains was significantly higher than in control brains free

of tau-containing lesions but significantly lower than in AD brains ($p = 0.0009$) (Fig. 4a-b). Representative images of tau seeding activity assays are depicted in Fig. 4a. Of note, a substantial patient to patient variability was noted in both groups, CTE and AD (Fig. 4b). Tau seeding activity in CTE cases closely correlated with the total burden of tau aggregates (%) measured in PHF-1 immunoreactivity ($r = 0.65$, $p = 0.0004$, Fig. 4c), as well as with the levels total tau oligomers ($r = 0.74$, $p < 0.0001$, Fig. 4e) but not total tau monomers ($r = 0.005$, n.s., Fig. 4d), and with levels of soluble phospho-tau monomers and

oligomers ($r = 0.89$, $p < 0.0001$ and $r = 0.85$, $p = 0.0001$, respectively, Figs. 4f-g), as measured by Western blot.

Discussion

We have examined the postmortem regional- and substrate-specific binding patterns of tau PET tracer [^{18}F]-AV-1541 in multiple ROIs from five autopsy-confirmed CTE cases. Our observations are derived from [^{18}F]-AV-1451 sensitive autoradiography, quantification of tau burden on immunostained sections, biochemical analysis of soluble tau content by Western blot and in vitro tau

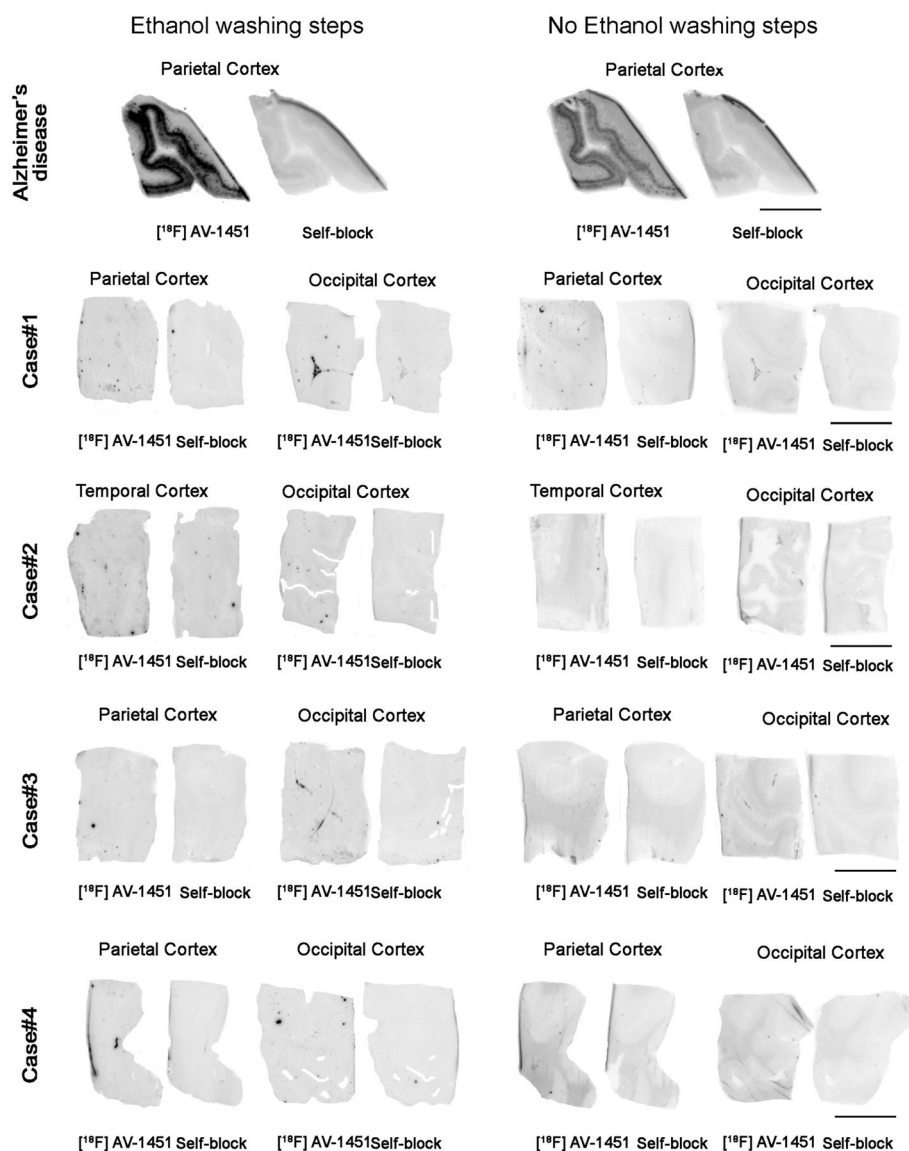
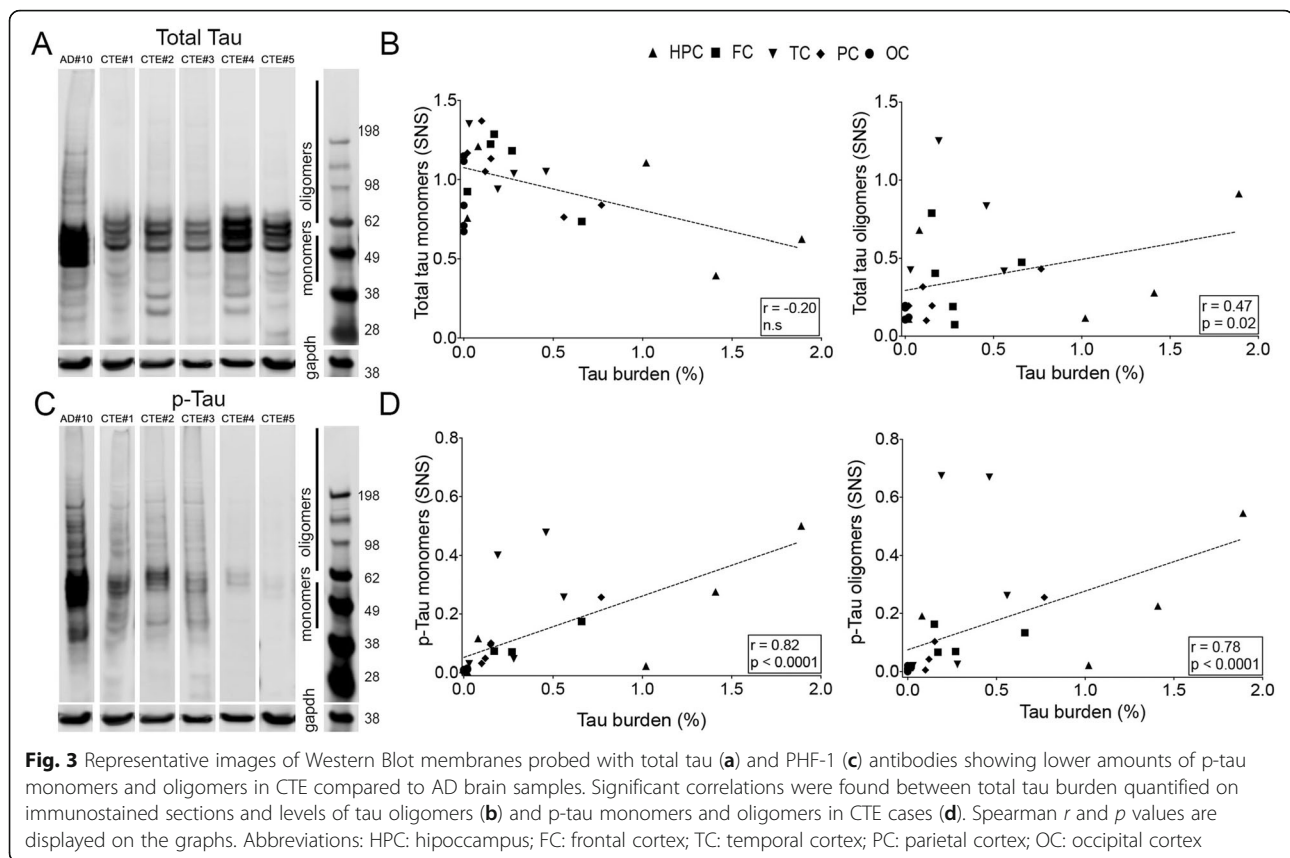


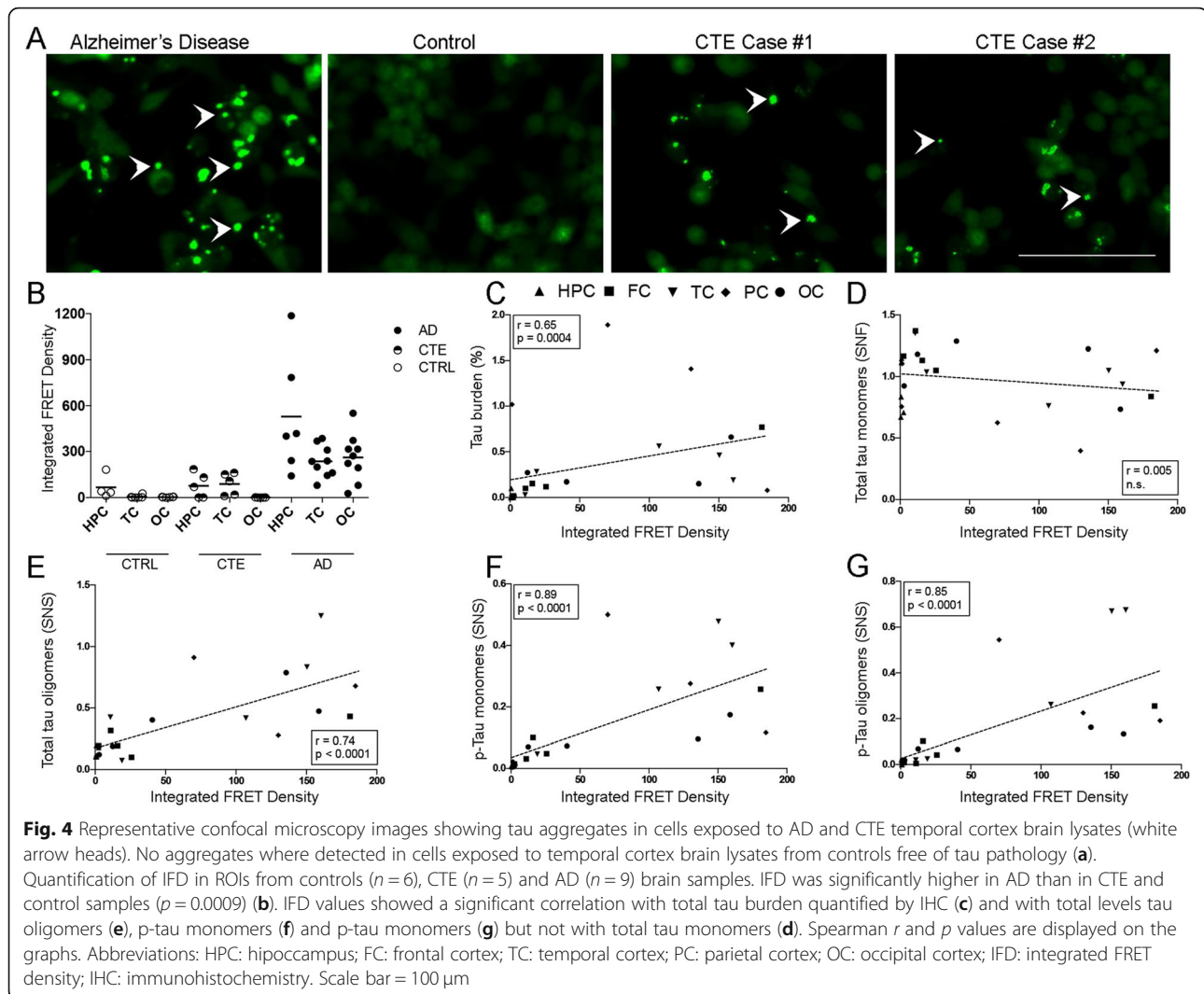
Fig. 2 Representative images of phosphor screen autoradiography experiments with and without ethanol washing steps. Identical results were observed in the head to head comparison of both protocols using adjacent brain tissue slices. A strong [^{18}F]-AV-1451 binding signal was observed in cortical regions containing tangles in AD but no [^{18}F]-AV-1451 binding was detected in CTE slices with the exception of the off-target to leptomenigeal melanocytes. Scale bar = 1 cm



seeding activity assays. In agreement with our previous observations, high resolution autoradiography experiments revealed strong binding of [^{18}F]-AV-1451 to NFTs in AD [20, 21], but negligible binding to tau aggregates in CTE brains. A strong [^{18}F]-AV-1451 binding to incidental leptomeningeal melanocytes present in two of the five CTE cases further confirmed tracer *off-target* binding to this biological substrate [20, 21]. These observations, along with the lack of correlation between [^{18}F]-AV-1451 autoradiographic regional binding at postmortem and the topographical distribution of tau aggregates or multiple other tau measures in these cases of CTE, suggest that [^{18}F]-AV-1451 may not have sufficient sensitivity to reliably detect and quantify tau pathology in CTE by in vivo neuroimaging particularly when confounding AD lesions are present in the context of aging.

As in other neurodegenerative conditions, the development of novel fluid and neuroimaging biomarkers potentially capable of facilitating an accurate diagnosis of CTE and of monitoring disease progression has become a priority in this research field [37, 42]. While tau PET tracer [^{18}F]-AV-1451 has recently shown great promise as a surrogate biomarker for tau-containing lesions in AD through its binding to NFTs with PHF conformation, the potential utility of this ligand in assessing the burden of the distinct tau-containing lesions of CTE remains

uncertain. To date, only very limited data from human in vivo [^{18}F]-AV-1451 PET imaging studies in patients with clinically suspected CTE have been published and they all, unfortunately, lack neuropathological confirmation of the diagnosis. Mitsis et al. reported a 71-year old retired NFL football player who had experienced multiple concussions and presented with progressive cognitive impairment in his 60s. [^{18}F]-Florbetapir PET was negative, excluding significant concomitant amyloid deposition, while [^{18}F]-AV-1451 PET showed increased uptake localized in globus pallidus, putamen, hippocampus and the substantia nigra [29]. However, we and others have described a nearly identical pattern of in vivo retention in elderly controls [17], that seems heavily influenced by the non-specific retention of this tracer in basal ganglia and its *off-target* to neuromelanin-containing neurons in the substantia nigra [21]. Dickstein et al. reported another 39-year old retired NFL football player with a history of multiple concussions who experienced cognitive decline, irritability and emotional lability in his 30s. [^{18}F]-Florbetapir PET was negative and [^{18}F]-AV-1451 showed increased retention in midbrain, globus pallidus and hippocampus, and also at gray-white matter junctions in multiple cortical areas, mirroring the described postmortem distribution of CTE tau lesions [7]. It should be noted though that, in the absence of a validated threshold for defining



signal with [^{18}F]-AV-1451, the authors relied on the value commonly used for the amyloid PET tracer florbetapir and thus, these results must be interpreted with caution [18]. Very recently, another study by Stern et al. has reported a significantly higher [^{18}F]-AV-1451 in vivo retention at the group level in three brain regions (bilateral superior frontal, bilateral medial temporal, and left parietal) in a cohort of 26 former National Football League (NFL) players with cognitive and neuropsychiatric symptoms compared to 31 asymptomatic men with no history of traumatic brain injury [36]. It remains unclear whether such differences were also present at individual level. Of note, the average in vivo retention values observed in the group of NFL players in that study were quite modest (SUVR values 1.09–1.12), with the exception of the medial temporal lobe (1.23); most fell within the range of in vivo retention values reported in normal elderly controls in multiple other studies [31]. Intriguingly, no association between [^{18}F]-AV-1451 in vivo retention and scores on

cognitive and neuropsychiatric tests could be demonstrated. The potential presence of age-related tau-containing lesions in the medial temporal lobe and tracer *off-target* binding to old hemorrhages, which are quite common after brain trauma, are potential confounders when interpreting these results.

All of the 5 CTE cases studied here demonstrated immunohistochemically confirmed abundant tau aggregates in a distribution consistent with the consensus diagnostic criteria. Importantly, we carefully selected the CTE cases included in this study ruling out the presence of substantial concomitant AD pathology as a confounder in our autoradiography experiments given the known strong affinity of [^{18}F]-AV-1451 to classic AD tau tangles. Our phosphor-screen autoradiography experiments, showed negligible binding of [^{18}F]-AV-1451 in brain regions with a high burden of tau lesions apart from *off-target* binding to leptomeningeal melanocytes present in two of the five cases. In contrast, tangle-

containing sections from AD brains, included here as positive control, exhibited strong [^{18}F]-AV-1451 binding signal as previously reported by us and others [19–22, 33, 41]. In agreement with these findings, high resolution nuclear emulsion autoradiography experiments showed high concentrations of silver grains colocalizing with NFTs in AD brains and incidental extracutaneous leptomeningeal melanocytes but no detectable silver grain accumulation colocalizing with CTE tau aggregates.

The possibility that the use of ethanol in the washing steps included in our traditional autoradiography protocol may have removed some weaker tracer binding was carefully ruled out by performing experiments which avoided the use of ethanol or other solvents in the washing conditions. Those parallel autoradiography studies yielded identical results.

The pathological tau burden in the CTE cases, quantified on immunostained sections containing multiple ROIs, significantly correlated with the levels of soluble p-tau monomers and oligomers, as assessed by Western blotting, and with tau seeding activity in the same ROIs. These measures of pathologic tau aggregates, however, were substantially lower than those found in a series of 9 AD cases that were used here for comparison. Intriguingly, a previous study by Woerman et al. reported increased tau seeding activity in CTE when compared to AD brains [40]. We believe that the discrepancies between that and the present study may be related to differences in sampling, given the highly focal nature of CTE [40], and/or the potential presence of concomitant AD pathology, a common finding in this condition [26], in older individuals with CTE. As noted above, our studies specifically excluded coincident neuropathologic processes, including the presence of substantial AD pathology, as a potential confounder through careful case selection.

Our results suggest that [^{18}F]-AV-1451 differs in its affinity for the tau aggregate-containing lesions of CTE and AD, despite both being comprised of 3 and 4 repeat isoforms of tau. Importantly, recent studies based on cryo-EM have elegantly demonstrated the existence of distinct conformers of assembled tau in different tauopathies [9, 10]. That work has demonstrated that, despite the presence of both 3 and 4 repeat isoforms, the tau filament structures in CTE are distinct from those of AD, as well as from the 3 repeat isoform containing tau aggregates of Pick disease. Even though similarly to AD, all six tau isoforms assemble into filaments in CTE, a conformation of the β -helix region creates a hydrophobic cavity that is absent in tau filaments in AD. Moreover, filaments in CTE have distinct protofilament interfaces to those of AD [10]. The distinct conformations of tau filaments in different tauopathies may not

only explain the phenotypic and neuropathologic diversity of these disorders but also underlie the differential affinity of PET ligands, like [^{18}F]-AV-1451, for tau aggregates in AD and non-AD tauopathies. This may, in part, reflect the process by which this compound was identified as potential tau imaging agents screening using cortical homogenates from AD brain tissue rich in NFT as the binding target. A potential limitation of the current study is the lack of females in the CTE group.

Conclusions

In conclusion, the results from this study further favor the idea that tau tracer [^{18}F]-AV-1451 binds with high affinity to tau aggregates in AD brains and that now established *off-target* binding must be carefully taken into account when interpreting its behavior *in vivo*. Our data also indicate that [^{18}F]-AV-1451 exhibits relatively low binding affinity to tau inclusions in CTE and suggest that this ligand may have a limited utility for the reliable detection and quantification of tau lesions in this non-AD tauopathy. The combination of the lower pathological tau load in CTE brains when compared to AD and the apparent differential affinity of this imaging agent for disease-specific molecular conformations of tau filaments suggest that [^{18}F]-AV-1451 may not be an optimal agent to use for assessment of CTE, particularly in older individuals where the presence of concomitant AD pathology is a frequent finding. Further neuro imaging-pathologic correlation studies are needed to accurately interpret what *in vivo* [^{18}F] AV-1451 PET positivity means. Although we cannot rule out with absolute certainty that [^{18}F] AV-1451 may exhibit some weak binding affinity for tau aggregates in CTE, we believe that selective screening using different tau conformations as binding targets may result in better and more reliable PET tracers for CTE and other non-AD tauopathies.

Acknowledgements

We are grateful to the study subjects, the Boston University ADRC and Massachusetts ADRC Brain Banks for providing the tissue samples, the MGH Gordon PET Core for providing the radiotracer and P41EB022544 for instruments used in this work, and to Dr. Peter Davies, from the Feinstein Institute for Medical Research, for kindly sharing the PHF-1 antibody.

Authors' contributions

MM and CA participated in study design, carried out immunostaining, phosphor screen and nuclear emulsion autoradiography, data analysis and drafted the manuscript. ACA carried out Western Blot experiments, analysis and interpretation of data. AVG participated in analysis, interpretation of data and drafted the manuscript. PR and MSTC carried out immunostaining and tau seeding assays. NSC carried out immunostaining and tau burden quantification. REB participated in analysis and interpretation of data. EEV, SWK and MD carried out phosphor screen autoradiography. VA prepared the tissue blocks from CTE cases. KAJ participated in the study design. ACM carried out the neuropathologic examination of CTE cases. MPF carried out the neuropathologic examination of AD and control cases, and participated in the study design, analysis and interpretation of data. TGI conceived the study and participated in its design and coordination, analysis and

interpretation of data and drafted the manuscript. All authors read and approved the final manuscript.

Availability of data and materials

Original slides and diagnostic material are retained. There are no novel reagents or materials for others to request.

Ethics approval and consent to participate

All procedures performed in studies involving human participants were in accordance with the ethical standards of the institutional and national research committee and with the 1964 Helsinki declaration and its later amendments.

Consent for publication

Informed consent was obtained from all individual participants included in the study and according to institutional procedures for autopsy consents for post-mortem tissue.

Competing interests

Marta Marquié received research funding from NIH grant AG005134 and AG036694. Marta Marquié currently works at Fundació ACE Institut Català de Neurociències Aplicades – Universitat Internacional de Catalunya in Barcelona, Spain.

Cintha Agüero received research funding from NIH grant AG036694 and AG061206.

Ana C. Amaral received research funding from NIH grant AG036694 and AG061206. Alberto Villarejo-Galende received research funding from the Instituto de Salud Carlos III (BA17/00035).

Prianca Ramanan received research funding from NIH grant AG036694 and AG061206. Michael Siao Tick Chong received research funding from NIH grant AG036694.

Eline Verwer received research funding from the Society of Nuclear Medicine and Molecular Imaging Education and Research Foundation.

Sally Ji Who Kim received research funding from NIH grant T32 EB013180.

Keith A. Johnson received research funding from NIH grants R01 EB014894, R21 AG038994, R01 AG026484, R01 AG034556, P50 AG00513421, U19 AG10483, P01 AG036694, R13 AG042201174210, R01 AG027435 and R01 AG037497 and the Alzheimer's Association grant ZEN-10-174210 K.

Ann C. McKee received research funding from NIH grants R01 AG062348, R01 AG057902, P30-AG13846, U01 NS086659, and the Nick and Lynn Buoniconti Foundation, Andlinger Foundation, National Football League and WWE. Matthew P. Frosch received research funding from NIH grants AG005134 and AG061206. Teresa Gómez-Isla received research funding from NIH grants AG005134, AG036694 and AG061206. Teresa Gómez-Isla participated as speaker in an Eli Lilly and Company sponsored educational symposium and serves in an Eli Lilly Data Monitoring Committee. Eli Lilly and Company currently owns Avid, the company that created AV-1451.

Author details

¹MassGeneral Institute for Neurodegenerative Disease, Charlestown, MA, USA.

²Department of Neurology, Massachusetts General Hospital, WACC Suite 715

15th Parkman St, Boston, MA 02114, USA. ³Department of Neurology,

Hospital Universitario Doce de Octubre, CIBERNED, Madrid, Spain. ⁴Gordon

Center for Medical Imaging, Division of Nuclear Medicine and Molecular

Imaging, Department of Radiology, Massachusetts General Hospital, Boston,

MA, USA. ⁵AP-HP, Department of Nuclear Medicine, Pitié-Salpêtrière Hospital,

Sorbonne University, UPMC Paris 06, CNRS UMR 7371, INSERM U1146, 75013

Paris, France. ⁶Departments of Neurology and Pathology, Boston University

School of Medicine, Boston, MA, USA. ⁷Department of Pathology and

Laboratory Medicine, VA Boston Healthcare System, Boston, MA, USA.

⁸Boston University Alzheimer's and CTE Center, Boston, MA, USA. ⁹C.S. Kubik

Laboratory for Neuropathology, Massachusetts General Hospital, Boston, MA,

USA.

Received: 5 August 2019 Accepted: 8 September 2019

Published online: 28 October 2019

References

- Brier MR, Gordon B, Friedrichsen K, McCarthy J, Stern A, Christensen J, Owen C, Aldea P, Su Y, Hassenstab J, Cairns NJ, Holtzman DM, Fagan AM, Morris JC, Benzinger TL, Ances BM (2016) Tau and Abeta imaging, CSF measures,

and cognition in Alzheimer's disease. *Sci Transl Med* 8:338ra366. <https://doi.org/10.1126/scitranslmed.aaf2362>

- Cairns NJ, Bigio EH, Mackenzie IR, Neumann M, Lee VM, Hatanpaa KJ, White CL 3rd, Schneider JA, Grinberg LT, Halliday G, Duyckaerts C, Lowe JS, Holm IE, Tolnay M, Okamoto K, Yokoo H, Murayama S, Woulfe J, Munoz DG, Dickson DW, Ince PG, Trojanowski JQ, Mann DM, Consortium for Frontotemporal Lobar D (2007) Neuropathologic diagnostic and nosologic criteria for frontotemporal lobar degeneration: consensus of the consortium for frontotemporal lobar degeneration. *Acta Neuropathol* 114:5–22. <https://doi.org/10.1007/s00401-007-0237-2>
- Cho H, Choi JY, Hwang MS, Kim YJ, Lee HM, Lee HS, Lee JH, Ryu YH, Lee MS, Lyoo CH (2016) In vivo cortical spreading pattern of tau and amyloid in the Alzheimer disease spectrum. *Ann Neurol* 80:247–258. <https://doi.org/10.1002/ana.24711>
- Cho H, Choi JY, Hwang MS, Lee JH, Kim YJ, Lee HM, Lyoo CH, Ryu YH, Lee MS (2016) Tau PET in Alzheimer disease and mild cognitive impairment. *Neurology* 87:375–383. <https://doi.org/10.1212/WNL.0000000000002892>
- Critchley M (1949) Punch-drunk syndromes: the chronic traumatic encephalopathy in boxers. In: *Homage a Clovis Vincent*. Maloine, Paris
- Critchley M (1957) Medical aspects of boxing, particularly from a neurological standpoint. *Br Med J* 1:357–362
- Dickstein DL, Dickstein DR, Janssen WG, Hof PR, Glaser JR, Rodriguez A, O'Connor N, Angstman P, Tappan SJ (2016) Automatic dendritic spine quantification from confocal data with neurolicuda 360. *Curr Protoc Neurosci* 77:1 27 21–21 27 21. <https://doi.org/10.1002/cpns.16>
- Dickstein DL, Pullman MY, Fernandez C, Short JA, Kostakoglu L, Knesarek K, Soleimani L, Jordan BD, Gordon WA, Dams-O'Connor K, Delman BN, Wong E, Tang CY, DeKosky ST, Stone JR, Cantu RC, Sano M, Hof PR, Gandy S (2016) Cerebral [18 F]T807/AV1451 retention pattern in clinically probable CTE resembles pathognomonic distribution of CTE tauopathy. *Transl Psychiatry* 6:e900. <https://doi.org/10.1038/tp.2016.175>
- Falcon B, Zhang W, Murzin AG, Murshudov G, Garringer HJ, Vidal R, Crowther RA, Ghetti B, Scheres SHW, Goedert M (2018) Structures of filaments from Pick's disease reveal a novel tau protein fold. *Nature* 561: 137–140. <https://doi.org/10.1038/s41586-018-0454-y>
- Falcon B, Zivanov J, Zhang W, Murzin AG, Garringer HJ, Vidal R, Crowther RA, Newell KL, Ghetti B, Goedert M, Scheres SHW (2019) Novel tau filament fold in chronic traumatic encephalopathy encloses hydrophobic molecules. *Nature* 568:420–423. <https://doi.org/10.1038/s41586-019-1026-5>
- Gavett BE, Ozonoff A, Doktor V, Palmisano J, Nair AK, Green RC, Jefferson AL, Stern RA (2010) Predicting cognitive decline and conversion to Alzheimer's disease in older adults using the NAB list learning test. *J Int Neuropsychol Soc* 16:651–660. <https://doi.org/10.1017/S155617710000421>
- Gavett BE, Stern RA, Cantu RC, Nowinski CJ, McKee AC (2010) Mild traumatic brain injury: a risk factor for neurodegeneration. *Alzheimers Res Ther* 2:18. <https://doi.org/10.1186/alzrt42>
- Gavett BE, Stern RA, McKee AC (2011) Chronic traumatic encephalopathy: a potential late effect of sport-related concussive and subconcussive head trauma. *Clin Sports Med* 30:179–188, xi. <https://doi.org/10.1016/j.csm.2010.09.007>
- Gordon BA, Friedrichsen K, Brier M, Blazey T, Su Y, Christensen J, Aldea P, McConathy J, Holtzman DM, Cairns NJ, Morris JC, Fagan AM, Ances BM, Benzinger TL (2016) The relationship between cerebrospinal fluid markers of Alzheimer pathology and positron emission tomography tau imaging. *Brain* 139:2249–2260. <https://doi.org/10.1093/brain/aww139>
- Holmes BB, Furman JL, Mahan TE, Yamasaki TR, Mirbaha H, Eades WC, Belaygorod L, Cairns NJ, Holtzman DM, Diamond MI (2014) Proteopathic tau seeding predicts tauopathy in vivo. *Proc Natl Acad Sci U S A* 111:E4376–E4385. <https://doi.org/10.1073/pnas.1411649111>
- Hyman BT, Phelps CH, Beach TG, Bigio EH, Cairns NJ, Carrillo MC, Dickson DW, Duyckaerts C, Frosch MP, Masliah E, Mirra SS, Nelson PT, Schneider JA, Thal DR, Thies B, Trojanowski JQ, Vinters HV, Montine TJ (2012) National Institute on Aging-Alzheimer's Association guidelines for the neuropathologic assessment of Alzheimer's disease. *Alzheimers Dement* 8: 1–13. <https://doi.org/10.1016/j.jalz.2011.10.007>
- Johnson KA, Schultz A, Betensky RA, Becker JA, Sepulcre J, Rentz D, Mormino E, Chhatwal J, Amariglio R, Papp K, Marshall G, Albers M, Mauro S, Pepin L, Alverio J, Judge K, Philiosaint M, Shoup T, Yokell D, Dickerson B, Gomez-Isla T, Hyman B, Vasdev N, Sperling R (2016) Tau positron emission tomographic imaging in aging and early Alzheimer disease. *Ann Neurol* 79: 110–119. <https://doi.org/10.1002/ana.24546>

18. Lee BG, Leavitt MJ, Bernick CB, Leger GC, Rabinovici G, Banks SJ (2018) A systematic review of positron emission tomography of tau, amyloid Beta, and Neuroinflammation in chronic traumatic encephalopathy: the evidence to date. *J Neurotrauma* 35:2015–2024. <https://doi.org/10.1089/neu.2017.5558>
19. Lowe VJ, Curran G, Fang P, Liesinger AM, Josephs KA, Parisi JE, Kantarci K, Boeve BF, Pandey MK, Bruinsma T, Knopman DS, Jones DT, Petrucelli L, Cook CN, Graff-Radford NR, Dickson DW, Petersen RC, Jack CR Jr, Murray ME (2016) An autoradiographic evaluation of AV-1451 tau PET in dementia. *Acta Neuropathol Commun* 4:58. <https://doi.org/10.1186/s40478-016-0315-6>
20. Marquie M, Normandin MD, Meltzer AC, Siao Tick Chong M, Andrea NV, Anton-Fernandez A, Klunk WE, Mathis CA, Ikonovic MD, Debnath M, Bien EA, Vanderburg CR, Costantino I, Makarets S, DeVos SL, Oakley DH, Gomperts SN, Growdon JH, Johnson KA, Frosch MP, Lucente D, Dickerson BC, Frosch MP, Hyman BT, Johnson KA, Gomez-Isla T (2017) Pathological correlations of [F-18]-AV-1451 imaging in non-alzheimer tauopathies. *Ann Neurol* 81:117–128. <https://doi.org/10.1002/ana.24844>
21. Marquie M, Normandin MD, Vanderburg CR, Costantino IM, Bien EA, Rycyna LG, Klunk WE, Mathis CA, Ikonovic MD, Debnath ML, Vasdev N, Dickerson BC, Gomperts SN, Growdon JH, Johnson KA, Frosch MP, Hyman BT, Gomez-Isla T (2015) Validating novel tau positron emission tomography tracer [F-18]-AV-1451 (T807) on postmortem brain tissue. *Ann Neurol* 78:787–800. <https://doi.org/10.1002/ana.24517>
22. Marquie M, Siao Tick Chong M, Anton-Fernandez A, Verwer EE, Saez-Calveras N, Meltzer AC, Ramanan P, Amaral AC, Gonzalez J, Normandin MD, Frosch MP, Gomez-Isla T (2017) [F-18]-AV-1451 binding correlates with postmortem neurofibrillary tangle Braak staging. *Acta Neuropathol* 134:619–628. <https://doi.org/10.1007/s00401-017-1740-8>
23. Martland M (1928) Punch drunk. *JAMA* 91:1103–1107
24. McKee AC, Cairns NJ, Dickson DW, Folkerth RD, Keene CD, Litvan I, Perl DP, Stein TD, Vonsattel JP, Stewart W, Tripodis Y, Cray JF, Bieniek KF, Dams-O'Connor K, Alvarez VE, Gordon WA, group TC (2016) The first NINDS/NIBIB consensus meeting to define neuropathological criteria for the diagnosis of chronic traumatic encephalopathy. *Acta Neuropathol* 131:75–86. <https://doi.org/10.1007/s00401-015-1515-z>
25. McKee AC, Cantu RC, Nowinski CJ, Hedley-Whyte ET, Gavett BE, Budson AE, Santini VE, Lee HS, Kubilus CA, Stern RA (2009) Chronic traumatic encephalopathy in athletes: progressive tauopathy after repetitive head injury. *J Neuropathol Exp Neurol* 68:709–735. <https://doi.org/10.1097/NEN.0b013e3181a9d503>
26. McKee AC, Stern RA, Nowinski CJ, Stein TD, Alvarez VE, Daneshvar DH, Lee HS, Wojtowicz SM, Hall G, Baugh CM, Riley DO, Kubilus CA, Cormier KA, Jacobs MA, Martin BR, Abraham CR, Ikezu T, Reichard RR, Wolozin BL, Budson AE, Goldstein LE, Kowall NW, Cantu RC (2013) The spectrum of disease in chronic traumatic encephalopathy. *Brain* 136:43–64. <https://doi.org/10.1093/brain/aws307>
27. McKeith IG, Boeve BF, Dickson DW, Halliday G, Taylor JP, Weintraub D, Aarsland D, Galvin J, Attems J, Ballard CG, Bayston A, Beach TG, Blanc F, Bohnen N, Bonanni L, Bras J, Brundin P, Burn D, Chen-Plotkin A, Duda JE, El-Agnaf O, Feldman H, Ferman TJ, Ffytche D, Fujishiro H, Galasko D, Goldman JG, Gomperts SN, Graff-Radford NR, Honig LS, Iranzo A, Kantarci K, Kaufer D, Kukull W, Lee VMY, Leverenz JB, Lewis S, Lipka C, Lunde A, Masellis M, Masliah E, McLean P, Mollenhauer B, Montine TJ, Moreno E, Mori E, Murray M, O'Brien JT, Orimo S, Postuma RB, Ramaswamy S, Ross OA, Salmon DP, Singleton A, Taylor A, Thomas A, Tiraboschi P, Toledo JB, Trojanowski JQ, Tsuang D, Walker Z, Yamada M, Kosaka K (2017) Diagnosis and management of dementia with Lewy bodies: fourth consensus report of the DLB consortium. *Neurology* 89:88–100. <https://doi.org/10.1212/WNL.0000000000004058>
28. Millsbaugh JA (1937) Dementia pugilistica. *Us Naval Med Bull* 35:297–303
29. Mitsis EM, Riggio S, Kostakoglu L, Dickstein DL, Machac J, Delman B, Goldstein M, Jennings D, D'Antonio E, Martin J, Naidich TP, Aloysi A, Fernandez C, Seibyl J, DeKosky ST, Elder GA, Marek K, Gordon W, Hof PR, Sano M, Gandy S (2014) Tauopathy PET and amyloid PET in the diagnosis of chronic traumatic encephalopathies: studies of a retired NFL player and of a man with FTD and a severe head injury. *Transl Psychiatry* 4:e441. <https://doi.org/10.1038/tp.2014.91>
30. Omalu B, Hammers JL, Bailes J, Hamilton RL, Kamboh MI, Webster G, Fitzsimmons RP (2011) Chronic traumatic encephalopathy in an Iraqi war veteran with posttraumatic stress disorder who committed suicide. *Neurosurg Focus* 31:E3. <https://doi.org/10.3171/2011.9.FOCUS11178>
31. Ossenkoppele R, Rabinovici GD, Smith R, Cho H, Scholl M, Strandberg O, Palmqvist S, Mattsson N, Janelidze S, Santillo A, Ohlsson T, Jogi J, Tsai R, La Joie R, Kramer J, Boxer AL, Gorno-Tempini ML, Miller BL, Choi JY, Ryu YH, Lyoo CH, Hansson O (2018) Discriminative accuracy of [18F] flortaucipir positron emission tomography for Alzheimer disease vs other neurodegenerative disorders. *JAMA* 320:1151–1162. <https://doi.org/10.1001/jama.2018.12917>
32. Pontecorvo MJ, Devous MD Sr, Navitsky M, Lu M, Salloway S, Schaefer FW, Jennings D, Arora AK, McGeehan A, Lim NC, Xiong H, Joshi AD, Siderowf A, Mintun MA, investigators FA-A (2017) Relationships between flortaucipir PET tau binding and amyloid burden, clinical diagnosis, age and cognition. *Brain* 140:748–763. <https://doi.org/10.1093/brain/aww334>
33. Sander K, Lashley T, Gami P, Gendron T, Lythgoe MF, Rohrer JD, Schott JM, Revesz T, Fox NC, Arstad E (2016) Characterization of tau positron emission tomography tracer [18F]AV-1451 binding to postmortem tissue in Alzheimer's disease, primary tauopathies, and other dementias. *Alzheimers Dementia* 12:1116–1124. <https://doi.org/10.1016/j.jalz.2016.01.003>
34. Schmidt ML, Zhukareva V, Newell KL, Lee VM, Trojanowski JQ (2001) Tau isoform profile and phosphorylation state in dementia pugilistica recapitulate Alzheimer's disease. *Acta Neuropathol* 101:518–524
35. Scholl M, Lockhart SN, Schonhaut DR, O'Neil JP, Janabi M, Ossenkoppele R, Baker SL, Vogel JW, Faria J, Schwimmer HD, Rabinovici GD, Jagust WJ (2016) PET imaging of tau deposition in the aging human brain. *Neuron* 89:971–982. <https://doi.org/10.1016/j.neuron.2016.01.028>
36. Stern RA, Adler CH, Chen K, Navitsky M, Luo J, Dodick DW, Alosco ML, Tripodis Y, Goradia DD, Martin B, Mastroeni D, Fritts NG, Jamagin J, Devous MD Sr, Mintun MA, Pontecorvo MJ, Shenton ME, Reiman EM (2019) Tau positron-emission tomography in former National Football League Players. *N Engl J Med* 380:1716–1725. <https://doi.org/10.1056/NEJMoa1900757>
37. Sundman M, Doraiswamy PM, Morey RA (2015) Neuroimaging assessment of early and late neurobiological sequelae of traumatic brain injury: implications for CTE. *Front Neurosci* 9:334. <https://doi.org/10.3389/fnins.2015.00334>
38. Vonsattel JP, Aizawa H, Ge P, DiFiglia M, McKee AC, MacDonald M, Gusella JF, Landwehrmeyer GB, Bird ED, Richardson EP Jr et al (1995) An improved approach to prepare human brains for research. *J Neuropathol Exp Neurol* 54:42–56. <https://doi.org/10.1097/00005072-199501000-00006>
39. Wang L, Benzinger TL, Su Y, Christensen J, Friedrichsen K, Aldea P, McConathy J, Cairns NJ, Fagan AM, Morris JC, Ances BM (2016) Evaluation of tau imaging in staging Alzheimer disease and revealing interactions between beta-amyloid and Tauopathy. *JAMA Neurol* 73:1070–1077. <https://doi.org/10.1001/jamaneurol.2016.2078>
40. Woerman AL, Aoyagi A, Patel S, Kazmi SA, Lobach I, Grinberg LT, McKee AC, Seeley WW, Olson SH, Prusiner SB (2016) Tau prions from Alzheimer's disease and chronic traumatic encephalopathy patients propagate in cultured cells. *Proc Natl Acad Sci U S A* 113:E8187–E8196. <https://doi.org/10.1073/pnas.1616344113>
41. Xia CF, Arteaga J, Chen G, Gangadharmath U, Gomez LF, Kasi D, Lam C, Liang Q, Liu C, Mocharla VP, Mu F, Sinha A, Su H, Szardenings AK, Walsh JC, Wang E, Yu C, Zhang W, Zhao T, Kolb HC (2013) [18F]FT807, a novel tau positron emission tomography imaging agent for Alzheimer's disease. *Alzheimers Dementia* 9:666–676. <https://doi.org/10.1016/j.jalz.2012.11.008>
42. Zetterberg H, Blennow K (2016) Fluid biomarkers for mild traumatic brain injury and related conditions. *Nat Rev Neurol* 12:563–574. <https://doi.org/10.1038/nrneurol.2016.127>

Publisher's Note

Springer Nature remains neutral with regard to jurisdictional claims in published maps and institutional affiliations.

Ready to submit your research? Choose BMC and benefit from:

- fast, convenient online submission
- thorough peer review by experienced researchers in your field
- rapid publication on acceptance
- support for research data, including large and complex data types
- gold Open Access which fosters wider collaboration and increased citations
- maximum visibility for your research: over 100M website views per year

At BMC, research is always in progress.

Learn more biomedcentral.com/submissions

